1993

Pulsed electrochemical detection of organic sulfur compounds at gold electrodes

Peter James Vandeberg
Iowa State University

Order Number 9414029

Pulsed electrochemical detection of organic sulfur compounds at gold electrodes

Vandeberg, Peter James, Ph.D.

Iowa State University, 1993

U·M·I
300 N. Zeeb Rd.
Ann Arbor, MI 48106

Pulsed electrochemical detection of organic sulfur compounds at gold electrodes

by

Peter James Vandeberg

A Dissertation Submitted to the

Graduate Faculty in Partial Fulfillment of the

Requirements for the Degree of

DOCTOR OF PHILOSOPHY

Department: Chemistry
Major: Analytical Chemistry

Approved:

Signature was redacted for privacy.

In Charge of Major Work

Signature was redacted for privacy.

For the Major Department

Signature was redacted for privacy.

For the Graduate College

Iowa State University
Ames, Iowa

1993

TABLE OF CONTENTS

	page
GENERAL INTRODUCTION	1
Explanation of dissertation format	1
Detection of organic sulfur compounds in liquid chromatography	2
Electrochemistry of organic sulfur compounds	7
Pulsed electrochemical detection	9
PAPER 1. PULSED AMPEROMETRIC DETECTION OF SULFUR COMPOUNDS: THIOUREA AT GOLD ELECTRODES	11
ABSTRACT	12
INTRODUCTION	13
EXPERIMENTAL	16
Reagents	16
Voltammetry	16
Flow-injection detection	17
Procedures	19
RESULTS AND DISCUSSION	20
Cyclic voltammetric response for thiourea	20
Pulsed voltammetric response for thiourea	27
Flow injection with pulsed amperometric detection (FI-PAD)	32
Analysis of adsorbed oxidation products	41

CONCLUSIONS 43

ACKNOWLEDGMENTS 45

REFERENCES 46

PAPER 2. A STUDY OF THE VOLTAMMETRIC RESPONSE OF THIOUREA AND ETHYLENETHIOUREA AT GOLD ELECTRODES IN ALKALINE MEDIA 48

ABSTRACT 49

INTRODUCTION 50

EXPERIMENTAL 52

Reagents 52

Voltammetry 52

Procedures 53

RESULTS AND DISCUSSION 54

Thiourea 54

Ethylenethiourea 73

CONCLUSIONS 85

ACKNOWLEDGMENTS 87

REFERENCES 88

PAPER 3. PULSED ELECTROCHEMICAL DETECTION OF CYSTEINE, CYSTINE, METHIONINE AND GLUTATHIONE AT GOLD ELECTRODES FOLLOWING THEIR SEPARATION BY LIQUID CHROMATOGRAPHY 90

ABSTRACT 91

INTRODUCTION 92

EXPERIMENTAL SECTION 95

Reagents 95

Voltammetry 95

Chromatography 96

RESULTS AND DISCUSSION 98

Voltammetric response in alkaline solutions 98

Voltammetric response in acidic solutions 101

Selection of PED waveform parameters 104

LC-PED results 108

CONCLUSIONS 116

ACKNOWLEDGEMENTS 117

REFERENCES 118

PAPER 4. COMPARISON OF PULSED AMPEROMETRIC DETECTION AND INTEGRATED VOLTAMMETRIC DETECTION OF ORGANIC SULFUR COMPOUNDS IN LIQUID CHROMATOGRAPHY 120

ABSTRACT 121

INTRODUCTION 122

EXPERIMENTAL SECTION 126

Reagents 126

Voltammetry 126

Chromatography 127

RESULTS AND DISCUSSION 129

Voltammetric response for cysteine in 0.1 M $HClO_4$ 129

Selection of PAD waveform parameters 132

Selection of IVD waveform parameters 134

Linearity of response and limits of detection 138

Baseline drift 139

Elimination of system peak for O_2 in the sample 140

Effect of a preadsorption step in PAD and IVD waveforms 142

Application of LC-IVD for mixtures of organosulfur compounds 146

CONCLUSIONS 150

ACKNOWLEDGEMENTS 151

REFERENCES 152

GENERAL CONCLUSIONS 154

LITERATURE CITED 155

ACKNOWLEDGEMENTS 159

GENERAL INTRODUCTION

Explanation of dissertation format. The four main sections of this dissertation consist of papers that were submitted for publication to various analytical and electrochemical journals. Although the content of this thesis deals with organic sulfur compounds in general, the emphasis is on thiourea and sulfur-containing amino acids and peptides. The four papers are preceded by a general introduction and followed by general conclusions and acknowledgements. References for both the introduction and conclusion will appear together following the conclusion. The four papers are each written in accordance to the format requirements of the journals to which they were submitted.

The research described in this dissertation was performed under the direction of Professor Dennis C. Johnson beginning in January 1991. Paper 1 is an investigation of the pulsed amperometric detection (PAD) of thiourea and was prompted by unpublished work by Jodi Kawagoe which revealed excessive fouling and peak-broadening when detecting thiourea at gold electrodes in a flow system. Paper 2 is a detailed voltammetric study of thiourea and ethylenethiourea performed to help understand the quantitative relationship between detector signal and analyte concentration. Paper 3 introduces a fast cyclic scan waveform for the determination of sulfur compounds and examines the selectivity seen for the detection of sulfur compounds under conditions of low pH. Paper 3 also contains several chromatographic applications for the detection of sulfur-containing amino-acids and peptides. Finally, Paper 4 takes a closer look at

the fast cyclic scan waveform, known as integrated voltammetric detection or IVD, and compares it to the traditional three-step waveform used with PAD. Each of the four papers includes an introduction, and hence, the general introduction to the dissertation is kept to a minimum.

Detection of organic sulfur compounds in liquid chromatography. The analysis of organic sulfur compounds is of great importance to the study of a wide range of environmental, biological and chemical systems. The atmospheric sulfur cycle, for example, is greatly influenced by organic sulfur compounds released by marine phytoplankton [1]. Thiocarbamates and thiophosphates are common pesticides and fungicides. Some classes of sulfur compounds are suspected carcinogens, including thiourea and ethylenethiourea [2]. Other sulfur compounds are thought to have anti-carcinogenic activity, including thiones closely related to ethylenethiourea [3]. Thiols and disulfides, in particular, play an important role in living systems. Of major importance in humans is glutathione, (glutamylcysteinylglycine, GSH) which participates in a wide variety of functions, including metabolism, removal of heavy metals and removal of free radicals and peroxides [4]. Depletion of cellular GSH results in the increased sensitivity of the cells to radiation and oxidative damage [4]. Low levels of GSH in tumor cells, on the other hand, may lead to a greater effectiveness of treatment by anticancer drugs and radiation [5]. Finally, thioethers formed during the metabolism of toxic compounds with GSH and other thiols may be used as a measure of exposure to those compounds [6].

High performance liquid chromatography (HPLC) provides many advantages for the analysis of organic sulfur compounds. The separation power of HPLC alleviates interference from other compounds. If an adequate detection method exists, determinations can be quite sensitive. In addition, a number of sulfur compounds can be determined in a single mixture.

There are three general detection schemes for detection of sulfur compounds of biological interest following liquid chromatography. Underivatized compounds may be detected directly with uv detection, compounds may be derivatized and detected with uv or fluorescence detection, or direct detection may be performed with electrochemical detection. Additional detection schemes, although less common, include chemiluminescence and mass spectroscopy.

In general, the ultraviolet adsorption characteristics of thiones, sulfides and disulfides are inadequate for sensitive LC detection. Adsorption occurs mainly in the region of 190-220 nm, where interference from solvents and matrices is common [7]. The thiolate anion of cysteine and glutathione is reported to have a fairly strong adsorption band at 237 nm (ϵ = 4000-6000 M^{-1} cm^{-1} for GSH) and uv detection should be adequate with postcolumn addition of alkaline media, but this has not been taken advantage of in LC analysis [7]. A method for the uv detection of ethylenethiourea at 233 nm has been reported, but only after preconcentration from a very simple groundwater matrix [8]. In addition, uv detection for methionine and methionine-hydroxy analogue has been used, but only where the two compounds have been major constituents of the sample [9].

Many biologically important sulfur compounds contain amine groups which may be derivatized with ninhydrin for uv detection [10]. More commonly, 1-fluoro-2,4-dinitrobenzene (DNP, Sanger's reagent) has been used with uv detection at 365 nm [11]. Detection limits for this method are reported at the nanomole level, but interferences from amino acids and other amines are encountered.

Thiols and thioethers can be determined after derivatization with 5,5'-dithiobis-(2-nitrobenzoic acid) (DTNB, Ellman's reagent) [12]. To distinguish between thiols and thioethers, the sample is divided into two separate parts with one fraction treated directly with DTNB. The other fraction is treated with DTNB following alkaline hydrolysis to convert the thioethers to thiolates. The DTNB derivatives are detected at 412 nm.

Organic sulfides used for mustard gas chemical warfare agents are treated with sodium benzenesulfochloramide (chloramine-B) to form the corresponding innocuous phenylsulfonylsulfilimines derivatives, which have a strong adsorption around 230 nm. Detection limits were reported on the order of 10 ng [13].

The sensitive and selective detection of thiols is possible with the use of fluorescence detection of thiol-derivatives. A much used fluorescence derivative is monobromobimane, which forms a thiol derivative. Detection limits of the bromobimane derivatized thiols are reported on the order of 1 pmol [14,15]. Much work has been published by Imai et al. using ammonium 7-fluorobenzo-2-oxa-1,3-diazole-4-sulphonate (SBD-F) [16-18]. Detection limits are reported in the range of 0.07 to 1.4 pmol for a variety of thiols including cysteine and glutathione. The SBD-F

is reportedly more stable than other fluorescence reagents, including the bromobimanes, which decompose, resulting in multiple chromatographic peaks [16].

The simultaneous determination of thiols and disulfides is possible with multiple derivitization steps. In one scheme, the free thiols are derivatized with 4-(aminosulfonyl)-7-fluoro-2,1,3-benzoxadiaxole (ABD-F). Next, the disulfides are reduced to their corresponding thiols and then finally derivatized with SBD-F [17]. Commonly, the difficulty in determining disulfides in the presence of thiols is solved by first determining the free thiols, then adding a reducing agent, such as mercaptoethanol or dithiothreitol, in excess, and then repeating the determination [19]. This two-stage determination can be problematic as a result of the relative concentrations of the thiol and corresponding disulfides which are found in biological fluids. For example, GSH is present in human whole blood at approximately 1 mM, but the GSH disulfide is at levels of only about 0.05 mM [20]. In addition, GSH is very easily oxidized by O_2 to the disulfide, thus if even a small fraction of the GSH is allowed to oxidize to the disulfide, large inaccuracies may be encountered for the disulfide determination.

A very novel indirect fluorescence method had been used for the detection of thiourea and its derivatives [21]. A calcein·palladium complex is added post-column to the mobile phase. Complexation with palladium efficiently quenches the calcein fluorescence, but when a sulfur compound is present, it will preferentially complex with the Pd(II), resulting in a release of the calcein and a corresponding increase in the fluorescence signal. Heat must be added to promote the ligand exchange reaction and

limits of detection are on the order of 10 pmol. The Pd complex is used at a level of *ca.* 10^{-5} M.

Electrochemical detectors for sulfur compounds have largely focussed on the use of Hg or Hg/Au electrode materials. Sulfur compounds form a Hg-complex in which the overpotential for Hg oxidation is decreased:

$$RSHg \rightarrow RSHg^{2+} + 2e^-$$

Although the application of an Hg detector for use with liquid chromatography has been extensively reported on, work relevant to this dissertation includes application of a dropping mercury electrode (DME) to the detection of thiourea derivatives [22,23]. A DME has also been used in this laboratory for the determination of inorganic sulfur species [24]. Application of a Hg pool electrode detection of sulfur-containing amino acids and related peptides was performed by Rabenstein, Saetre and coworkers [25-26]. The use of Hg/Au amalgam electrodes for the detection of sulfur compounds was reported in 1981[27]. The Hg/Au electrode was successfully used by Allison and Shoup at Bionalytical Systems (BAS) to determine GSH in blood in both the reduced and oxidized forms [20]. Detection of the disulfide is made possible by first reducing it at an upstream electrode and then detecting it as the thiol. The success of Shoup and coworkers at BAS has lead to the commercialization of the Hg/Au electrode. It has been used for determination of ethylenethiourea [28-29] and is the detection method for an official Association of Official Analytical Chemists method [30]. A problem with the Hg/Au electrode is surface preparation. The Hg surface generally lasts about three weeks of use before it must be renewed by polishing and treatment with fresh liquid

Hg. Furthermore, when the new Hg surface has been applied, it must be allowed to equilibrate at least two days prior to use to attain reproducible response [30-31].

Glassy carbon (GC) electrodes have been applied as detectors for a number of sulfur compounds [32-35]. GC electrodes require a high detection potential which results in interference from other electroactive species often including solvent oxidation. Selectivity may be enhanced by if the compounds of interest are able to be detected at a potential where interfering compounds are not oxidized. Use of anodic pretreatment has been used to lower the detection potential for methionine [33] and the use of photolysis has been used for both methionine and cystine [35]. A variety of specially modified carbon electrodes have been successfully used for detection of sulfur compounds. Mixed-oxide Ru has been used by Cox and co-workers for detection of sulfur-containing amino acids and related compounds [36]. Detection limits are on the order of 50 pmol. Several workers have reported the use of cobalt phthalocyanine modified carbon paste electrodes for the detection of thiols [37-38]. An LOD of 3 pmol was reported [37]. Special electrode preparations are required for the Ru and Co modified electrodes and the electrode surfaces must be frequently replaced or polished to maintain reproducibility.

Electrochemistry of organic sulfur compounds. Electrochemical studies of organic sulfur compounds at solid electrodes have been viewed as difficult because of the tendency of the sulfur compounds to produce films which coat the electrode surface and poison electrode activity [39-40]. A vast amount of literature exists dealing with

the electrochemistry of sulfur compounds, much of it in non-aqueous media [40].

Literature reports on the electrochemical aspects of thiourea are more thoroughly discussed in Papers 1 and 2, but some of the more important aspects will be examined briefly here. The adsorption of thiourea on gold has been investigated using radiotracer methods [41-42] and ac voltammetry and surface enhanced raman spectroscopy (SERS) [43]. These studies concluded that strong adsorption occurs over a wide potential range. Under acidic conditions, oxidative desorption of thiourea takes place with the rupture of the C-S bond but adsorbed thiourea cannot be completely removed by negative polarization of the electrode. Anodic desulfurization of adsorbed thiourea and related compounds has been reported by several workers [44-46]. Desulfurization may result in a fairly stable coating of surface sulfide which diminishes electrode activity, but may be stripped cathodically. In fact, cathodic stripping has been used for the quantitative determination of thioamides at silver electrodes [46].

Relatively few studies of the oxidation of cysteine, cystine and glutathione have been performed at gold and platinum electrodes [47-53]. Cysteine is believed to undergo a one e^- oxidation, resulting in an adsorbed radical species (RS•) [50]. A similar radical species results from the dissociative adsorption of cystine, which is oxidized to cysteic acid during formation of the surface oxide [49]. Cysteic acid, however, when adsorbed to the Au surface, is speculated to undergo further oxidation, resulting in desulfurization [53]. Oxidation of both the reduced and oxidized forms of glutathione similarly takes place with the formation of surface oxide [51].

Because the oxidation of sulfur compounds occurs concurrently with the

formation of the surface oxide, a better understanding of the oxide formation process is of great importance. Studies of surface oxide formation have been performed by a number of researchers, including Burke et al. [54-55]. The pH dependence of surface oxide catalyzed oxidation of sulfite was noted by Vitt et al. [56]. Recent studies of oxide formation kinetics from our own group have led to a better understanding of time limitations on the general surface oxide formation process [57].

Pulsed electrochemical detection. Many classes of polar, aliphatic compounds are catalytically oxidized at noble metal electrodes. Constant potential detection, however, is not possible as a result of the fouling of the electrode surfaces by surface oxide and/or organic oxidation products. Active electrode surfaces may be regained by application of anodic cleaning pulse and a cathodic regeneration pulse. Application of a repetitive waveform in this manner is the basis for pulsed electrochemical detection (PED).

PED has been reviewed recently [58-60], and hence it is unnecessary to review more than the most important details relating to the work contained in this dissertation. Polta and Johnson demonstrated the use of a three-step pulsed amperometric detection (PAD) waveform for sulfur compounds on Pt under alkaline conditions [61-62]. In using thiourea as a model compound, they achieved a limit of detection of about 200 pmol. Response deviated negatively from linearity with increasing concentration, but linear calibration curves could be obtained by plotting the inverse of the peak signal as a function of the inverse of the concentration. Initial work done by Polta at Au

electrodes, showed better sensitivity than Pt for sulfur compounds [63]. PAD was successfully applied to chromatographic separations of thiocarbamate [64] and thiophosphate [65] pesticides in acetate buffers containing acetonitrile.

Significant to the development of PED for sulfur compounds was the introduction of the potential-sweep pulsed coulometric detection (PS-PCD) waveform by Neuburger and Johnson [66]. Because the detection of sulfur compounds requires concomitant formation of Au surface-oxide, amperometric measurement of the signal results in a large background from the surface oxide. When the current is integrated over surface oxide formation and reduction, the background from the surface oxide is automatically subtracted. Use of a PS-PCD waveform resulted in lower limits of detection. In addition, the PS-PCD waveform enabled use of small pH and organic modifier gradients which cause large baseline shifts with PAD because of their effect on the surface oxide formation [67].

PAPER 1.

PULSED AMPEROMETRIC DETECTION OF SULFUR COMPOUNDS: THIOUREA AT GOLD ELECTRODES[1]

[1] Published in Vandeberg, P.J.; Kawagoe, J.L. and Johnson, D.C., *Anal. Chim. Acta*, **1992**, *260*, 1-11.

ABSTRACT

Cyclic and pulsed voltammetry at a rotated disk electrode and pulsed amperometric detection (PAD) in a flow-injection cell are applied in studies of the anodic response of thiourea at Au electrodes in 0.1 M NaOH. The greatest voltammetric response corresponds to a peak-shaped anodic wave catalyzed by the oxide-formation process on the electrode surface. This anodic response is under mixed transport-surface control with sulfate concluded to be the predominate oxidation product. For high thiourea concentrations, electrode fouling can occur from accumulation of atomic sulfur formed by the incomplete oxidation of thiourea. Electrode fouling during PAD can be avoided using a pulsed waveform in which the cathodic reactivation process occurs at a potential < -1.0 V vs. SCE to achieve cathodic desorption of atomic sulfur. A change in the slope of calibration data for concentrations > 0.01 mM is interpreted to be a consequence of (i) the decreased efficiency for oxidation of thiourea and (ii) a positive shift in the potential for the peak anodic response as concentration is increased.

INTRODUCTION

The past decade has witnessed a tremendous growth in the use of amperometric detection in liquid chromatography (LC) and flow-injection (FI) methodology. Advantages of amperometric detection, when applicable, include high sensitivity and moderately low cost. Work in our laboratory has focused on development of the amperometric detection of polar aliphatic organic compounds at Au and Pt electrodes in LC and FI systems [1,2]. The consensus, based on experience with detection at constant applied potentials, is that aliphatic compounds are not readily detected at solid electrodes. We have demonstrated the successful application of pulsed potential-time (E-t) waveforms at Au and Pt electrodes for the sensitive Pulsed Amperometric Detection (PAD) of numerous polar aliphatic compounds. Compounds detected include alcohols (simple and complex), carbohydrates, (aldoses and ketoses, monosaccharides and oligosaccharides), amino alcohols, amino sugars, amino acids and a variety of sulfur compounds. Detection limits in LC-PAD are commonly in the range of 1-10 pmoles.

Among our current interests is the optimization of PAD waveforms for detection of organo-sulfur compounds. Such compounds are commonly found in pesticides and their biodegradation products, and other agrochemicals. Many organo-sulfur compounds do not adsorb strongly in the uv-visible region of the electromagnetic spectrum and their detection by conventional photometric methodology is inadequate without prior chemical derivatization. Application of PAD to organo-sulfur

compounds has offered several challenges [3-6], including electrode fouling during prolonged exposure to some compounds [7], and a better understanding of the detection process is being sought to enable enhancement of detector performance.

Thiourea has been used as a model compound for studies using pulsed waveforms at Pt [3,4] and Au [8] electrodes. Thiourea was chosen as a model organo-sulfur compound primarily because of its electrochemical behavior is representative of many organo-sulfur compounds [3]. It also has a low volatility and does not produce the foul odor characteristic of many organo-sulfur compounds. Furthermore, thiourea derivatives are known degradation products of ethylenebisdithiocarbamate fungicides [9] and are, therefore, natural targets for LC-PAD applications. Thiourea has been labeled as having carcinogenic activity [10]; hence, all work with this compound should be performed with the greatest of care to prevent direct exposure of researchers and contamination of the environment.

Initial studies indicated a higher sensitivity for PAD at Au in comparison to Pt electrodes [5,11]; however, the detection mechanism is believed to be very similar for these two electrode materials. The mechanism for anodic detection of sulfur compounds is believed to involve adsorption via the sulfur atom onto oxide-free metal atoms in the electrode surface. A prerequisite for adsorption apparently is the presence of a non-bonded electron pair on the S-atom. For example, thiols and sulfoxides are detected, but sulfones and sulfonic acids are not detected. Anodic detection of adsorbed sulfur compounds occurs during anodic formation of oxide on the noble metal electrodes with concomitant oxidative desorption of the sulfur species. In the PAD

waveform, the anodic current is sampled during this surface-catalyzed oxidation process. The reactions below have been proposed to account for PAD response of various sulfur compounds in alkaline media [12]:

$$R\text{-}S^- + 6OH^- \rightarrow R\text{-}SO_3^- + 3H_2O + 6e^- \quad (1)$$

$$R\text{-}SO\text{-}R' + 2OH^- \rightarrow R\text{-}SO_2\text{-}R' + H_2O + 2e^- \quad (2)$$

$$(RO)_3PS + 10OH^- \rightarrow (RO)_3PO + SO_4^{2-} + 5H_2O + 10e^- \quad (3)$$

$$SCN^- + 8OH^- \rightarrow CN^- + SO_4^- + 4H_2O + 6e^- \quad (4)$$

Because of the significance of preadsorption in the detection mechanisms of sulfur compounds, the anodic response is expected to be strongly influenced by the adsorption isotherms of the compounds. Hence, linear calibration curves are expected for very dilute solutions with severe negative deviations from linearity for highly concentrated solutions. An additional complication expected for high concentrations of sulfur compounds is that the corresponding high surface coverage of adsorbate ($\Theta \rightarrow 1$) can inhibit the rate of surface oxide formation. Hence, the presence of the adsorbed sulfur compounds interferes with the process that is required to enable the detection mechanism. Thus, at high concentrations, distortions to the shapes of FI and LC peaks can be expected in addition to the non-linear PAD response. It is also conceivable, for strongly adsorbed sulfur compounds, that their oxidative desorption can be hindered so severely that the PAD waveform is unable to regenerate the activity of the clean electrode surface.

EXPERIMENTAL

Reagents. All chemicals were Analytical Reagents (Fisher Scientific Co.) and were used without further purification. Water was purified by passage in a serial fashion through ion-exchange cartridges (Culligan) and a Milli-Q purification system (Millipore Corp.).

Voltammetry. Voltammetric experiments were performed with a Model RDE-4 potentiostat, a Au rotated disk electrode (RDE; 0.20 cm^2), and a MSR rotator and speed controller (Pine Instrument Co.). Data were recorded by a Model 2000 X-Y recorder (Houston Instruments Co.) or by a PC-XT computer (IBM) with a DAS-8PGA data acquisition board (MetraByte Corp.) and ASYST-2.0 software (ASYST Software Technologies). Waveforms for pulsed voltammetry were generated with the ASYST software and directed to the potentiostat via a DT-2800/5716 data acquisition board (Data Translation).

The electrochemical cell (250 mL) was constructed of pyrex glass with three side-arms. Two side-arms accommodated the counter electrode (16-ga. Pt wire) and the reference electrode (SCE; Fisher Scientific) in *ca.* 10 mL of supporting electrolyte which was separated from the test solution by porous glass disks. All electrode potentials are reported with respect to the SCE. The third side-arm was fitted with a three-way stopcock to direct N_2 over the test solution, or through a fritted glass membrane (medium) in the test solution for the removal of dissolved oxygen.

Flow-Injection Detection. FI-PAD studies were performed with a PAD-2 detector (Dionex Corp.). The pump was an APM-1 LC pump (Dionex) and injections were made with a Model 7010 injection valve (Rheodyne) using a 50-μL injection loop. Data were recorded on a Model SR-255-B strip-chart recorder (Heath Co.) or by the computer interface described above using Snapshot software (HEM Data Corp.).

An inexpensive flow-through electrolysis cell was constructed in the departmental shop according to the diagram in Figure 1. The cell body was assembled from a Kel-f coupler (P-111) and two tube-end fittings (P-110) commonly available for assembly of LC systems (Upchurch). The bore of the coupler was enlarged to *ca.* 0.10 in. and a 0.10-in. hole was drilled also through the body of the coupler approximately at its center in a direction perpendicular to the axis of the coupler. This hole allowed fluid to exit from the cell after flowing over the working electrode.

The working electrode was the end surface of a Au wire (0.040-in. dia.) inserted through a short length (*ca.* 1 in.) of 1/32-in. i.d. PTFE tubing (1/16th-in. o.d.). After insertion of the Au wire through the tubing, the end surface of the wire and the surrounding PTFE were made approximately co-planar by cutting with a sharp razor blade and polishing with P-1200 abrasive cloth (SIAWAT). A leak-free seal was secured between the Au wire and the tubing when compressed by the flange in the tube-end fitting when the fitting was turned tightly into the coupler. Electrical contact to the Au wire was made by a clip attached at the exposed end of the wire.

A second tube-end fitting was modified by removing the flange with a 1/32-in. bit. The end of the PTFE tube (1/32-in. i.d., 1/16-in. o.d.) used for solution delivery

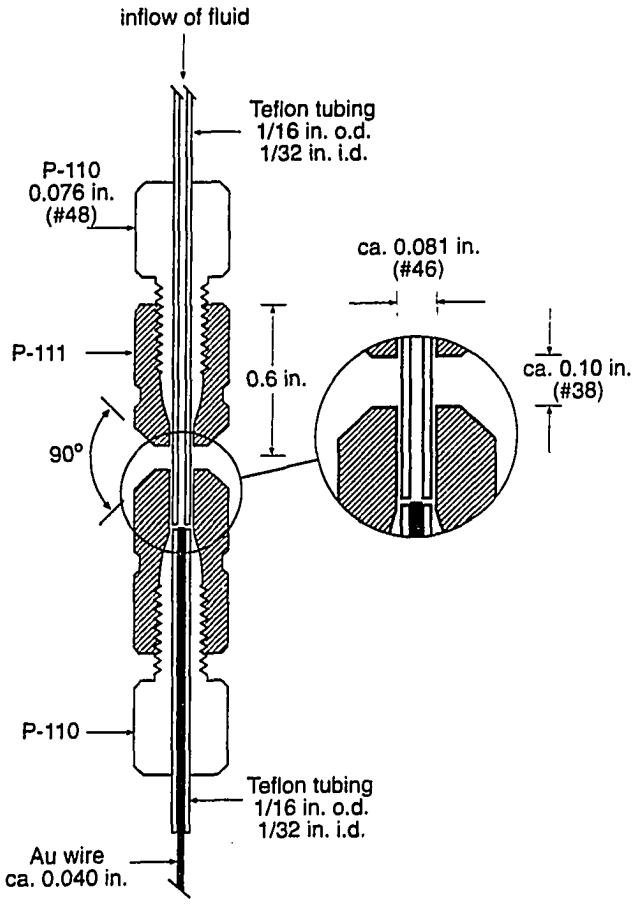

Figure 1. Diagram of gold wire flow-through electrolysis cell.

was then slipped through this modified tube-end fitting and the fitting turned into the upper end of the coupler. The fitting was turned to gentle tightness and the PTFE delivery tube was pushed deeper within the coupler until the end was in very close proximity to the Au wire and the fitting was then turned to finger tightness. Although detector response was observed to have some dependence on the spacing between the tube end and the Au wire, the response of the assembled cell remained consistent within *ca.* $\pm 1\%$ relative deviation for moderate thiourea concentrations (0.5 - 1 mM). The cell was placed in a *ca.* 75-mL beaker which had been modified by attaching a side arm to drain excess fluid to a waste container and the beaker filled with 0.1 M NaOH.

Procedures. The supporting electrolyte was 0.1 M NaOH for all experiments. Dissolved O_2 was removed from all solutions used for voltammetric studies at the Au RDE using dispersed N_2 (99.99%, Air Products). The Au RDE was polished daily with 0.05-μm alumina on microcloth (Buehler Ltd.) using H_2O as the lubricant. No attempt was made to deoxygenate solutions in FI-PAD experiments because of the O_2 permeability of the PTFE tubing used to assemble the FI apparatus.

RESULTS AND DISCUSSION

Cyclic voltammetric response for thiourea. The residual voltammetric response for the Au RDE in 0.1 M NaOH is shown by the dashed line in Figure 2. Wave a, observed for E > *ca.* 0.3 V during the positive scan, corresponds to the anodic formation of surface oxide and Wave b, for E > 0.6 V, is the result of O_2 evolution. Cathodic Peak c, obtained in the region 0.0 to 0.2 V during the negative scan, corresponds to reduction of the surface oxide. When dissolved O_2 is present, a cathodic wave is obtained in the region E < *ca.* -0.2 V.

The voltammetric response for 0.5 mM thiourea is shown by the solid line in Figure 2. Wave d, obtained at *ca.* 0.0 V just prior to the onset of oxide formation during the positive scan, has been attributed to a one-electron oxidation of the S-atom of thiourea with subsequent dimerization to form formamidine disulfide [13] as indicated by:

$$2H_2NC(S)NH_2 \rightarrow HN{=}C(NH_2)SSC{=}NH(NH_2) + 2e^- + 2H^+ \qquad (5)$$

A cathodic peak, attributed to reduction of adsorbed formamidine disulfide, is obtained at *ca.* -0.8 V during the negative scan if the positive scan limit is set at *ca.* 0.1 V so that surface oxide is not formed. However, if surface oxide is allowed to form during the positive scan, no cathodic peak is seen at -0.8 V for the reduction of the disulfide. This indicates that the adsorbed dimeric species is further oxidized at E > 0.2 V, probably by a process catalyzed by the formation of surface oxide.

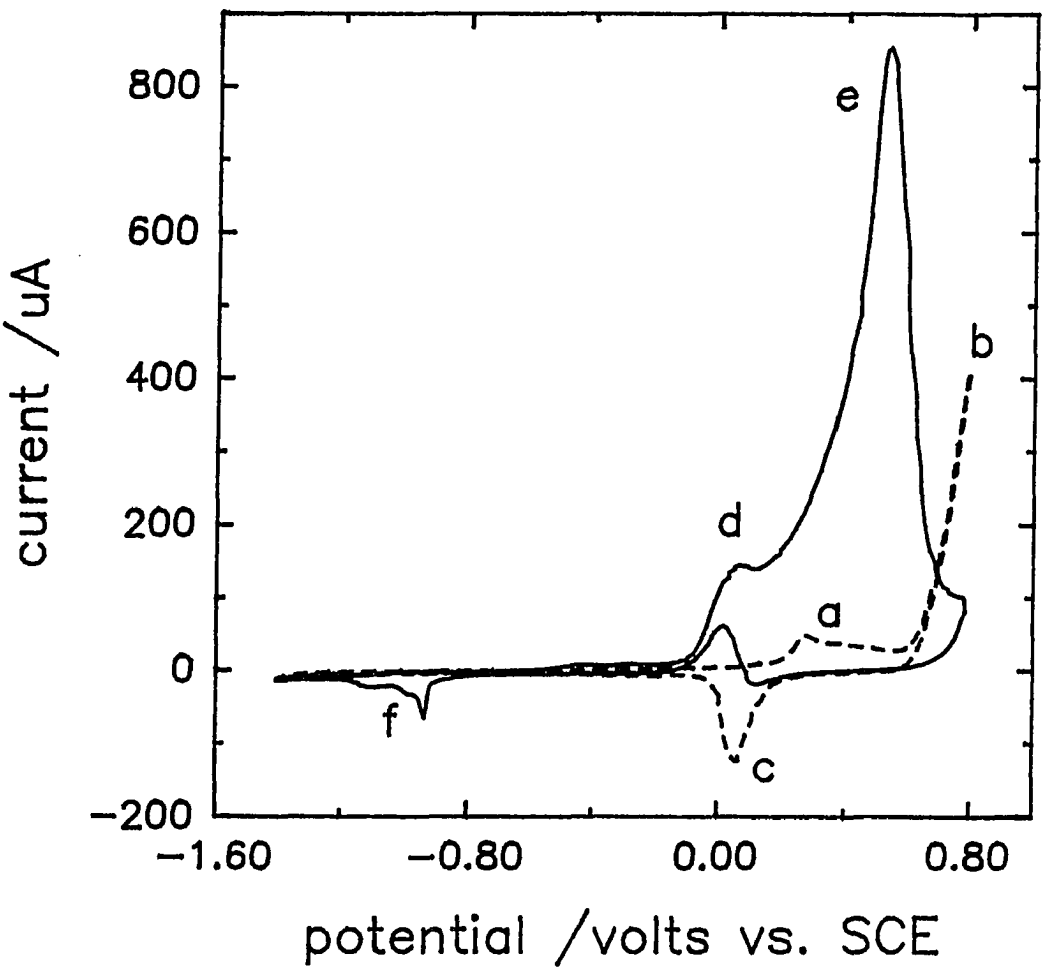

Figure 2. Voltammetric response for thiourea at the gold RDE in 0.1 M NaOH. Rotation speed: 1000 revolutions min^{-1}. Scan rate: 100 mV s^{-1}. Concentration (mM): (---) 0.00; (—) 0.5.

The peak current (i_p) for Wave d obtained in a solution of 0.5 mM thiourea was determined to be a linear function of the square root of rotation speed ($\omega^{0.5}$), for values of ω in the range 400 to 3600 rev min^{-1}, with a nonzero intercept. This is evidence that a component of the total anodic current for Wave d is under control by the mass-transport process. This observation for alkaline media is in agreement with that of Zacharov et al. [13] for thiourea at a Au electrode in acidic media. The observation of a nonzero intercept in the linear i_p-$\omega^{0.5}$ plot is consistent with the existence of a component of the total current resulting from oxidation of preadsorbed thiourea. Significant negative deviation from the linear i_p-$\omega^{0.5}$ relation was observed at concentrations higher than 1 mM. The plot of i_p vs. scan rate (ϕ) for Wave d was linear, for ϕ in the range 33 to 133 mV s^{-1}, with a nonzero intercept. This evidence is consistent with the conclusion that the anodic process yielding Wave d occurs under mixed control by mass-transport and surface processes.

Peak e in Figure 2 observed at 0.5 V during the positive scan exhibits positive but nonlinear dependence on both ϕ and $\omega^{0.5}$, which is evidence of an anodic process under mixed control by surface and mass-transport processes. The addition of Ba^{2+} following extensive oxidation under these voltammetric conditions ($>$ 100 cycles) gave an affirmative indication for the voltammetric production of SO_4^{2-}; the test was negative when applied to a fresh solution of thiourea. Therefore, Peak e is tentatively concluded to result, at least in part, from oxidation of the sulfur atom in thiourea to produce sulfate, as indicated by:

$$H_2NC(S)NH_2 + 10OH^- \rightarrow SO_4^{-2} + H_2NC(O)NH_2 + 8e^- + 10\ H_2O \qquad (6)$$

The fact that anodic oxidation of thiourea at E > 0.2 V yields a peak (e) rather than a plateau response is an indication that the faradaic process is severely attenuated for E > *ca.* 0.5 V. This attenuation might be the result of severe fouling of the electrode by formation of inert surface oxide (AuO) and/or by adsorption of reaction products. The anodic process producing Peak e ceases completely at *ca.* 0.6 V shortly after the scan reversal at 0.8 V. However, when the oxide is cathodically dissolved (Peak c) during the negative scan, the anodic process forming formamidine disulfide resumes and the net current swings briefly from cathodic to anodic at ca. 0.1 V. Whereas the formation of surface oxide at E > 0.2 V is believed to be an essential component of the anodic mechanism producing Peak e, the generation of a high surface coverage of the oxide at E >> 0.2 V is concluded to be the primary cause of the attenuation observed for the anodic process.

Cathodic Peaks f are observed at E < -0.9 V on the negative scan only following oxidation of thiourea in the voltammetric region of Peak e. Separate experiments in 0.1 M NaOH containing SO_4^{2-} confirmed our suspicion that sulfate is not electroactive. Hence, although the production of sulfate is confirmed for the voltammetric oxidation of thiourea, Peaks f definitely are not the result of SO_4^{2-} reduction. Instead, we conclude that Peaks f correspond to the cathodic desorption of a product of incomplete oxidation of thiourea produced simultaneously with sulfate at E > 0.2 V. The existence of cathodic peaks corresponding to our Peaks f was not

shown in previous electrochemical studies of thiourea at Au [13-15], although the existence of a cathodic process was mentioned as being the result of an adsorbed thiourea product [16]. A very similar cathodic process was reported for thiourea at Pd electrodes and was attributed to the reduction of elemental sulfur generated by anodic decomposition of thiourea [17]. Elemental sulfur is known to be liberated from formamidine disulfide at high pH [18]. Furthermore, results obtained at Pt and glassy carbon electrodes led to speculations that elemental sulfur can be released from by products of thiourea oxidation [18].

Voltammetric experiments for thiourea at concentrations $\geq$ 5 mM revealed that the surface activity of the Au RDE was severely diminished during sequential cyclic scans when the negative scan limit was set at a value $>$-0.8 V so that the process producing Peaks f did not occur. A bronze colored film was to develop on the electrode surface during many voltammetric scans which is evidence for the buildup of an extensive quantity of a strongly adsorbed substance. Conversely, when the negative scan limit was set at -1.4 V, so that Peaks f were obtained during each cyclic scan, a high level of electrode surface activity persisted and a constant value of peak height was observed for Peak e. Furthermore, no film was observed to be formed on the Au surface in these experiments, even for 10 mM thiourea.

Figure 3 shows the effects of electrode passivation from oxidation of thiourea. After fifty voltammetric cycles, using positive and negative scan limits of +0.80 V and -0.75 V, respectively, the current response for thiourea oxidation is observed to be decreased by almost 50% (see dashed line). The first negative scan to a new limit of

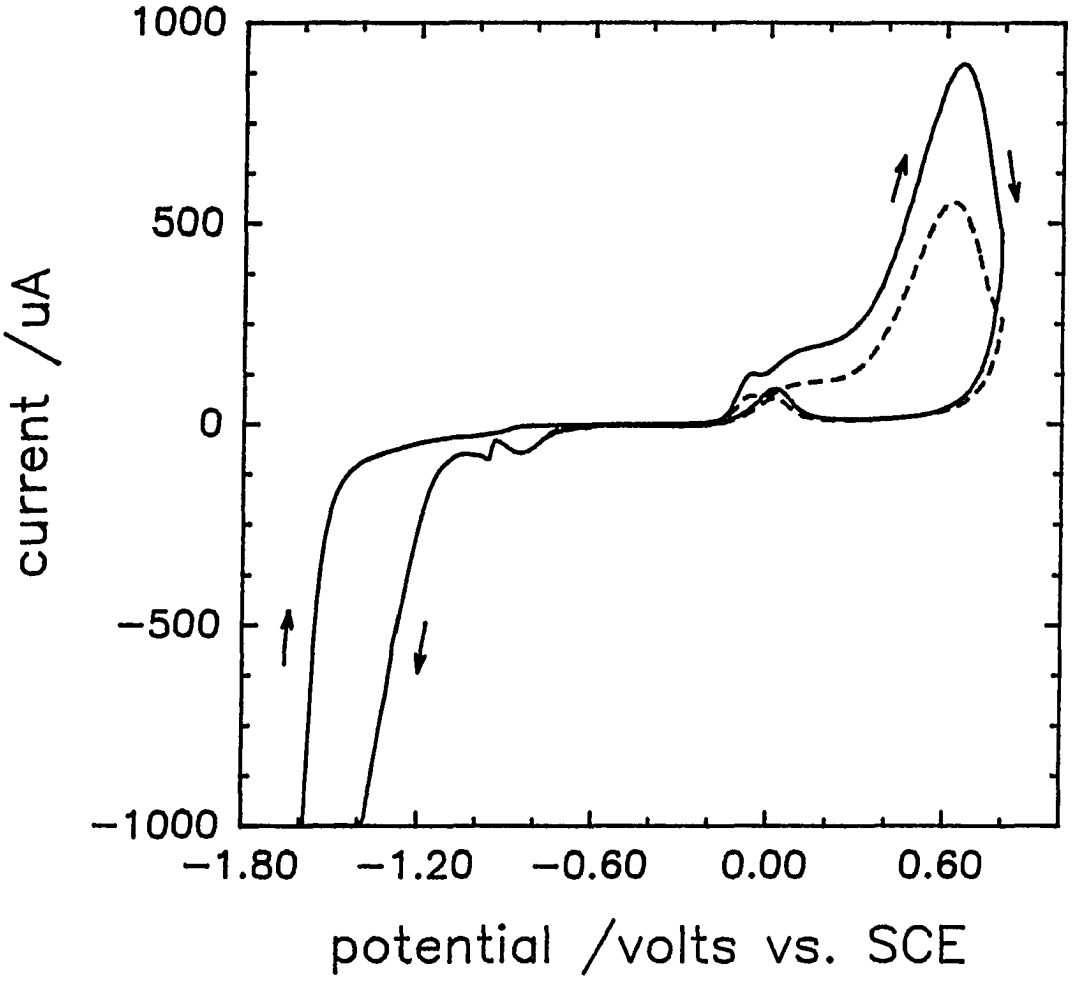

Figure 3. Voltammetric response for 20 mM thiourea as a function of negative scan limit at a gold RDE. Dashed line is for 20th cycle between -0.75 and 0.80 V. Solid line is 1st scan in negative direction to -1.60 V with subsequent positive scan to 0.80 V. Rotation speed: 1000 revolutions min^{-1}. Scan rate: 100 mV s^{-1}.

-1.6 V (solid line) produced a small peak at ca. -0.8 V which we tentatively attribute to the cathodic desorption of formamidine disulfide generated by the anodic process in the region -0.20 to +0.20 V. Continuation of the negative scan produced a very large cathodic response in the region -1.0 to -1.6 V which corresponds approximately to the region for Peaks f (see Figure 2). This is evidence for the buildup of a large quantity of adsorbate which undergoes cathodic desorption to produce the large signal for E < -1.0 V. The subsequent positive scan yields a substantially larger anodic response throughout the region -0.2 to 0.8 V (Peaks d & e) for oxidation of thiourea. Subsequent negative scans show the cathodic process at ca. -1.0 V to be virtually identical to Peaks f shown in Figure 2. Clearly, the cathodic process producing Peaks f is responsible for the significant increase in electrode activity observed in the region of Peaks d & e.

The surface activity of a severely fouled Au electrode can be restored by one of two procedures: (i) polishing with 0.05-μm alumina to mechanically remove the fouled surface layers of the electrode, or (ii) transfer to fresh electrolyte solution followed by multiple potential cycles between the limits for onset of cathodic and anodic evolution of H_2 and O_2, respectively. The voltammetric renewal of activity for severely fouled electrodes can require many cycles of potential (> 100) and the time required can be decreased by application of a PAD waveform. Voltammetric evidence indicating a fouled condition of the Au electrode is the observation in fresh electrolyte solution that the anodic current at E > 0.2 V (positive scan) and the cathodic current at E < -0.9 V (negative scan) are larger than is characteristic for the residual response of a

mechanically polished electrode. To illustrate, i-E curves are shown in Figure 4 for a polished electrode (dashed line) and a previously fouled electrode (solid line) after 150 cycles in 0.1 M NaOH between the limits -1.4 and +0.7 V. Clearly, for optimal PAD performance, it is essential that cathodic reactivation of the Au electrode occur at a potential < *ca.* -1.2 V to eliminate surface fouling.

Pulsed voltammetric response for thiourea. An important consideration in the optimization of PAD waveforms for thiourea is the choice of detection potential corresponding to the peak anodic response (E_p) in the region of Peak e. For concentrations ≤ 0.2 mM, E_p is constant at *ca.* 0.45 V; however, with the increase of concentration in the range 0.5 to 2 mM, E_p is observed to increase as shown in Figure 5. Factors causing this negative shift of E_p with increasing thiourea concentration, in seemingly decreasing order of probability, are as follows: (i) inhibition of surface-oxide formation caused by adsorbed thiourea, (ii) surface fouling by adsorbed oxidation products, and (iii) change in oxidation mechanism. Values of E_p are constant at 0.65 V for concentrations in the range 5 to 10 mM.

It can be expected that values of E_p obtained by cyclic voltammetry do not accurately predict peak PAD response. Therefore, the pulsed voltammetric response of thiourea was obtained using a PAD waveform in which the detection potential was scanned across the region of anodic response. In the three-step waveform, oxidative cleaning was at E_2 = 0.80 V (t_2 = 60 ms) and cathodic reactivation was at E_3 = -1.30 V (t_3 = 300 ms). This value of E_3 is sufficiently negative of the potential region for

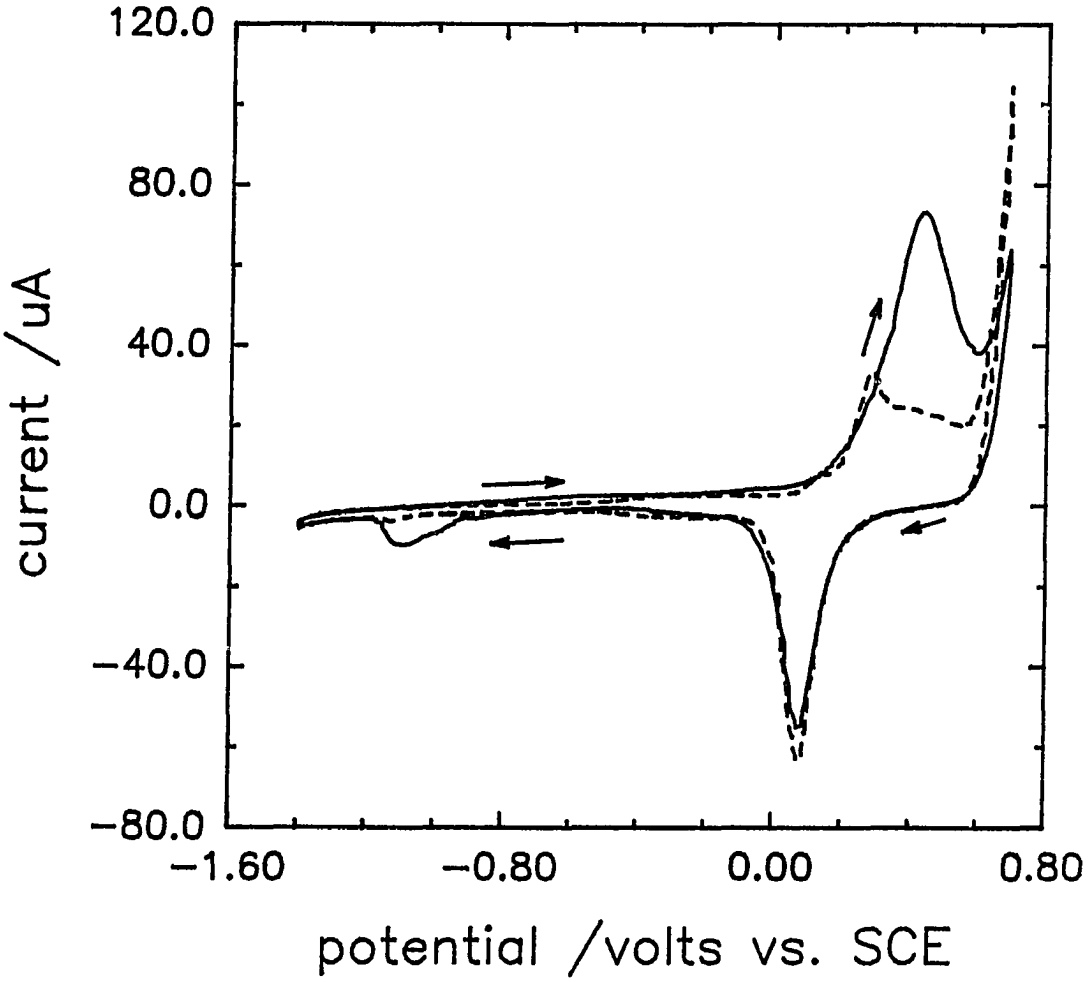

Figure 4. Voltammetric response of a fouled gold RDE in fresh 0.1 M NaOH (solid line). Residual for a clean gold RDE (dashed line). Rotation speed: 1000 revolutions min^{-1}. Scan rate: 100 mV s^{-1}.

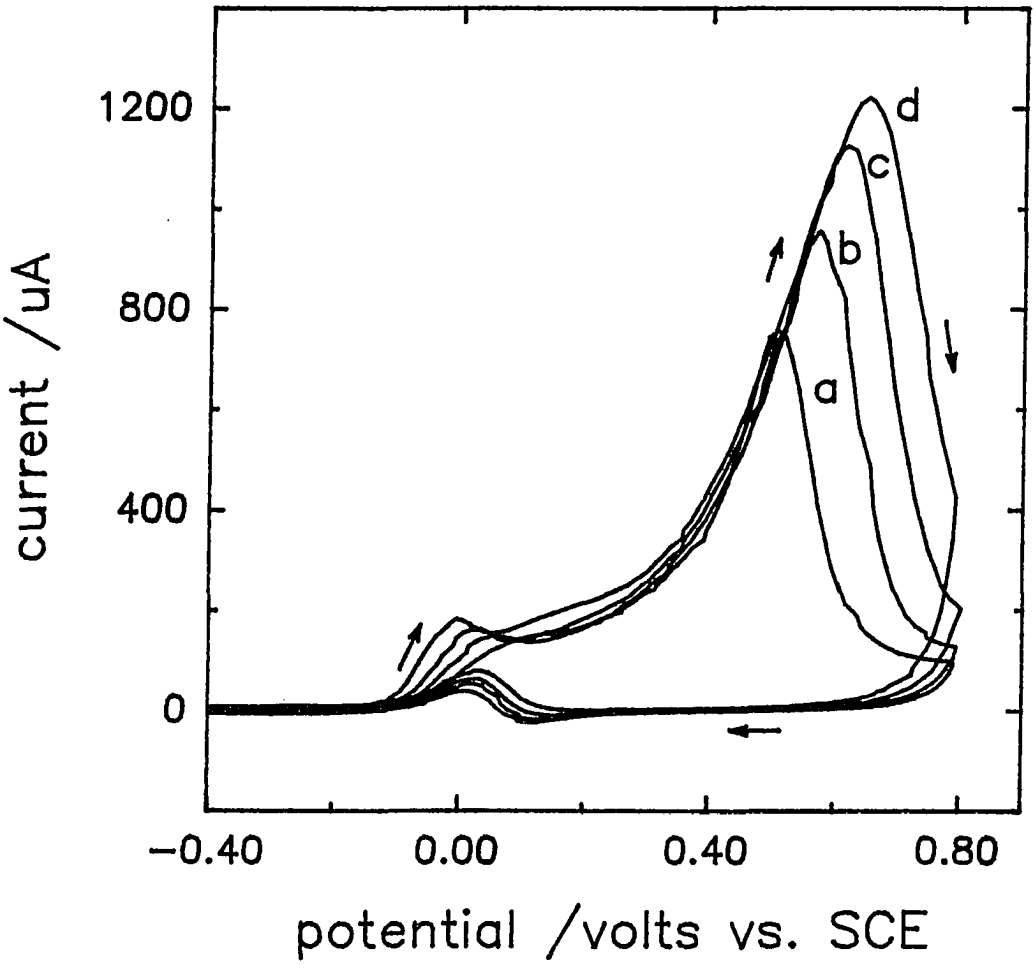

Figure 5. Voltammetric response of gold RDE in 0.1 M NaOH as function of thiourea concentration. Rotation speed: 1000 revolutions min^{-1}. Scan rate: 100 mV s^{-1}. Concentration (mM): (a) 0.5, (b) 1.0, (c) 2.0, (d) 5.0.

Peaks f (see Figure 2) so the Au electrode remains in a uniformly high state of surface activity. The detection potential (E_1, t_1 = 540 ms) was scanned in a positive direction starting from -0.40 V with potential increments (ΔE_1) of 20 mV. Following a 300-ms delay period (t_d) after each step of E_1, the anodic current was sampled during a period (t_s) of 1 ms.

The pulsed voltammetric response for thiourea is shown in Figure 6 as a function of concentration in the range 0.5 to 5.0 mM. These results are similar to those obtained by cyclic voltammetry in the tendency for a peaked anodic response. However, the values of peak potential (E_p) obtained by pulsed voltammetry are significantly different than those obtained by cyclic voltammetry. For example, for 0.5 mM thiourea, E_p is 0.40 V for pulse voltammetry and 0.50 V for cyclic voltammetry.

It is believed for E_3 = -1.30 V that adsorption of thiourea is minimized prior to application of the detection potential (E_1) in the PAD waveform. Hence, the tendency for preadsorbed thiourea to inhibit oxide formation at E_1 is also minimized. This expectation is in agreement with the observation that E_p values for pulsed voltammetry remained constant for concentration values up to *ca.* 2 mM, whereas for cyclic voltammetry, E_p began to shift to more positive values for concentrations above *ca.* 0.2 mM.

There remains the possibility for very large thiourea concentrations that some adsorption might occur shortly after initiation of the potential step from E_3 to E_1 and prior to oxide formation with the result that E_p is shifted. Results of a recent kinetic study of oxide formation at Au electrodes in 0.1 M NaOH indicate that an induction

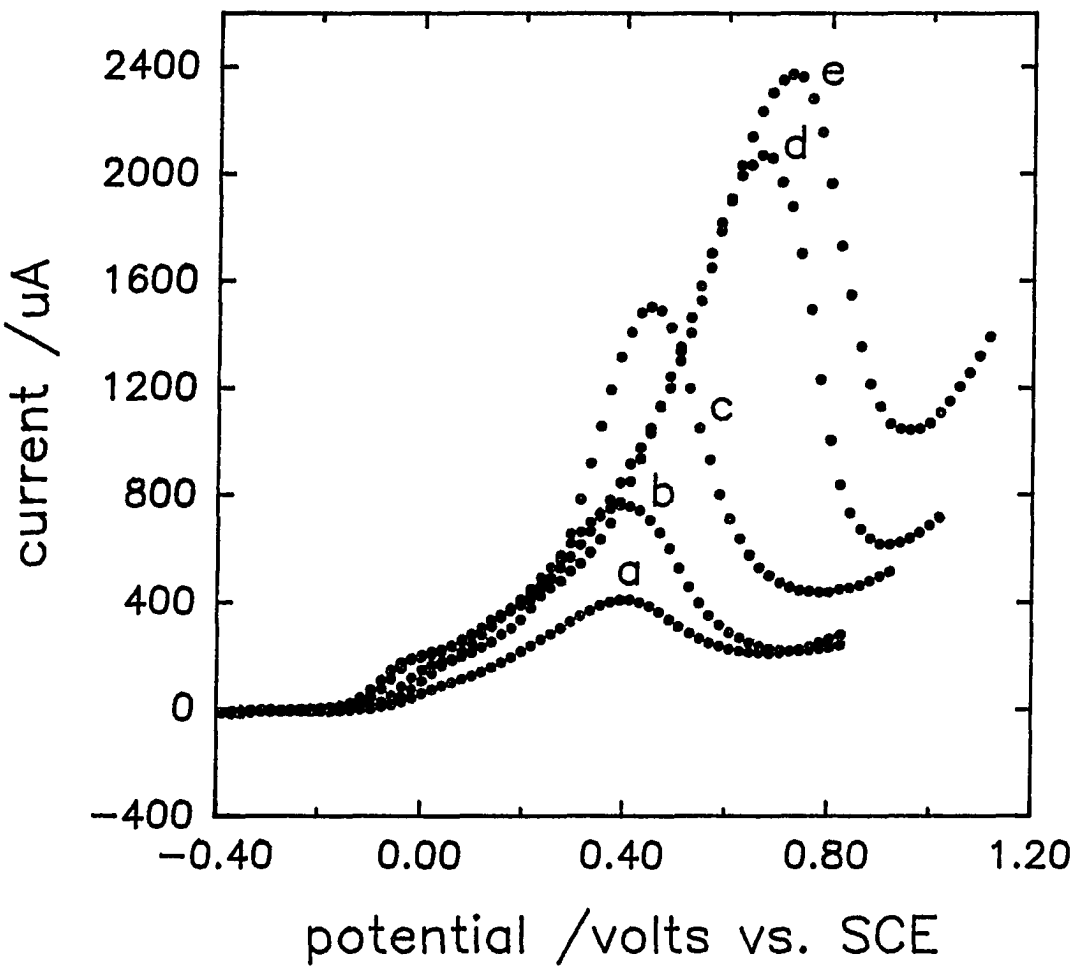

Figure 6. Pulsed voltammetric response of the thiourea at the gold RDE in 0.1 M NaOH as a function of concentration. PAD waveform: E_1 = varied, t_1 = 540 ms, t_d = 300 ms; E_2 = 0.80 V, t_2 = 60 ms; E_3 = -1.30 V, t_3 = 300 ms. Concentration (mM): (a) 0.5, (b) 1.0, (c) 2.0, (d) 5.0.

period of *ca.* 3 ms exists for oxide formation following the positive potential step [20]. Furthermore, these results indicate that the equilibrium oxide coverages are virtually achieved within *ca.* 20 ms, even though a small anodic current persists for up to 1000 ms beyond the potential step. Integration of the flux for 10 mM thiourea at a RDE rotated at 1000 rev min^{-1} indicates that 10% of a monolayer of adsorbed thiourea (*ca.* $1x10^{-9}$ mol cm^{-2}) can be achieved in *ca.* 3 ms. Hence, we attribute the positive shift of E_p observed for large thiourea concentrations to the inhibition of oxide formation resulting from a small amount of thiourea adsorbed during the induction period for oxide formation.

Flow injection with pulsed amperometric detection (FI-PAD). A three-step PAD waveform was chosen with E_1 = 0.50 V and variable t_1. Use of small t_1 values offers the benefit of large anodic response with the disadvantage of large background currents due to anodic formation of surface oxide [1]. Use of large t_1 values offers the benefit of small background currents but the disadvantage of decreased anodic response due to loss of surface activity from formation of inert oxide and/or adsorbed oxidation products. The optimum value of t_1 is chosen ultimately as a compromise between the desire to diminish background current, and its associated noise, and the need to minimize surface fouling. Results are shown here for t_1 = 300 and 500 ms. Of greater importance for thiourea is the need to maintain a reductive pulse (E_3) at a sufficiently negative value to achieve the cathodic process (Peaks f in Figure 2) of desorption of the adsorbed product of partial thiourea oxidation.

Calibration data were obtained by FI-PAD for concentrations of thiourea in the range $1x10^{-6}$ to $1x10^{-2}$ M. Representative detection peaks are shown in Figure 7. Linear regression analysis of the data indicated two distinct regions of linear response and the corresponding regression statistics are given in Table 1. For concentrations in the range 10^{-6} to 10^{-5} M (Region 1), the sensitivities are very similar for the two t_1 values. However, for the range 10^{-5} to 10^{-3} M (Region 2), the sensitivities differ and the waveform for t_1 = 300 ms exhibits a sensitivity > 30 % larger than for t_1 = 540 ms. Significant deviation from linear response was observed for concentrations above $2x10^{-3}$ M regardless of the t_1 value. It is likely that this deviation is the consequence of the shift in the potential of peak response (E_p) to values positive of the detection potential (E_1) chosen for the PAD waveform.

Table 1. Linear regression statistics for FI-PAD response as a function of thiourea concentration in 0.1 M NaOH (Conditions: flow-rate, 0.8 ml min^{-1}. PAD waveform: E_1 = 0.50 V, t_1 = variable; E_2 = 0.80 V, t_2 = 60 ms; E_3 = -1.30 V, t_3 = 300 ms)

Region	t_1 (ms)	Range (M)	Slope (10^3 μA M^{-1})[a]	Intercept (μA)[a]	*r*	*n*
1	300	10^{-6} - 10^{-5}	62.1 (±1.4)	-0.05 (±0.02)	0.9992	12
1	540	10^{-6} - 10^{-5}	62.5 (±2.6)	-0.03 (±0.02)	0.9973	12
2	300	10^{-5} - 10^{-3}	40.4 (±0.7)	1.24 (±0.35)	0.9991	18
2	540	10^{-5} - 10^{-3}	28.8 (±0.4)	0.96 (±0.19)	0.9995	18

[a] Uncertainty represents ±90% confidence interval.

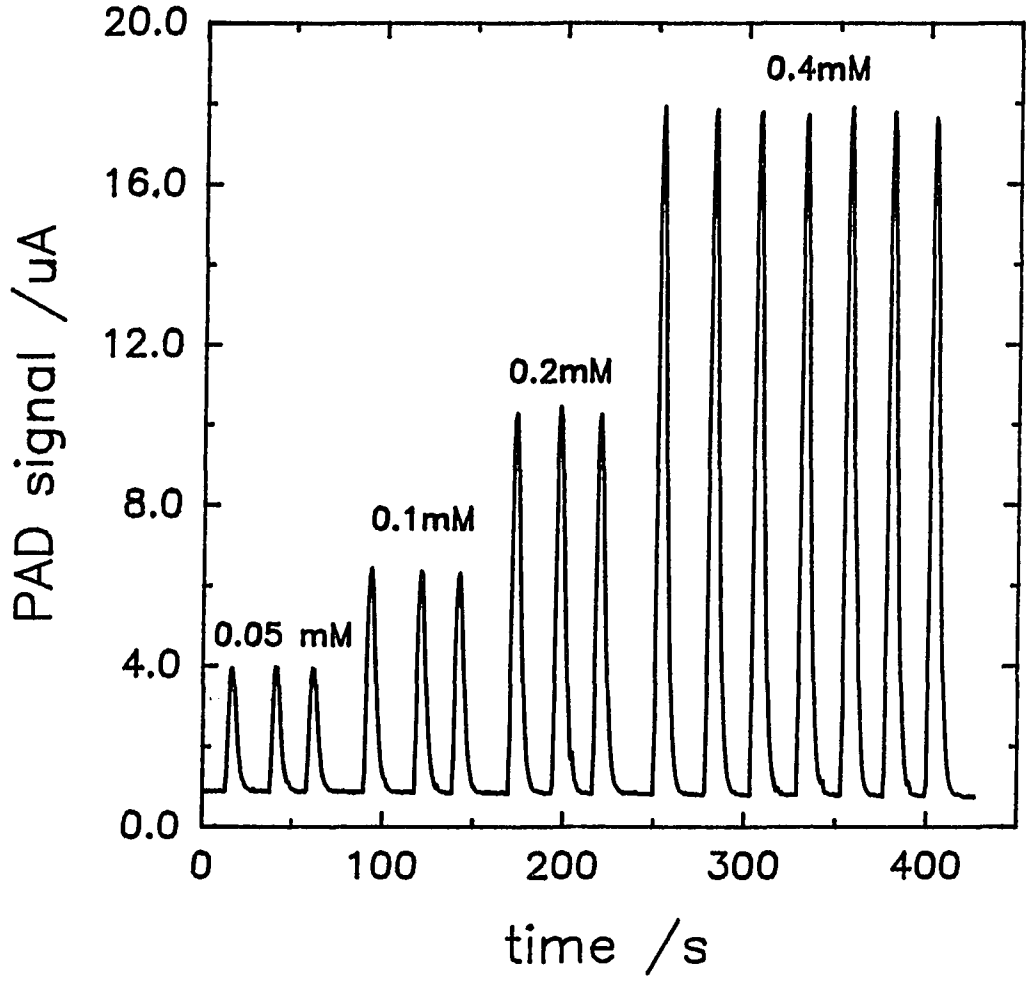

Figure 7. Representative FI-PAD peaks for thiourea in 0.1 M NaOH. Flow-rate: 0.8 ml min^{-1}. Concentration (mM): shown in figure. PAD waveform: E_1 = 0.50 V, t_1 = 300 ms; E_2 = 0.80 V, t_2 = 60 ms; E_3 = -1.30 V, t_3 = 300 ms.

The calibration data are summarized graphically in Figure 8 by log-log plots of the normalized peak signal (I_p) vs. the analytical concentration (C). Values of I_p were calculated according to eqn. 7 [21] where i_p is the observed peak current, and *a* and *b* are the intercept and slope, respectively, obtained by linear regression analysis in the two concentration regions.

$$I_p = [i_p - a]/bC \qquad (7)$$

The benefit of plotting calibration data in this manner is that the graphical representation of relative uncertainty is independent of concentration [21]. The dashed lines in Figure 8 indicate relative uncertainties of $\pm$10% and $\pm$30%. The two regions indicated in Figure 8 correspond to the two separate regression ranges indicated in Table 1. Based on these results for Range 1, the detection limits (S/N = 3) for a50-μL injection of thiourea are 4.9 ng (65 pmol) and 2.4 ng (32 pmol) for t_l = 300 and 540 ms, respectively.

There is reason to suspect that the observation of two linear regions for thiourea response might be indicative of a change in the detection mechanism for thiourea as concentration increases. For example, at low concentrations, the oxide-catalyzed oxidation of thiourea to sulfate (Eq. 6) is likely to occur with higher efficiency, corresponding to a larger number of transferred electrons. Furthermore, the difference in sensitivity as a result of change in t_l might be due to the electrode being more able to efficiently oxidize the thiourea at shorter times. This would support the idea that fouling occurs more readily from incomplete oxidation of adsorbed thiourea at large

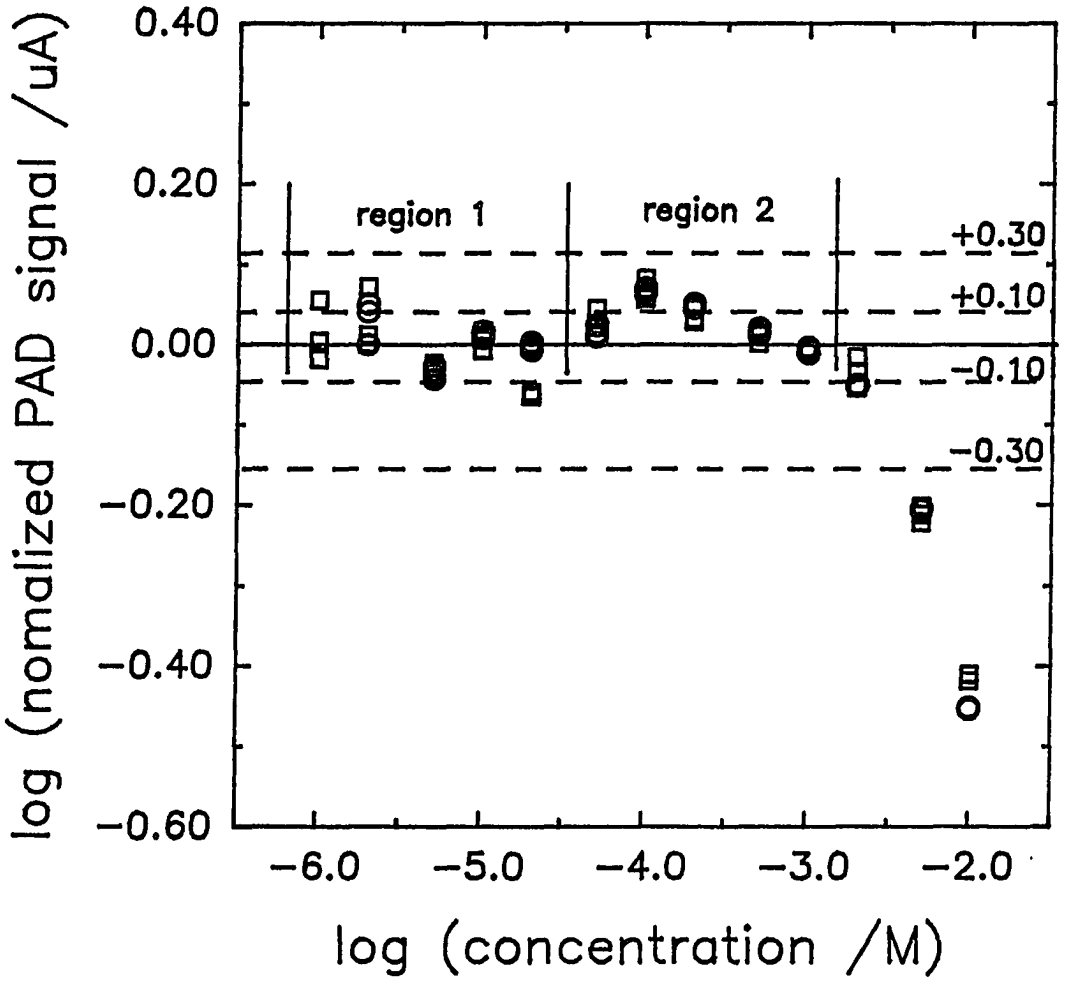

Figure 8. Calibration curve for thiourea in 0.1 M NaOH by FI-PAD. The two regions represent the linear segments specified in Table 1. Flow-rate: 0.8 ml min^{-1}. PAD waveform: E_1 = 0.50 V, t_1 = 300 (○), 500 (□) ms; E_2 = 80 V, t_2 = 60 ms; E_3 = -1.30 V, t_3 = 300 ms.

concentration.

The shapes of FI-PAD peaks are observed to be influenced by choice of t_1 and E_1, as is illustrated in Figure 9 & 10. The peaks in Figure 9, obtained for t_1 = 540 ms with a 50-μL injection of 10 mM thiourea, exhibit a significant loss of sensitivity with decreases in E_1 from 0.70 to 0.30 V (Peaks e to a), with concomitant peak broadening. In contrast, peaks in Figure 10, obtained for t_1 = 180 ms, do not exhibit significant broadening for the same decrease in E_1 values. The shape of FI-PAD peaks obtained for 50 mM $K_4Fe(CN)_6$, which is not complicated by oxide formation or electrode fouling, was virtually identical to that for Peak e in Figure 9. The distortion of peaks observed in Figure 9 for 10 mM thiourea was not observed for 1 mM thiourea using the same t_1 value.

The fact that the detection of organo-sulfur species is dependent on preadsorption at the electrode surface indicates that PAD signals should be enhanced by use of a preadsorption step. In addition, at high surface coverage, evidence of an adsorption isotherm should be seen. To test these possibilities, the three-step PAD waveform was applied with E_3 = -0.2 V to permit adsorption of thiourea prior to the detection step at E_1. The PAD response (i_p) is plotted in Figure 11 as a function of adsorption time ($t_{ads} = t_3$) for several thiourea concentrations. It was determined for concentrations $\leq$ 0.01 mM that increased values of t_{ads} had very little effect on the PAD response. This is probably an indication that the small quantity of thiourea adsorbed during t_{ads} was quickly and efficiently oxidized during the delay period (t_d) prior to current sampling at E_1. For 0.1 mM thiourea, the increase in PAD response

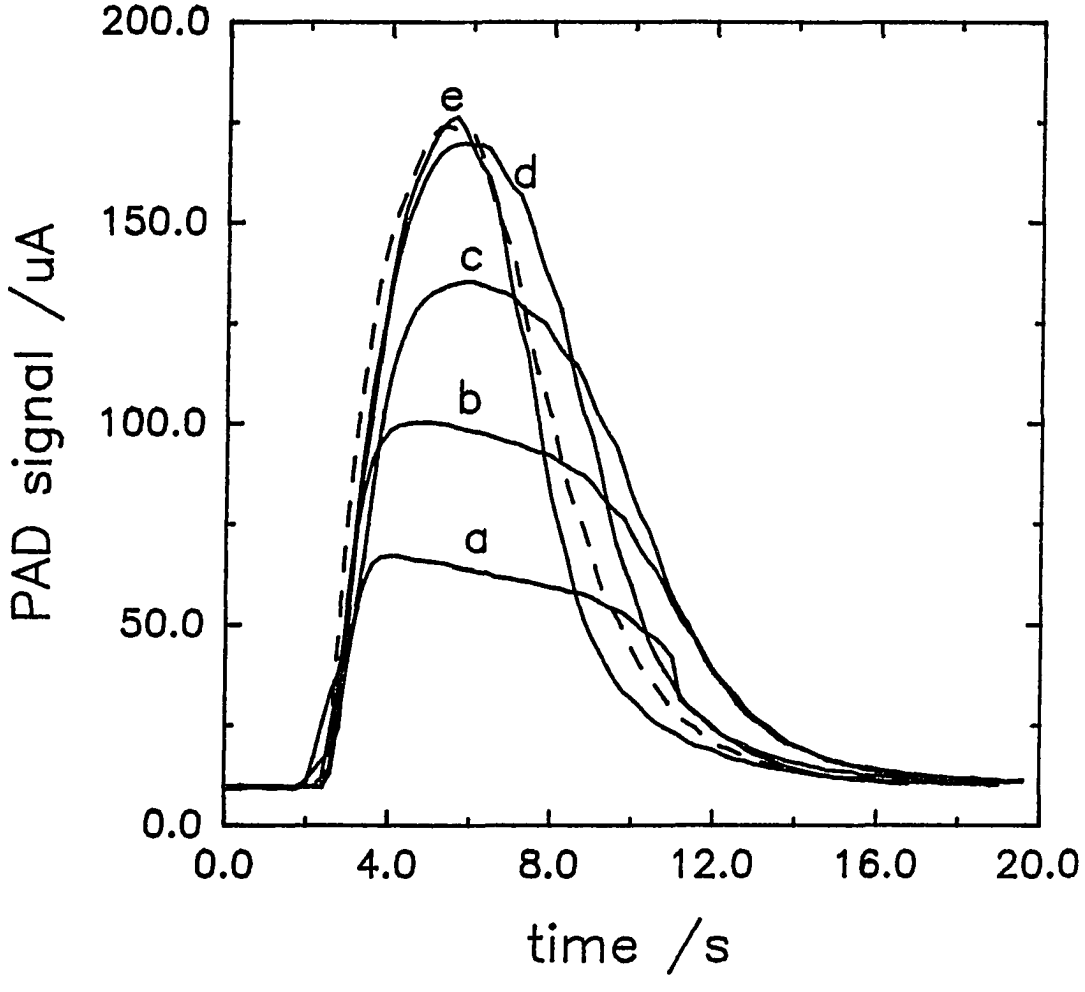

Figure 9. Effect of detection potential (E_1) on peak shape for 10 mM thiourea in 0.10 M NaOH using t_1 = 540 ms. The dashed line is 50 mM $K_4Fe(CN)_6$ as a reference for an ideal peak. Flow-rate: 0.8ml min^{-1}. PAD waveform: E_1 = (variable), t_1 = 540 ms; E_2 = 0.80 V, t_2 = 60 ms; E_3 = -1.30 V, t_3 = 300 ms. E_1 (V) : (a) 0.30, (b).40, (c) 0.50, (d) 0.60, (e) 0.70.

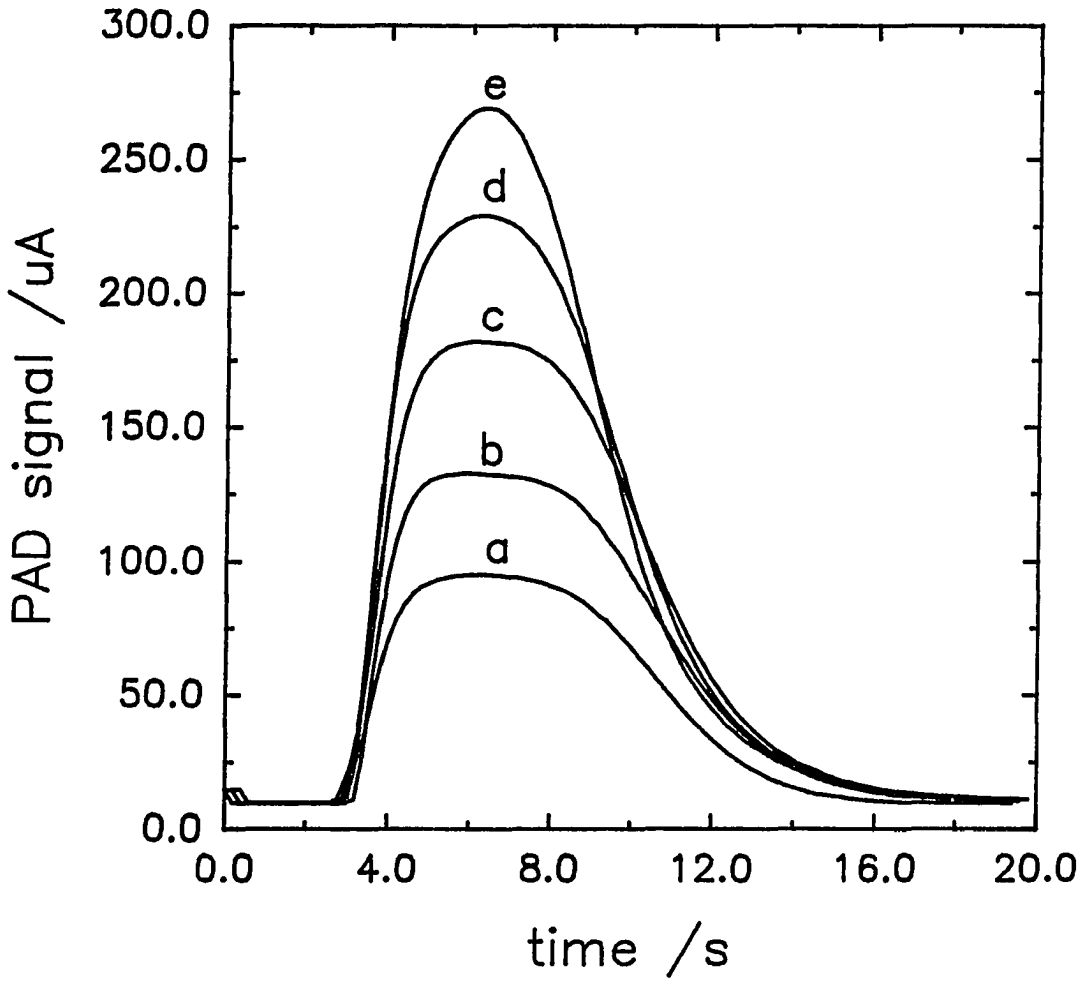

Figure 10. Effect of detection potential (E_1) on FI-PAD peaks for 10 mM thiourea in 0.1 M NaOH. Flow-rate: 0.8 ml min^{-1}. PAD waveform: E_1 = (variable), t_1 = 180 ms: E_2 = 0.80 V, t_2 = 60 ms: E_3 = -1.30 V, t_3 = 300 ms. E_1 (V): (a) 0.30, (b) 0.40, (c) 0.50, (d) 0.60, (e) 0.70.

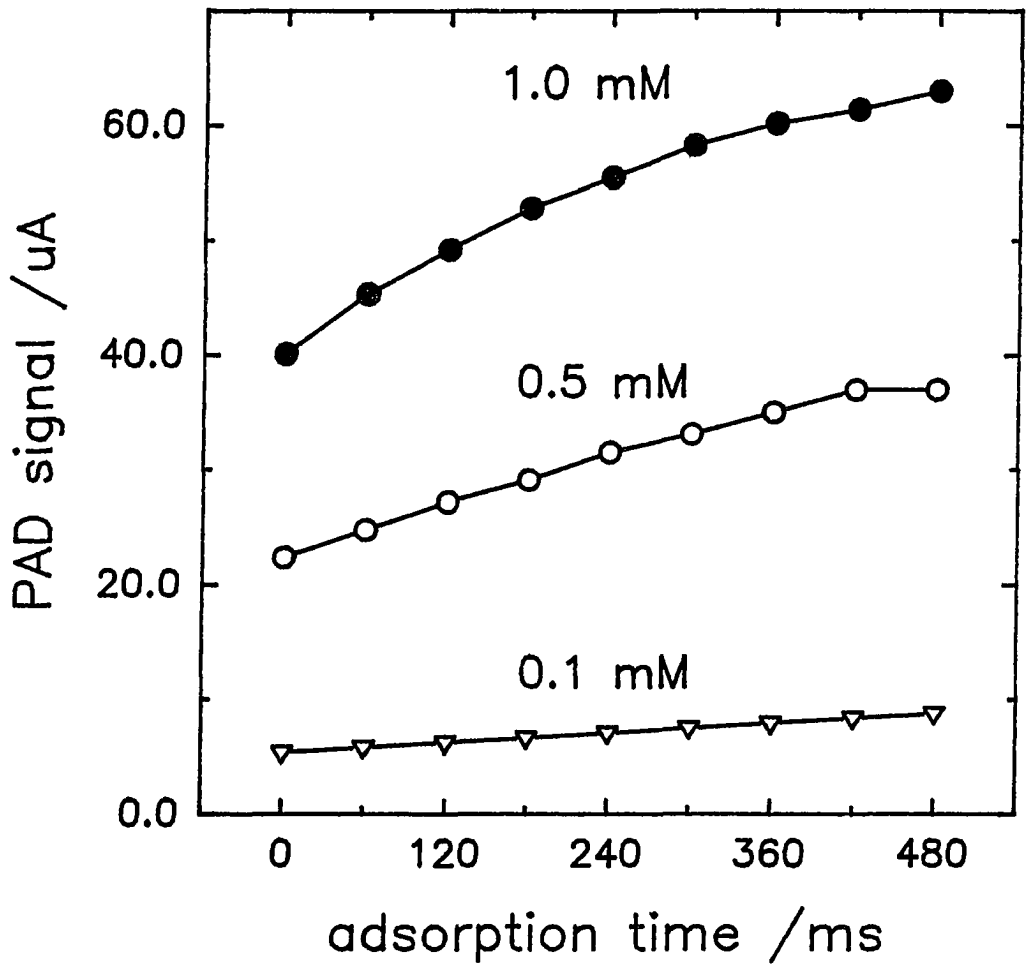

Figure 11. Plot of FI-PAD peak response as a function of adsorption time for thiourea in 0.1 M NaOH. Flow-rate: 0.8 ml min^{-1}. PAD waveform: E_1 = 0.50 V, t_1 = 300 ms; E_2 = -1.30 V, t_2 = 300 ms; E_3 = -0.20 V, t_3 = t_{ads} = variable.

with increasing t_{ads} appears nearly linear which is an indication that a minimal fraction of surface area is covered by adsorbed thiourea. For 0.5 and 1 mM, curvature is seen in the i_p-t_{ads} plots, indicating that maximum surface coverage is being approached for large t_{ads}.

It should be noted for each concentration represented in Figure 11, the majority of the PAD response is under mass-transport control, as indicated by the response for $t_{ads} = 0$. Pre-adsorption effects, as determined from i_p-t_{ads} plots were almost identical for $E_3 = -0.75$ and -0.20 V. In sharp contrast, there was no indication of pre-adsorption for $E_3 = -1.30$ V.

Analysis of Adsorbed Oxidation Products. The Au RDE was extensively fouled, according to the conditions described in Figure 3 for 20 mM thiourea, and aportion of the resulting bronze-colored film was removed for analysis by gentle wiping with a clean Kimwipe^R tissue (Kimberly-Clark). The film could not be removed from the Au surface by a strong stream of H_2O; however, the majority of the film was easily removed by wiping with the tissue, leaving the Au surface with only a slightly tarnished appearance. The Au wire electrode in the flow cell was fouled by making several 1.4-mL injections of 10 mM thiourea while applying a PAD waveform for which $E_3 = -0.75$ V. The exposed wire surface turned the characteristic bronze color and the end was cut off with a razor for analysis.

Elemental analysis of the film from the RDE surface was performed using Scanning Electron Microscopy (SEM) with detection by Energy Dispersive

Spectroscopy (EDS). The analysis showed the film to consist of sulfur and gold in an atomic ratio of *ca.* 5:1. This quantity of Au is significantly larger than would be obtained by the same gentle rubbing of a clean Au surface with the tissue. Carbon and nitrogen were not detected and, therefore, thiourea and formamidine disulfide are not present in the films at detectable levels. The SEM-EDS indicated the absence of oxygen from the film and we conclude that sulfate is not present. It was not possible to determine if the film represented a discreet compound of gold and sulfur; however, we note that the color of the film (bronze) is inconsistent with the colors of common gold sulfides (AuS and Au_2S_3, brown-black). The SEM-EDS results for the fouled Au-wire electrode were consistent with these conclusions.

CONCLUSIONS

The SEM-XDS results are interpreted to indicate that the bronze-colored films from the fouled electrodes contain elemental S and Au. This conclusion is in agreement with previous conjecture that thiourea is anodically decomposed to yield atomic S at Pd [17] and Pt [19] electrodes. The detailed mechanism for production of the atomic S is not yet fully understood.

We speculate that adsorbed atomic S becomes physically incorporated within multi-layered oxide films produced on the Au surface at $E > 0.2$ V. Subsequently, during cathodic reduction of the oxide film, the atomic S interferes with surface migration of Au atoms, thereby interfering with the restructuring of the Au surface with the result that a thin film is generated which is composed of dispersed atomic S and Au. A thick surface film containing S and Au is the result of many consecutive cycles of oxide formation and dissolution. This thick film has the effect of physically blocking access by thiourea to the conductive Au substrate and the electrode is described as "fouled". The thick film is not an electronic insulator, however, as is indicated by only a slight decrease in the area of the cathodic peak for oxide reduction (Peak c in Figure 2) observed for an extensively fouled surface.

Cathodic desorption of very thin films of adsorbed atomic S, perhaps as S^{2-} in alkaline media, is achieved very efficiently by the process producing Peaks f at $E < -0.9$ V (see Figure 2). Conversely, cathodic reactivation of an extensively fouled surface bearing a thick film of dispersed atomic S and Au is not very efficient, and

mechanical polishing is prescribed in such cases. Hence, to prevent loss of electrode activity during pulsed amperometric detection (PAD) of thiourea, it is essential that the PAD waveform include a cathodic reactivation step to a potential $E_3 < -1.0$ V to achieve cathodic desorption of any adsorbed atomic S generated during the detection process at E_1.

ACKNOWLEDGMENTS

The authors are grateful to Marc D. Porter, Brian Lamp and William R. LaCourse for helpful discussions of the data. This work was supported by the National Science Foundation under contract CHE-8914700.

REFERENCES

1. D.C. Johnson and W.R. LaCourse, Anal. Chem., 62 (1990) 589A.

2. W.R. LaCourse and D.C. Johnson, in C.A. Marsden (Ed.) "Electrochemical Detection and Liquid Chromatography in the Biosciences," Royal Society of Chemistry: London.

3. T.Z. Polta and D.C. Johnson, J. Electroanal. Chem., 209 (1986) 159.

4. T.Z. Polta, G.R. Luecke and D.C. Johnson, J. Electroanal. Chem., 209 (1986) 171.

5. T.Z. Polta and D.C. Johnson, Chromatogr. Forum, 1 (1986) 37.

6. A. Ngoviwatchai and D.C. Johnson, Anal. Chim. Acta, 215 (1988) 1.

7. D.C. Johnson and D.G. Williams, unpublished.

8. G.G. Neuburger and D.C. Johnson, Anal. Chem., 60 (1988) 2288.

9. National Research Council, Regulating Pesticides in Food, National Academy Press: Washington, D.C., (1987) 208.

10. U.S. Department of Health and Human Services, Fourth Annual Report on Carcinogens, GPO, Washington, DC (1985) 423.

11. T.Z. Polta, Ph.D. Dissertation, Iowa State University, Ames, IA, (1986).

12. D.C. Johnson, J.A. Polta, T.Z. Polta, G.G. Neuburger, J.L. Johnson, A.P-C. Tang, I-H. Yeo and J. Baur, J. Chem. Soc., Faraday Trans. 1, 82 (1986) 1081.

13. V.A. Zakharov, I.M. Bessarabova, O.A. Songina and M.A. Timoshkin, Elektrokhim., 7 (1971) 1215.

14. H. Wroblowa and M. Green, Electrochim. Acta, 8 (1963) 679.

15. R. Holze and S. Schomaker, Electrochim. Acta, 35 (1990) 613.

16. V.N. Andreev and V.E. Kazarinov, Elektrokhim., 10 (1974) 1736.

17. R.V. Bucur and P. Marginean, Electrochim. Acta, 29 (1984) 1297.

18. P.W. Preisler and L. Berger, J. Amer. Chem. Soc., 69 (1947) 322.

19. J. Kirchnerovà and W.C. Purdy, Anal. Chim. Acta, 123 (1981) 83.

20. R. Roberts and D.C. Johnson, Electroanalysis, in press.

21. D.C. Johnson, Anal. Chim. Acta, 204 (1988) 1.

PAPER 2.

A STUDY OF THE VOLTAMMETRIC RESPONSE OF THIOUREA AND ETHYLENETHIOUREA AT GOLD ELECTRODES IN ALKALINE MEDIA[2]

[2] Published in Vandeberg, P.J.; Johnson, D.C., *J. Electroanal. Chem.*, in press.

ABSTRACT

The voltammetric response of thiourea (TU) and ethylene thiourea (ETU) is influenced by strong adsorption of these sulfur-containing compounds. Interpretation of the current-potential curves obtained at a Au rotated disk electrode (RDE) is aided by the results of shielding and collection data obtained with a Au-Au rotated ring-disk electrode (RRDE). Pulsed amperometric detection (PAD) was applied at the ring of the RRDE to avoid loss of electrode response to TU and ETU that is observed for a constant (dc) applied potential. The largest response for both compounds is in the form of an anodic peak obtained for the positive potential scan in the region ca. +0.1 to +0.6 V vs. SCE for 0.10 M NaOH. This current peak is composed of contributions from the formation of surface oxide, oxidation of TU and ETU adsorbed in the potential region < 0.1 V, and oxidation of TU and ETU transported to the electrode simultaneously with the appearance of the anodic peak. The relative contributions of each component is dependent on the concentration of TU and ETU, the rotational velocity of the electrode, and the potential scan rate. Voltammetric data indicate ETU is adsorbed to a greater extent than TU and, furthermore, that adsorbed TU undergoes desulfurization with accumulation of adsorbed S^{o} in the region -0.6 to -0.1 V.

INTRODUCTION

Our laboratory has been very active in the development of so-called *pulsed electrochemical detection* (PED) at Au and Pt electrodes for application to liquid chromatography (LC). PED is based on multi-step *E-t* waveforms and has been demonstrated to be applicable for numerous polar aliphatic organic compounds including monosaccharides, disaccharides and oligosaccharides; alcohols, glycols and polyalcohols; and amines, alkanolamines and amino acids [1-3]. Efforts to extend the application of PED to various organic sulfur compounds have been challenging as a result of the strong adsorption of these compounds at the noble metal surfaces [4,5].

Investigation of the fundamental basis of response mechanisms in PED has consistently benefited from hydrodynamic voltammetry at rotated disk electrodes (RDEs). However, rotated ring-disk electrodes (RRDEs) until recently have not been successfully applied in these studies because of the rapid loss of activity of the ring electrode when operated at constant (dc) potentials in *collection* and *shielding* experiments. Loss of electrode activity is especially problematic for dc detection of sulfur compounds at noble metal electrodes because the anodic response requires generation of adsorbed hydroxyl radicals ($\cdot OH_{ads}$) during concomitant formation of surface oxides at the noble metal surfaces. Furthermore, the electrodes can become fouled by adsorbed atomic sulfur [5-7]. However, application of PED waveforms at the ring of RRDEs has been demonstrated recently to be successful for maintaining ring activity throughout *collection* and *shielding* experiments [8] and ring-disk techniques

are now considered useful even for sulfur compounds.

Here we report on voltammetric studies of thiourea (TU) and ethylene thiourea (ETU; 2-imidazolidinethione) at Au disk and Au-Au ring-disk electrodes. ETU has significance because it is a carcinogenic metabolite of ethylene bis-dithiocarbamate fungicides. Whereas voltammetric studies have been reported for TU at Au electrodes in acidic media [9-12], no studies have been reported for alkaline media, perhaps because of the severe fouling of electrode surfaces under these conditions. TU has been used frequently in our laboratory as a model compound to test the utility of PED for organic sulfur compounds because it has a low vapor pressure, is readily soluble in aqueous solvents, and does not produce the foul stench associated with many thiols and sulfides. Furthermore, TU and its derivatives are carcinogenic [13] and development of LC-PED technology for quantitative determinations of these compounds in complex samples can have great environmental benefit. TU undergoes a multi-electron oxidation at Au electrodes concomitantly with formation of the surface oxide [4-5]. An oxide-catalyzed anodic mechanism is generally characteristic of organic sulfur compounds on both Au and Pt electrodes [4]. Reports of voltammetric studies for imidazoladinethiones have been limited to Hg [14] and Pt [15].

EXPERIMENTAL

Reagents. Sodium hydroxide and TU were Analytical Reagent Grade from Fisher Scientific, and ETU was from ChemService. Other chemicals were Standards Grade (Fisher). All chemicals were used as received without further purification. Water was purified in a serial fashion by passage through ion-exchange cartridges from Culligan and a Milli-Q system from Millipore.

Voltammetry. A Au disk electrode (0.4762-cm o.d.) and Au-Au ring-disk electrode (disk: 0.4623-cm o.d.; ring: 0.4874-cm i.d., 0.5385-cm o.d.) were constructed by Pine Instrument Co. These electrodes were rotated in a MSR rotator with affiliated speed controller (Pine).

Potentiostatic control of the RDE, as well as the disk electrode of the RRDE, was achieved using the K-1 unit of a Model RDE-4 bipotentiostat (Pine). In ring-disk experiments, control of the ring under multistep potential-time (*E-t*) waveforms was achieved using a PAD-2 potentiostat (Dionex Corp.). A single saturated calomel electrode (SCE, Fisher Scientific) and Pt wire served as the potential reference and counter electrode, respectively, for both potentiostats. To prevent interference between the two potentiostatic systems, the PAD unit was operated with a floating ground. Furthermore, a 0.3-s RC filter was inserted between the SCE and the reference input of the bipotentiostat to match the filter in the PAD unit. Voltammetric data were recorded digitally by an IBM-compatible 386 PC using a DAS-1602 data acquisition board and Asyst 4.0 software from Keithley-Metrabyte-Asyst.

The electrochemical cell (200 mL) was constructed from Pyrex glass with two side arms (5 mL) joined to the cell via fritted glass disks (medium porosity) to accommodate the reference and counter electrodes.

Procedures. All data were obtained using 0.10 M NaOH as the supporting electrolyte. Stock solutions of all chemical reagents were made fresh each week and their purity was verified by LC-PAD and LC-UV analyses. Test solution were prepared just prior to use by dilution of the appropriate aliquots of stock solutions with 0.10 M NaOH. Dissolved O_2 was removed from test solutions by dispersion of N_2 (99.99%, Air Products) through a fritted glass disk (medium) and a N_2 atmosphere was maintained over the test solutions during experimentation. The disk and ring-disk electrodes were polished daily with 0.05-μm alumina on microcloth using water as the lubricant.

Values of n (eq mol^{-1}) for mass-transport controlled processes at the RDE were estimated on the basis of the Levich Equation for the transport-limited current (i_{lim}) [16]:

$$i_{lim} = 0.62nFAD^{2/3}\omega^{1/2}\nu^{-1/6}C^b \qquad (1)$$

In Eqn. 1, A is the electrode area (cm^2), D is the diffusion coefficient (cm^2 s^{-1}), ω (rad s^{-1}) is rotational velocity, ν is kinematic viscosity (cm^2 s^{-1}), F is the Faraday constant (96,485 coul eq^{-1}), and C^b is the bulk concentration (mol cm^{-3}).

RESULTS AND DISCUSSION

Thiourea.

Voltammetric response. The residual response obtained at the Au RDE in 0.1 M NaOH is shown Fig. 1 and is consistent with previous descriptions [17-22]. During the positive potential scan in the absence of dissolved O_2, charging of the double-layer region is the sole source of the small anodic current in the region ca. -1.2 to -0.6 V. The small anodic wave (**a**) in excess of the charging current in the region -0.4 to 0.1 V has been attributed to formation of a sub-monolayer of adsorbed hydroxyl species ($AuOH_{ads}$) [17,18]. More recently, this species has been described as a hydrous oxide (AuOH) [19-21]]. Whatever the exact chemical nature of this species, it is thought to have catalytic properties for oxidation reactions of various compounds including polyalcohols and carbohydrates [18-21] that involve transfer of oxygen from H_2O to the oxidation products. The larger anodic wave (**b**) for $E >$ ca. +0.2 V is the result of formation of surface oxide (AuO) and discharge of H_2O to produce O_2 (**c**) occurs at $E > 0.7$ V. The small unlabeled step just prior to wave **b** has been attributed to onset of oxide formation [21]. During the subsequent negative scan, cathodic dissolution of AuO produces a peak (**d**) in the region +0.2 to 0.0 V and, finally, cathodic discharge of H_2O generates H_2 at ca. -1.4 V (**e**). When present, dissolved O_2 produces a cathodic wave at $E <$ ca. -0.2 V.

The voltammetric response for TU is shown in Fig. 2 for three different concentrations. A complex set of anodic signals is obtained in the region -0.5 to

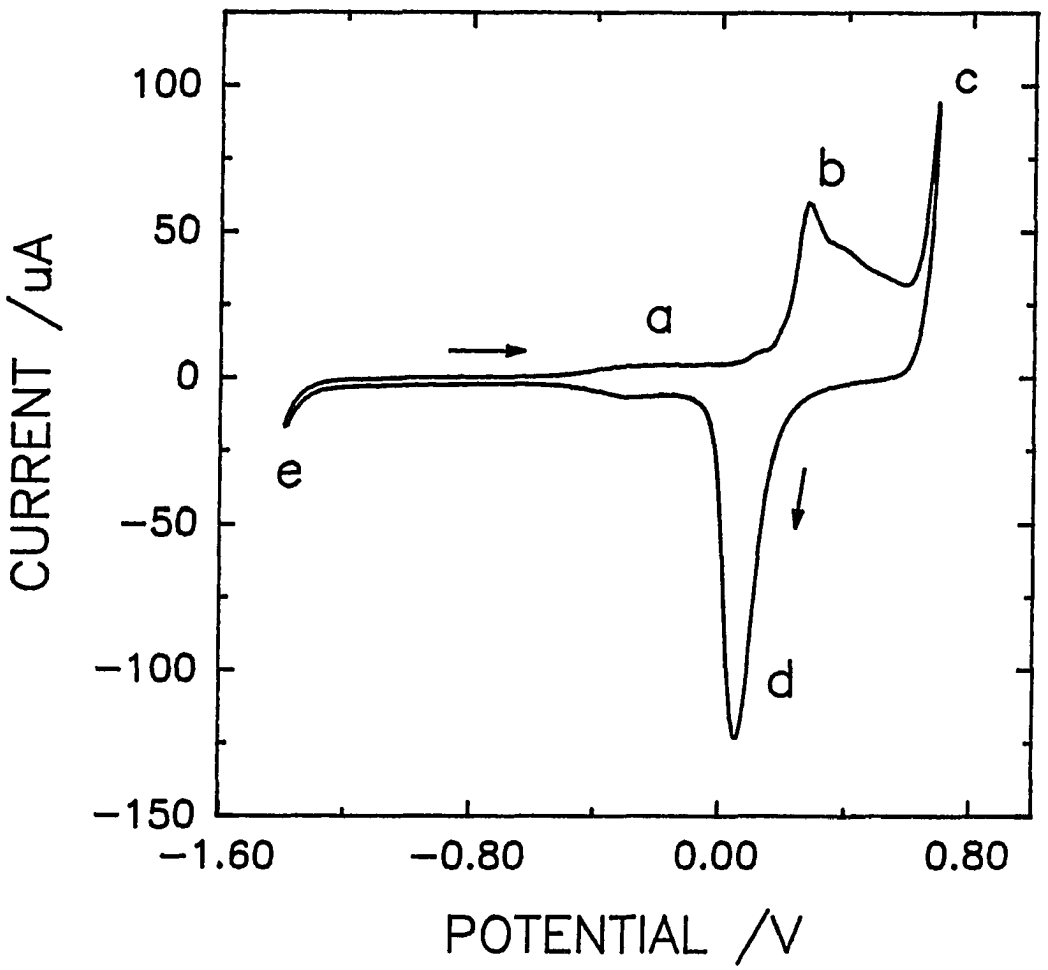

Figure 1. Residual voltammetric response at the Au RDE in 0.10 M NaOH. Rotational velocity: 104.7 rad s^{-1}. Scan rate: 100 mV s^{-1}.

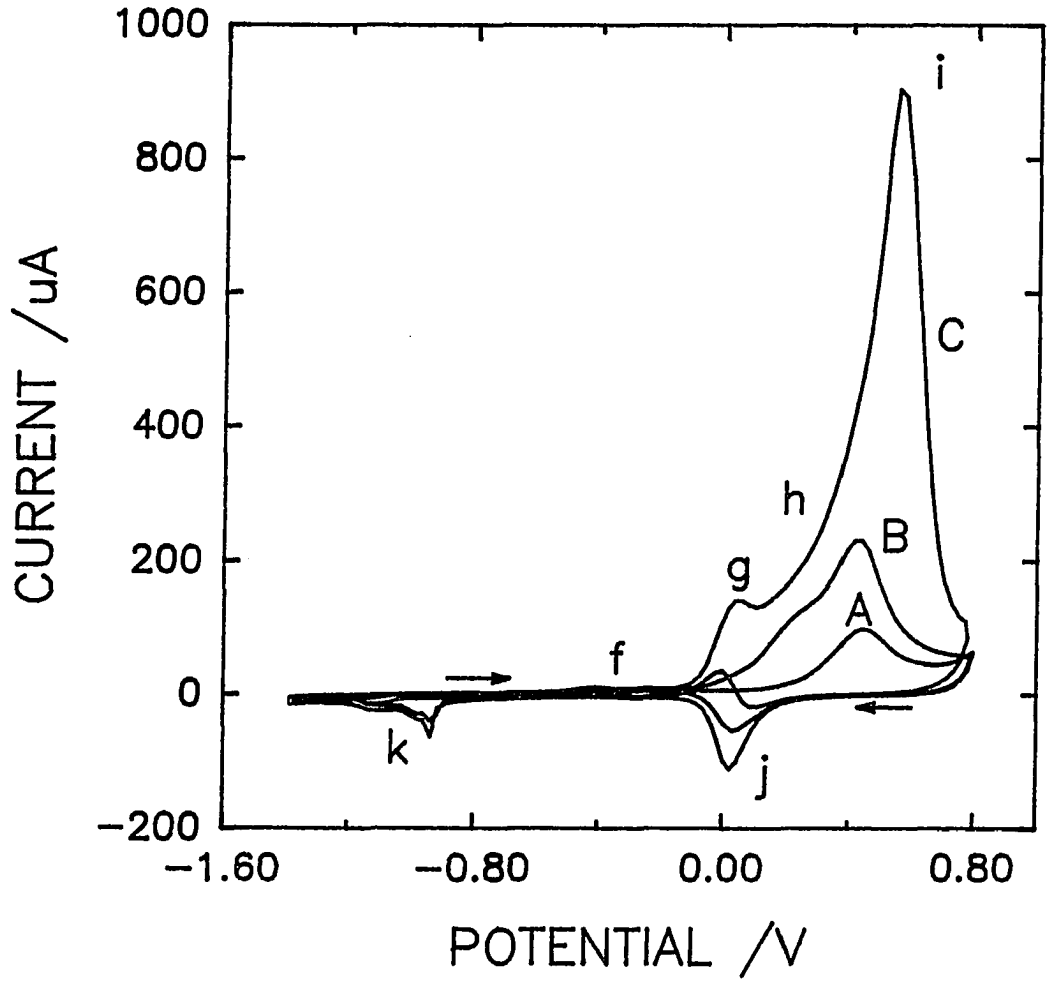

Figure 2. Voltammetric response for thiourea at the Au RDE as a function of concentration. Rotational velocity: 104.7 rad s^{-1}. Scan rate: 100 mV s^{-1}. Concentration (mM): (A) 0.01, (B) 0.1, (C) 1.0.

+0.8 V during the positive scan. The small anodic wave (f) in the region -0.5 to -0.1 V results from formation of the sub-monolayer of AuOH and corresponds to wave **a** in Figure 1. In acidic and neutral media, a wave corresponding to our peak **g** has been attributed to the one-electron oxidation of TU to the corresponding free-radical product with subsequent dimerization to form formamidine disulfide [12,23] according to:

$$2\ H_2NC(S)NH_2 \rightarrow HN{=}C(NH_2)S\text{-}SC{=}NH(NH_2) + 2e^- + 2H^+ \qquad (2)$$

The tentative conclusion that wave **g** in alkaline media might also correspond to formation of formamidine disulfide receives some support from the observations that this disulfide is unstable in alkaline media, with decomposition to produce atomic sulfur, and that Au electrodes have been observed to become fouled by atomic sulfur during voltammetric experiments in alkaline media containing TU at high concentrations [5]. However, as will be shown, wave **g** is observed to be under mass-transport control for low TU flux and surface control for high TU flux. Hence, it seems possible that the product of the reaction corresponding to wave **a** might be the adsorbed free-radical product of the one-electron oxidation of TU.

Wave **h** at ca. 0.2 V has been attributed to the oxidation of TU to sulfinic acid [9,23] according to:

$$H_2NC(S)NH_2 + 4OH^- \rightarrow H_2NC{=}NH(SO_2H) + 4e^- + 2H_2O \qquad (3)$$

Wave **h** occurs in the potential region where a small step is observed in the Au residual response just prior to oxide formation (wave **b** in Fig. 1) and, hence, is suspected to

becatalyzed by onset of AuO formation. Oxidation of amines also is observed to occur in this potential region [24]. Wave **h** is not well defined, appearing clearly only under conditions of intermediate TU flux, e.g., 0.1 mM concentration and 104.7 rad s^{-1} rotational velocity (curve **B** in Fig. 2). The large anodic peak (**i**) observed during the positive scan in the region ca. +0.3 to +0.7 V (Fig. 2) clearly dominates the voltammetric response for TU. This peak has been concluded to correspond primarily to the production of sulfate by oxidation of the sulfur in TU which has been previously adsorbed as well as that which is transported to the electrode surface simultaneously with the appearance of peak **i** [5]:

$$H_2NC(S)NH_2 + 10OH^- \rightarrow SO_4^{2-} + H_2NC(O)NH_2 + 8e^- + 5H_2O \qquad (4)$$

The oxidative detection of adsorbed and transported TU occurs simultaneously with formation of AuO and is concluded to occur by a catalytic mechanism in which oxygen from AuOH formed as an intermediate product in generation of AuO is transferred to the products of TU oxidation [4,5]. As formation of the oxide layer (AuO) nears completion (> +0.6 V), the rate of TU oxidation is severely attenuated resulting in the peak-shaped response. In very dilute solutions of TU (< ca. 0.1 mM), the peak potential (E_{peak}) is virtually unchanged with increases in concentration. However, for high TU concentrations of TU (> ca. 0.5 mM), which result in high surface coverage by the adsorbed sulfur-containing species, oxide formation is inhibited causing a positive shift in the potential for onset of AuO formation. Hence, there occurs a positive shift in E_{peak}, as is readily apparent by comparison of curves **B** and **C** (Fig. 2).

Following scan reversal at +0.8 V, the anodic response for TU quickly falls to zero because of the absence of further generation of AuOH and the inertness of the existent AuO film. The onset of cathodic dissolution of AuO at ca. 0.05 V (peak **d**, Fig. 1) allows the process generating wave **g** to recommence. Hence, because the net current during the negative scan in the region +0.1 to -0.1 V is the algebraic sum of the currents from cathodic dissolution of AuO and anodic oxidation of TU, peak **j** can appear as a simple cathodic peak or a combination cathodic-anodic peak, depending on the amount of oxide being reduced, the rate of potential scan (ϕ), and the flux of TU.

The final feature of note in Figure 2 is the set of cathodic peaks (**k**) obtained during the negative scan in the region ca. -0.9 to -1.2 V. We have previously reported on the basis of voltammetry and scanning electron microscopy with energy dispersive spectroscopy (SEM-EDS) that these peaks correspond to the cathodic desorption of adsorbed S° generated by incomplete oxidation of adsorbed TU [5]. Peaks **k** are strikingly similar to those observed in sodium sulfide solutions [25-27], and might have contributions from adsorbed polysulfides (S_x^{2-}).

Variation of rotation speed. The voltammetric response for 0.1 M TU at the Au RDE is shown in Fig. 3 for three values of rotational velocity (ω, rad s^{-1}). Wave **f** has virtually no dependency on ω, which is indicative of a surface-controlled faradaic origin for these signals. Peaks **g** and **h** show a strong positive dependence on ω for 0.1 M TU. However, because these waves are poorly defined, it is difficult to estimate values of plateau currents for the purpose of testing adherence to the i-$\omega^{1/2}$

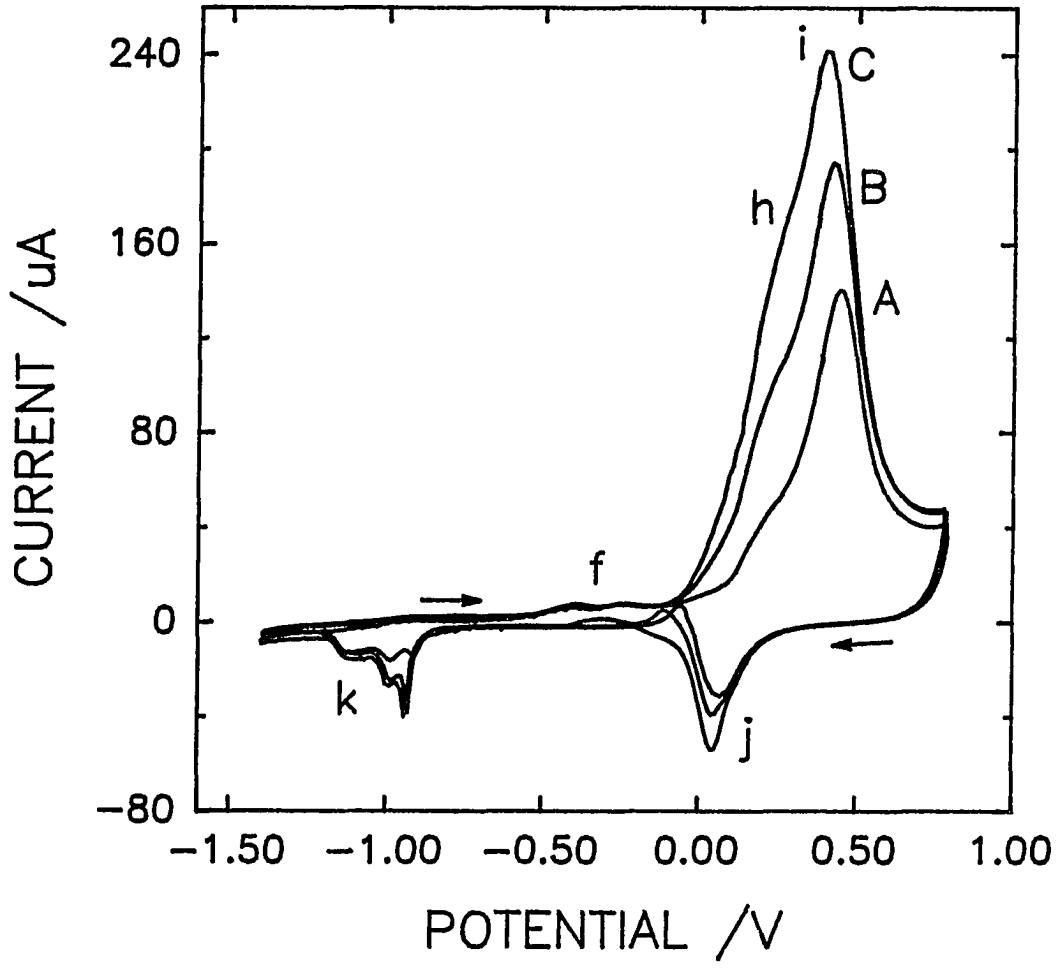

Figure 3. Voltammetric response for 0.10 mM thiourea at the Au RDE as a function of rotation speed. Conditions: 100 mV s^{-1} scan rate. Rotational velocity (rad s^{-1}): (A) 10.5, (B) 94.2, (C) 167.6.

relationship predicted by Equation (1). At higher TU concentrations (> 1 mM), dependence on ω is lost for peak **g**, and wave **h** becomes indistinguishable from peak **i**. Peak **i** exhibits a linear i-$\omega^{1/2}$ relationship at low TU concentrations (< 1 mM) with a large positive intercept. This behavior is indicative of mixed response involving transport- and surface-controlled faradaic processes. Peak **i** will be discussed later in more detail.

The dependence of peak **j** on ω during the negative scan is made complex because of the multiple processes occurring. To summarize: peak **j** becomes more anodic in appearance with increasing ω and reaches a maximum value for approximately the same flux at which the ω dependence is lost for wave **g**. Peaks **k** exhibit ω dependence only at very low TU concentrations (< 0.05 mM).

Variation of scan rate. The voltammetric response for 0.10 mM TU is shown in Figure 4 as a function of potential scan rate (ϕ). Peaks **f** and **k** exhibit a virtual linear dependence on ϕ, indicative of their surface-controlled origins. In contrast, the ϕ dependence of peak **g** and wave **h**, as well as peaks **i** and **j**, is more complicated. Peak **g** is not well resolved from wave **h** at low TU concentrations (< 1 mM). At higher concentrations, peak **g** exhibits a linear dependence on ϕ, indicating that the corresponding reaction is under surface control.

Wave **h** in Figure 4 shows strong scan rate dependence at ϕ < 20 mV s^{-1} but is virtually independent of scan rate at ϕ > 20 mV s^{-1}. Results illustrated in Figure 3 demonstrate that, for ϕ = 100 mV s^{-1}, wave **h** varies linearly with $\omega^{1/2}$. Hence, we

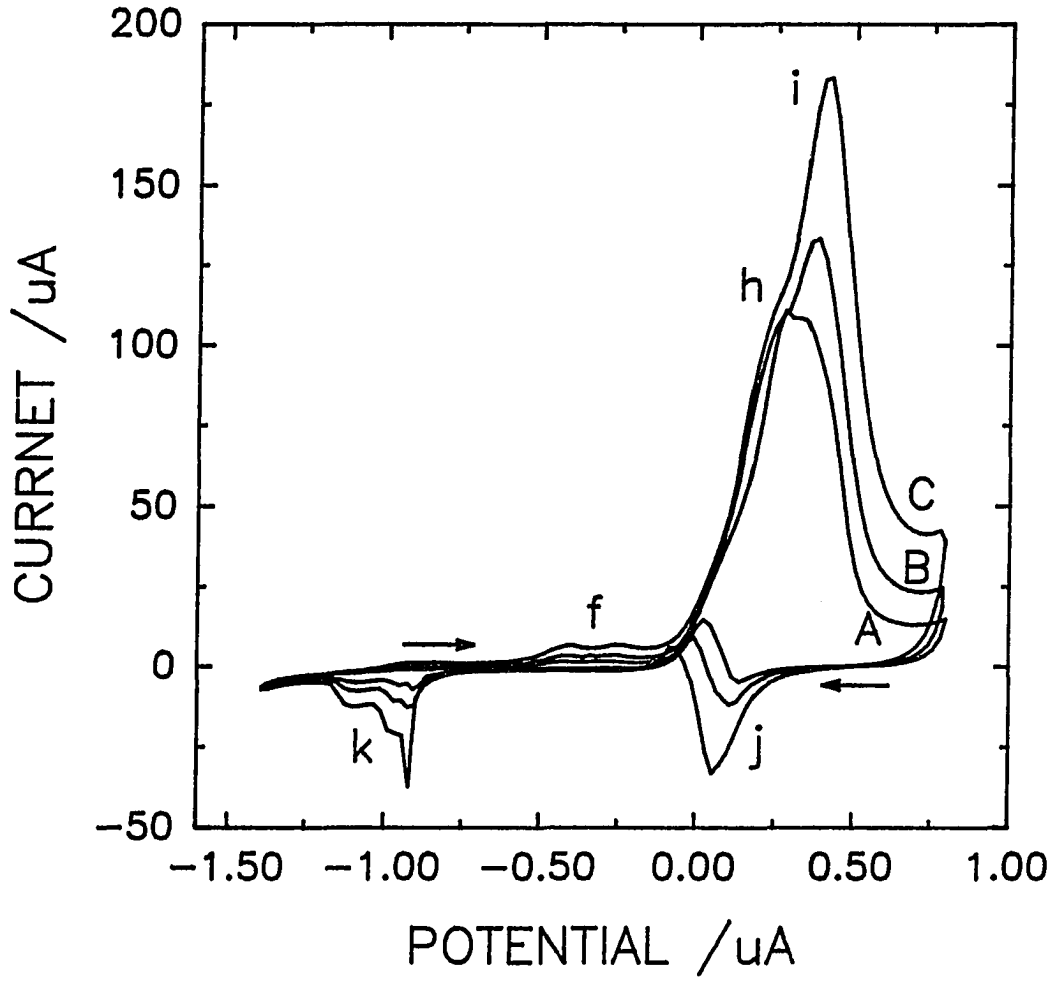

Figure 4. Voltammetric response for 0.10 mM thiourea at the Au RDE as a function of scan rate. Rotational velocity: 104.7 rad s^{-1}. Scan rate (mV s^{-1}): (A) 20, (B) 40, (C) 80.

conclude that the component of current corresponding to oxidation of TU being transported to the RDE undergoes a transition from surface control at $\phi < 20$ mV s^{-1} to transport control at $\phi > 20$ mV s^{-1}. This is consistent with a mechanism catalyzed by the generation of AuOH during production of AuO but, for which, the AuO ultimately blocks reactivity of the electrode.

Plots of peak current for peak **i** (i_{peak}) vs. ϕ are linear and have a non-zero intercept that is a virtual linear function of $\omega^{1/2}$. These results are consistent with our conclusions that Peak **i** represents the total signal from formation of surface oxide and oxidative desorption of adsorbed TU, both of which exhibit dependence on ϕ, and the oxidation of TU simultaneously being transported to the electrode, which is dependent on ω.

The sharpness of peak **i** is observed to be dependent both on scan rate and concentration. Broad peaks, as shown in Figure 4, are obtained for low TU concentrations and high ϕ values (e.g., 0.05 mM and 100 mV s^{-1}) whereas the peaks are very sharp when obtained for high concentrations and low ϕ values (e.g., $\geq$ 0.1 mM and 10 mV s^{-1}). These results are additional evidence of the complex nature of peak **i** as discussed above. We explain the sharp peaks as follows: High TU concentrations result in a high surface coverage by the adsorbed sulfur species which inhibits onset of oxide formation with the consequential shift of peak **i** to higher potential values ($>$ +0.2 V). However, when oxide formation does begin at the higher potentials, oxidative desorption quickly escalates to produce a very rapid rise in anodic response. Slow scan rates allow oxide coverage to reach its equilibrium

potential-dependent value with the consequential sharp attenuation of peak **i** (> 0.4 V). The maximum currents for the narrow peaks also exhibit a positive linear dependence on ϕ, as is observed for the broader peaks described earlier.

Ring-disk study. The amperometric response at the ring electrode of the RRDE is shown vs. the disk potential (E_d) in Figure 5B for 0.05 mM TU. The detection potential (E_{det}) was 0.50 V in the PAD waveform applied at the ring and values for the other waveform parameters are given in the caption to Figure 5B. The response at the Au RDE is repeated in Figure 5A for 0.2 mM TU to assist in the interpretation of the ring response. The waves and peaks in Figure 5A are designated in a manner consistent with Fig. 2. The choice of 0.2 mM TU for Figure 5A optimized the features of the disk response, whereas the choice of 0.05 mM TU for Figure 5B minimized the contribution to the background current from detection of adsorbed TU.

The very slight cathodic signal in the i_d-E_d response (Fig. 5A) -1.2 V, not seen in Figure 2, is the result of a low level of dissolved O_2. Whereas reduction of O_2 in the absence of TU occurs for E < ca. -0.2 V, reduction in the presence of TU is confined to E < ca. -1.0 V, probably as a consequence of interference by adsorbed TU in the reduction mechanism for O_2. Examination of Figure 5B reveals that shielding of the TU flux at the ring electrode occurs during the positive E_d scan in the region ca. -1.0 to -0.7 V, undoubtedly as a result of TU adsorption at the disk electrode. Further shielding of the TU flux at the ring electrode (Fig. 5B) occurs during the positive E_d

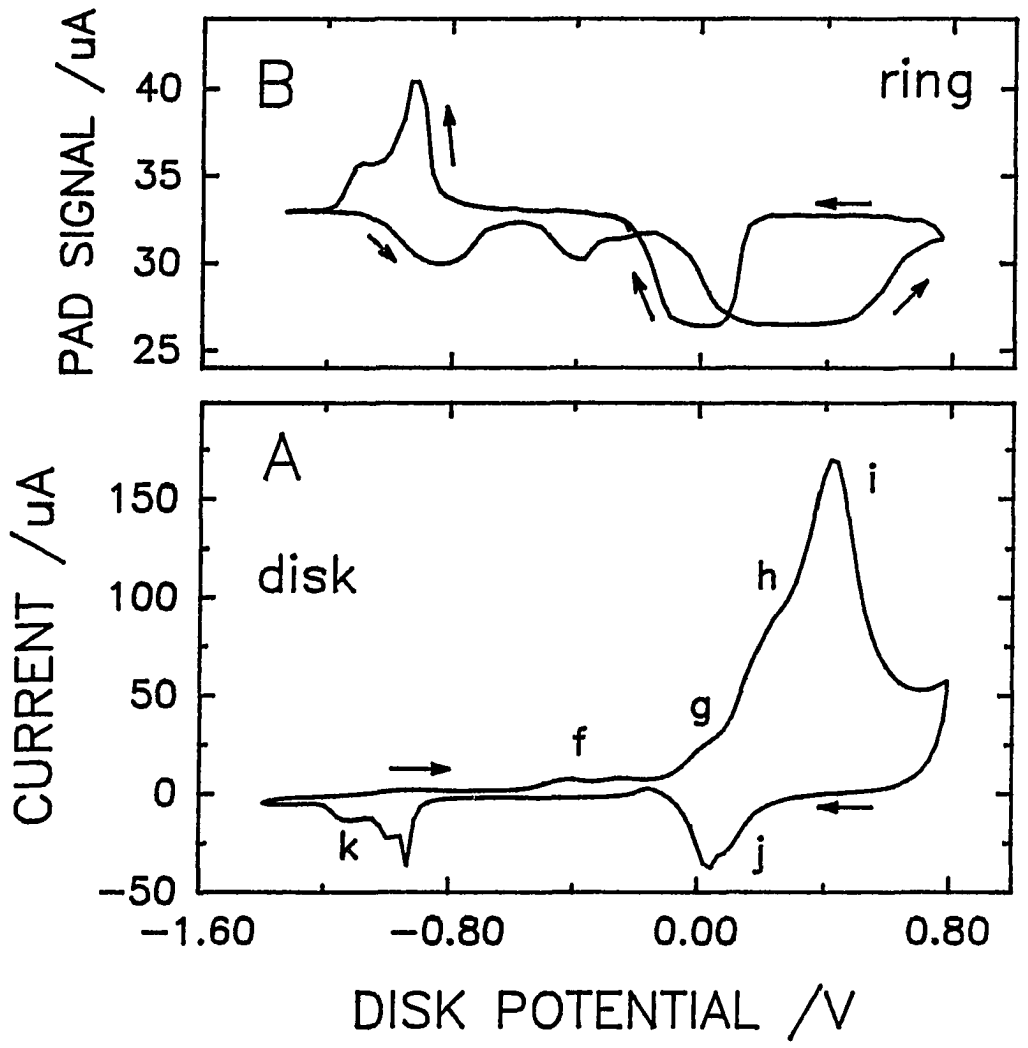

Figure 5. Voltammetric response for 0.20 mM thiourea at the disk (A) and 0.05 mM thiourea at the ring (B) of the Au-Au RRDE. Rotational velocity (rad s^{-1}): (A) 10.5, (B) 104.7. E_d scan rate: 50 mV s^{-1}. (B) 0.05. PAD waveform at ring (B): E_{det} = 0.50 V, t_{det} = 300 ms (t_{del} = 200 ms, t_{samp} = 100 ms), E_{oxd} = 0.80 V, t_{oxd} = 60 ms, E_{red} = -1.30 V, t_{red} = 180 ms.

scan in the region of the small anodic wave **f** at the disk electrode (Fig. 5A), indicating additional TU adsorption at the disk surface. Further discussion of wave **f** will be given below.

Shielding of the TU flux at the ring electrode also occurs during the positive scan for E_d > ca. -0.2 V and is virtually constant throughout the region +0.1 to +0.5 V. This is concluded to indicate that a component of the total disk current in this region (peak **g**, wave **h**, and peak **i**) corresponds to transport-limited oxidation of TU. This is consistent with our earlier conclusions for peak **i** based observed linear dependence of the peak current on ϕ and $\omega^{1/2}$. Shielding of TU flux at the ring electrode is rapidly attenuated for E_d > +0.5 V, following appearance of the maximum signal for peak **i** at the disk electrode, and the shielding ceases completely upon scan reversal.

Ring-disk data obtained for low TU concentrations (e.g., 0.01 mM), low rotational velocities (e.g., 105 rad s^{-1}), and moderately fast scan rates (> 50 mV s^{-1}) demonstrated transport-limited shielding throughout the E_d region ca. -1.0 to +0.6 V during the positive E_d scan. Hence, under conditions of low flux, the equilibrium surface coverage by adsorbed TU at the disk electrode is not achieved during the E_d scan from -1.0 to -0.1 V.

During the negative E_d scan, shielding of the TU flux at the ring electrode recommences with onset of peak **j** at the disk electrode, corresponding to reduction of surface oxide, and reaches the same limiting value as observed during the positive E_d scan in the region ca. +0.1 to -0.2 V. This indicates that the processes of TU

oxidation and adsorption at the disk electrode following cathodic dissolution of surface oxide occur at a transport-limited rate. Continuing with the negative E_d scan, a large collection signal is observed in the i_r-E_d curve (Fig. 5B) simultaneously with cathodic peaks **k** in the i_d-E_d curve (Fig. 5A). This is consistent with cathodic desorption of an electroactive species from the disk which is detected anodically at the ring. Previously, we concluded that peaks **k** correspond to desorption of S° as HS^-, a two-electron process. Therefore, detection at the ring electrode will correspond primarily to oxidation of HS^- to SO_4^{2-}, an eight-electron process. This explains the large anodic collection signal at the ring (Fig. 5B) relative to the very small cathodic desorption signals at the disk (peaks **k** in Fig. 5A).

Estimation of n (eq/mol). Values of i_{peak} for peak **i** obtained during the positive scan at the Au RDE are plotted in Figure 6 as a function of the bulk concentration (C^b) of TU for three values of ω. Each plot exhibits two linear regions. For low C^b values, peak **i** is dominated by the components from formation of surface oxide and oxidative desorption of TU adsorbed during the positive scan in the region -1.0 to -0.1 V. The fact that i_{peak} for C^b < ca. 0.05 mM TU exhibits ω dependence is a consequence of the importance of the mass-transport process in establishing the equilibrium surface coverage of adsorbed TU. Indeed, the time integral of the flux ($\int J\partial t = \int i\partial t/nFA$, mol) during the scan from -1.0 V to -0.1 V can be used to estimate the value of C^b at which a monolayer of adsorbed TU can be achieved for specified values of rotational velocity. On the basis of the integrated flux, assuming

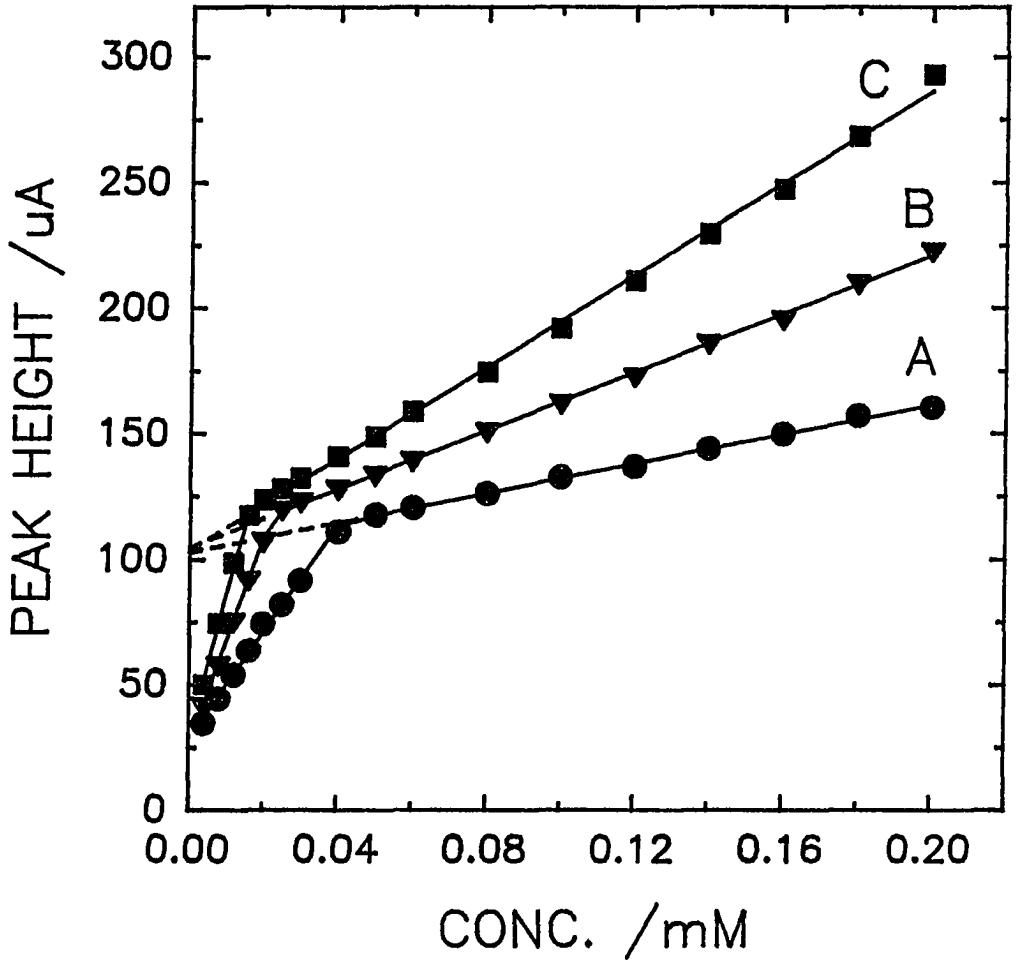

Figure 6. Anodic peak height at +0.40 V for thiourea at the Au RDE as a function of concentration and rotation speed. Scan rate: 100 mV s^{-1}. Rotational velocity (rad s^{-1}): (A) 10.5, (B) 41.9, (C) 94.2.

transport-limited TU adsorption and using 10^{15} sites/cm^2 for the estimated density of adsorption sites, values of C^b necessary to achieve formation of a complete monolayer of adsorbed TU were estimated to be within $\pm$ 20% of the C^b values corresponding to the intersections of the linear regions in the curves shown in Fig. 6. The value n (eq mol^{-1}) for anodic adsorption of TU was also estimated to be 0.98 $\pm$ 0.07 eq mol^{-1} on the basis of the anodic charge passed during the positive scan in the region -1.0 to -0.1 V and the assumption of transport-limited adsorption of TU.

For C^b > ca. 0.05 mM at the rotational velocities used to obtain Fig. 6, the surface coverage by adsorbed TU is at a maximum value and, hence, there is a constant contribution to peak **i** from the surface-controlled processes of oxide formation and oxidative desorption of adsorbed TU. Hence, variation of i_{peak} with increasing C^b and ω reflects the contribution to total current from the oxidation of TU transported to the electrode simultaneously with the appearance of peak **i**. Furthermore, the linear plots of i_{peak} vs. C^b for C^b > 0.05 mM are extrapolated to a non-zero intercept which is independent of ω. This intercept corresponds to the sum of the contributions from oxide formation and oxidative desorption of previously adsorbed TU. Hence, as expected for surface-controlled faradaic processes, the intercept is independent of ω but is a linear function of ϕ.

Values of n for the transport-limited oxidation of TU corresponding to peak **i** were calculated from the linear plots in Fig. 6 for C^b > 0.05 mM using D = 1.2x10^{-5} cm^2 s^{-1} [23] in eqn. (9). The resulting n values are 6.6 $\pm$ 0.13, 6.6 $\pm$ 0.07 and 6.9 $\pm$ 0.07 eq mol^{-1} for ω = 10.5, 41.9 and 94.2 rad s^{-1}, respectively. Values of n calculated

from linear i_{peak}-$\omega^{1/2}$ plots are 6.9 ± 0.04, 6.7 ± 0.15 and 7.4 ± 0.19 eq mol^{-1} for 0.10, 0.20 and 0.50 mM TU, respectively. These n values are below the value 8 eq mol^{-1} expected for oxidation of TU according to eqn. (4). Hence, it appears that not all sulfur atoms in TU are oxidized to sulfate.

Anodic desulfurization. Wave **g** (Fig. 2) is tentatively concluded to correspond to the one-electron oxidation of TU with the possibility of subsequent formation of formamidine disulfide. Formamidine disulfide is unstable in alkaline media and decomposes with release of S° [23,28]. Furthermore, the observation of n < 8 eq mol^{-1} for TU oxidation in peak **i** might also result because of production of some S°. Thus, we conclude that S° can be formed simultaneously with the appearance of both wave **g** and peak **i**. We have previously concluded that adsorbed S° is cathodically desorbed from the disk electrode to produce peaks **k** (see Figs. 2-4) during the negative scan in the region -0.9 to -1.2 V [5].

When the positive scan limit is decreased from +0.6 to -0.6 V, so that peaks **g** and **i** are not observed (pos. scan), peaks **k** are still obtained (neg. scan). Figure 7 shows the effect on peaks **k** of scan interruption at -0.4 V with variation of holding time prior to resumption of negative scan for a stationary electrode. It is apparent that increasing the holding time at -0.4 V results in an increased cathodic response for peaks **k**; a maximum peak current is obtained for holding times ≥ ca. 120 s. The anodic peak on the subsequent positive scan in the region ca. -1.2 to -1.0 V (Fig. 7) is not obtained if the Au electrode is rotated. Hence, we conclude this anodic peak at

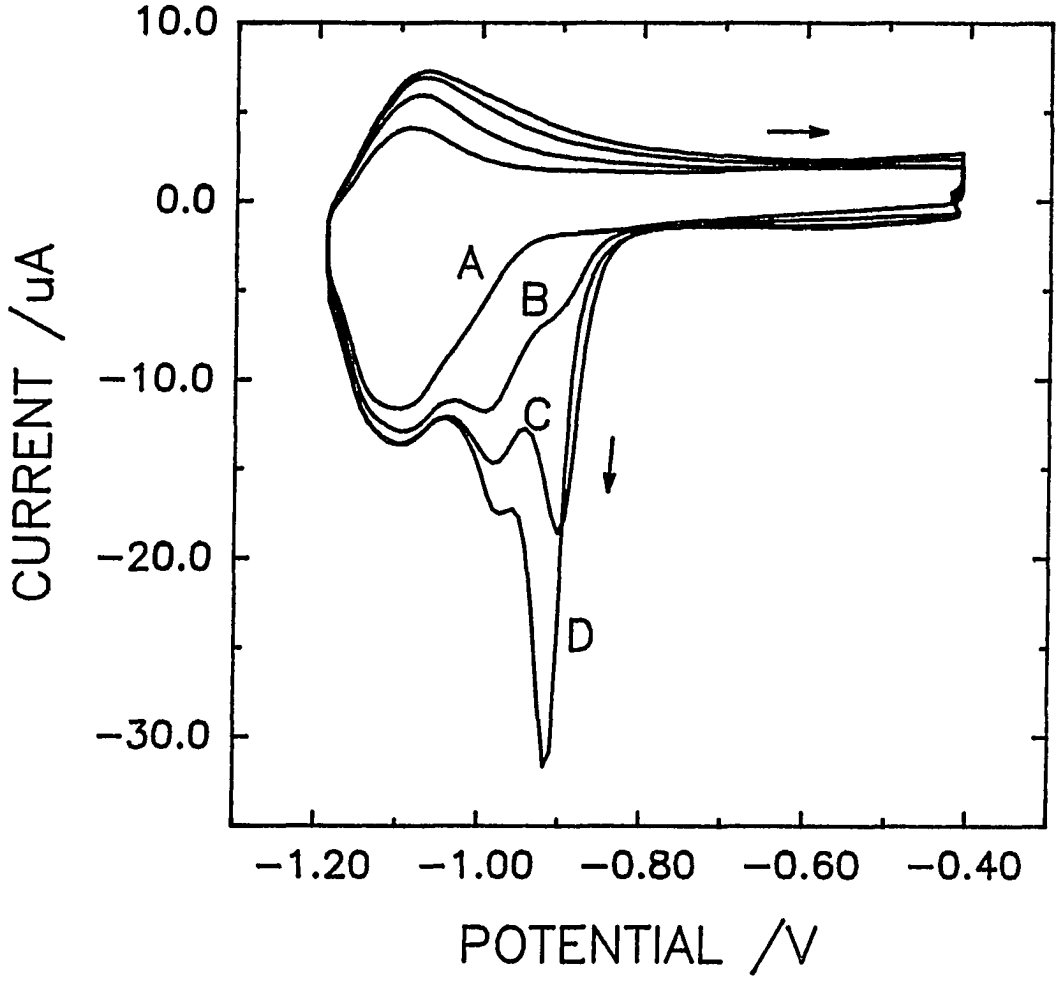

Figure 7. Voltammetric response of 0.020 mM thiourea at the stationary Au RDE as a function of hold time at -0.40 V prior to scan. Scan rate: 100 mV s^{-1}. Hold time (s): (A) 0, (B) 30, (C) 60, (D) 120.

the stationary electrode corresponds to anodic readsorption of HS^- desorbed during thepreceding negative scan to produce peaks **k** and, furthermore, that the anodic desorption of TU does not occur in the region ca. -1.2 to -1.0 V (pos. scan). The voltammetric response is virtually identical for the same experiments performed in solutions containing HS^- in place of TU.

As noted above from ring-disk experiments, adsorption of TU does occur during the positive scan for $E >$ ca. -1.0 V; however, no accompanying anodic peak is seen. The small anodic peaks from about -0.6 to -0.1 V (wave **f**, Fig. 5, n = ca. 1 eq mol^{-1}) might be the result of the anodic desulfurization of adsorbed TU:

$$H_2NC(S)NH_2 + Au \rightarrow (H_2N)_2CS\text{-}Au \quad (5)$$

$$(H_2N)_2CS\text{-}Au + OH^- \rightarrow H_2NC(O)NH_2 + HS\text{-}Au + e^- \quad (6)$$

We speculate that a greater packing density (mol cm^{-2}) can exist for adsorbed HS^- than for the larger adsorbed TU. As desulfurization occurs, more surface sites become available and further adsorption of TU can occur, as indicated by the shielding at the ring electrode at about -0.4 V (Fig. 6). Continued desulfurization of TU would explain why wave **f** (Fig. 2 - 4) has a second small anodic peak at ca. -0.2 V following the appearance of the initial peak at ca. -0.4 V.

The desulfurization of TU at Au electrodes in alkaline media is consistent with conclusions regarding cathodic peaks observed at Ag [29] and Pd [30] electrodes in alkaline media. Furthermore, numerous metal cations are known to form undissociated compounds with thiourea which undergo subsequent desulfurization with precipitation of the metal sulfides [31].

Ethylenethiourea.

Voltammetric Response. The voltammetric response for ETU at the Au RDE in 0.1 M NaOH is shown in Figure 8 as a function of concentration. The response in the region -1.4 to 0.0 V is marked by two small peaks at ca. -1.0 V (**l**) and -0.5 V (**m**). Similarly small peaks are obtained on the negative scan at ca. -0.6 V (**m'**) and -1.1 V (**l'**), and these peaks are concluded to correspond to quasi-reversible surface-controlled redox couples. These peaks are observed regardless of the choice of values > -0.4 V for the positive scan limit. Hence, the **l-l'** and **m-m'** peaks are not a consequence of processes occurring for E > -0.4 V.

The first major wave (**n**) during the positive scan appears at ca. 0.2 V. By analogy with the oxidation of TU, this wave might correspond to a one-electron oxidation of ETU to form the adsorbed free-radical species or the dimeric product [7], as described by:

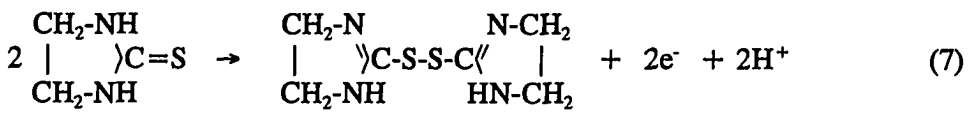

$$2\ \begin{matrix} CH_2\text{-}NH \\ | \quad \rangle C{=}S \\ CH_2\text{-}NH \end{matrix} \rightarrow \begin{matrix} CH_2\text{-}N \qquad\quad N\text{-}CH_2 \\ | \quad \rangle C\text{-}S\text{-}S\text{-}C\langle \quad | \\ CH_2\text{-}NH \qquad HN\text{-}CH_2 \end{matrix} + 2e^- + 2H^+ \qquad (7)$$

Alternately, as also suggested for the comparable wave obtained for TU, the product of this reaction might be the adsorbed free-radical product of the one-electron oxidation of ETU. Wave **n** is poorly resolved from the larger peak **o** and appears only as a shoulder to peak **o** for 0.01 mM ETU. For 10 mM ETU, wave **n** is shifted to ca. +0.4 V (Figure 9).

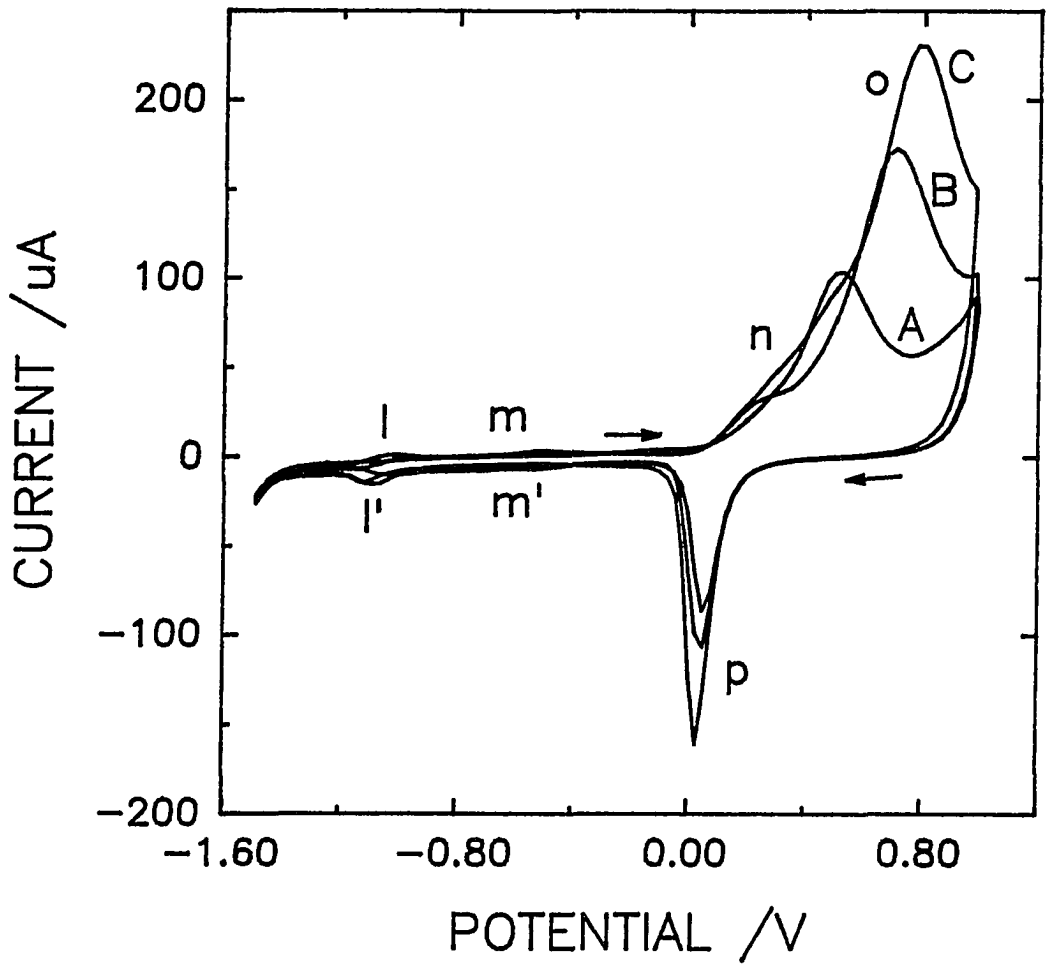

Figure 8. Voltammetric response for ethylenethiourea at the Au RDE as a function of concentration. Rotational velocity: 104.7 rad s^{-1}. Scan rate: 100 mV s^{-1}. Concentration (mM): (A) 0.01, (B) 0.1, (C) 0.4.

Peak **o** appears with a peak potential (E_p) increasing in the range ca. +0.5 to +1.0 V for ETU concentrations increasing from 0.01 to 10 mM. The primary product of the oxidation corresponding to peak **o** was concluded to be SO_4^{2-}, on the basis of a positive $BaSO_4$ test for an ETU solution after extensive voltammetric study followed by neutralization. Based on published reports for studies of the homogeneous oxidative decomposition of ETU by various oxidizing agents [32,33], and by comparison to the oxidation of TU, the following reaction is proposed for peak **o**:

$$\begin{array}{l} CH_2\text{-}NH \\ |\quad\rangle C{=}S \\ CH_2\text{-}NH \end{array} + 10OH^- \rightarrow \begin{array}{l} CH_2\text{-}NH \\ |\quad\rangle C{=}O \\ CH_2\text{-}NH \end{array} + SO_4^{2-} + 5H_2O + 8e^- \qquad (8)$$

Similar to the behavior of peak **i** for TU, the anodic response for ETU in peak **o** is sharply attenuated by accumulation of surface oxide during the positive scan and the anodic signal goes dramatically to zero upon scan reversal at +0.8 V. The peak potential (E_{peak}) for peak **o** is observed to be shifted positive for increasing concentrations even as low as 0.01 mM. By comparison, E_{peak} for peak **i** observed for TU does not shift until concentrations are increased above ca. 0.5 mM. For extremely large ETU concentrations (e.g., 10 mM), the shift in E_{peak} is so pronounced that peak **o** becomes a shoulder to the wave for O_2 evolution at $E > +1.0$ V. The possibility was tested that sulfate, believed to be a major product of the reaction yielding peak **o**, might adsorb and cause the positive shift in E_{peak}. This possibility was discredited, however, on the basis of observations that *i-E* curves for 0.01 mM ETU are identical with and

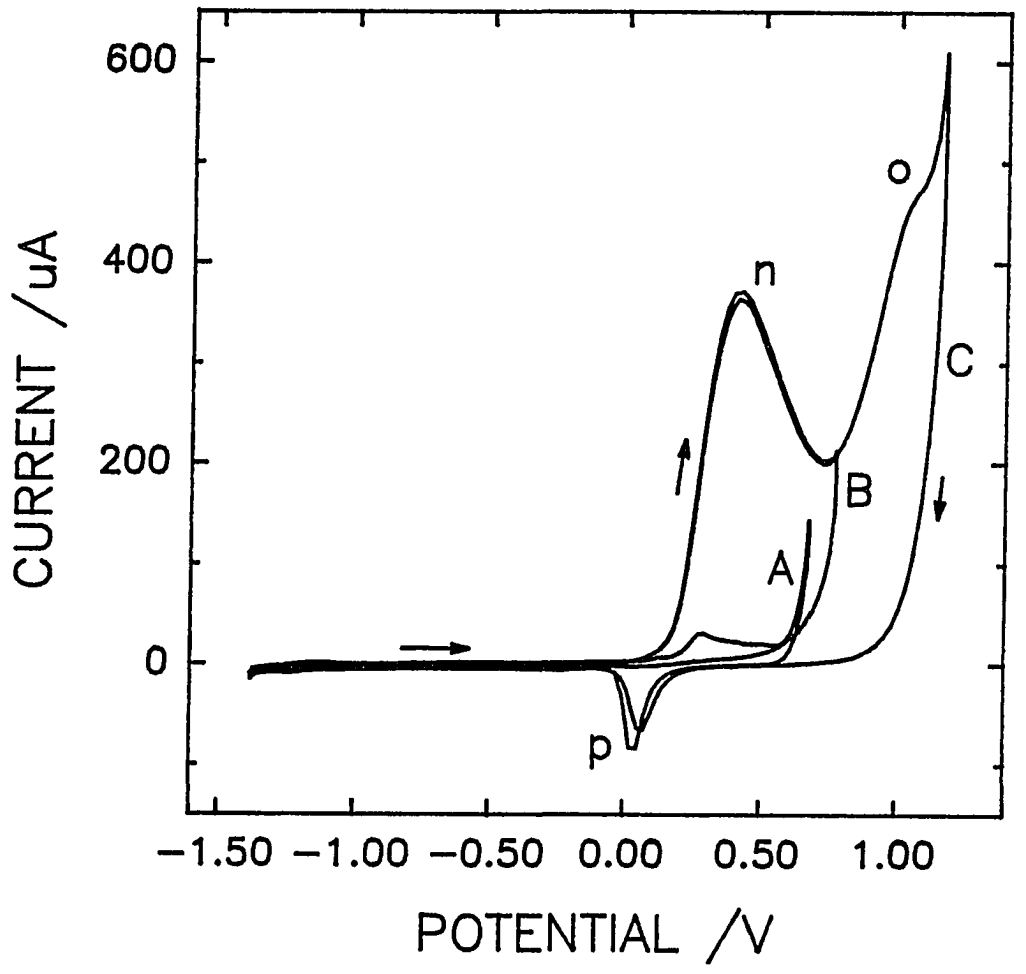

Figure 9. Voltammetric response of 10 mM ethylenethiourea at the Au RDE. Rotational velocity: 104.7 rad s^{-1}. Scan rate: 100 mV s^{-1}. Curves: (A) residual response, (B) upper scan limit = 0.80 V, (C) upper scan limit = 1.20 V.

without the presence of 10 mM Na_2SO_4. Because peak **o** for ETU corresponds to the oxide-catalyzed oxidation of absorbed and transported ETU, the remarkably large shift in E_{peak} might be indicative of a significantly greater extent of adsorption for ETU, in comparison to TU, with a resulting larger inhibition in the anodic formation of surface oxide. Alternately, the large shift in E_{peak} might be indicative of greater hydrophobicity for the ETU-covered electrode with a resulting decreased access by H_2O to the Au surface.

Cathodic peak **p** in Figure 8 corresponding to the dissolution of surface oxide during the negative scan in seen clearly at ca. 0.1 V. However, the peak height for the presence of ETU is significantly smaller than observed in the residual response for the absence of ETU. This is believed to indicate that not all the adsorbed ETU is oxidatively desorbed during the positive scan to +0.8 V and, hence, less surface oxide is formed in the presence of ETU. This is illustrated more clearly by *i-E* curves in Fig. 9 obtained for 10 mM ETU as a function of the positive scan limit. There is no evidence of an oxide reduction peak in the presence of ETU for a positive scan limit of +0.8 V (curve B). Furthermore, onset of significant O_2 evolution is shifted to approximately ca. +1.1 V (curve C) as compared to ca. 0.60 V in the absence of ETU (curve A). A second factor contributing to the smaller size of peak **p** in the presence of ETU might be the simultaneous oxidation of ETU (n = 1 eq mol^{-1}) on the oxide-free Au sites generated during oxide dissolution.

It is also significant in Figs. 8 and 9 that there is no evidence for cathodic desorption of S° starting at ca. -0.9 V during the negative scan. Hence, we conclude

that desulfurization of ETU does not occur as a significant product of the anodic reactions for wave **n** and peak **o**.

The i_{peak}-C^b plots for peak **o** obtained for ETU are shown in Fig. 10. Similar to the analogous plots for TU (Fig. 6), the plots are characterized by an extreme change in slope for C^b values increasing above ca. 0.02 to 0.05 mM, depending on rotational velocity. As observed for TU, the values of i_{peak} for ETU for small C^b values correspond primarily to the simultaneous processes of oxidation of adsorbed ETU and formation of surface oxide. However, in marked contrast to TU, the plots for large C^b values exhibit severe negative deviation from linearity for $\omega > 10.5$ rad s^{-1}. This indicates that detection of ETU is not under transport control in the region of peak **o**. An attempt was made to estimate n from the approximately linear portions of the i_{peak}-C^b plots for C^b values just above the breaks in these plots. These calculated n values are in the range 3 to 5 eq mol^{-1} which is considerably below the expected value of 8 eq mol^{-1} for the reaction in eqn. (8).

Variation of rotational velocity and scan rate. Figure 11 contains the voltammetric response of 0.1 M ETU for three values of ω. Variation of ω has virtually no effect on peaks **l** and **m**, and wave **n**, and only a slight effect on peak **o**. For $C^b > 1$ mM, all evidence of ω dependence is lost for peak **o**. This is clear evidence that the anodic detection of ETU, regardless of the value of n, occurs with a heterogeneous rate constant sufficiently large to result in a transport-limited contribution to peak **o**.

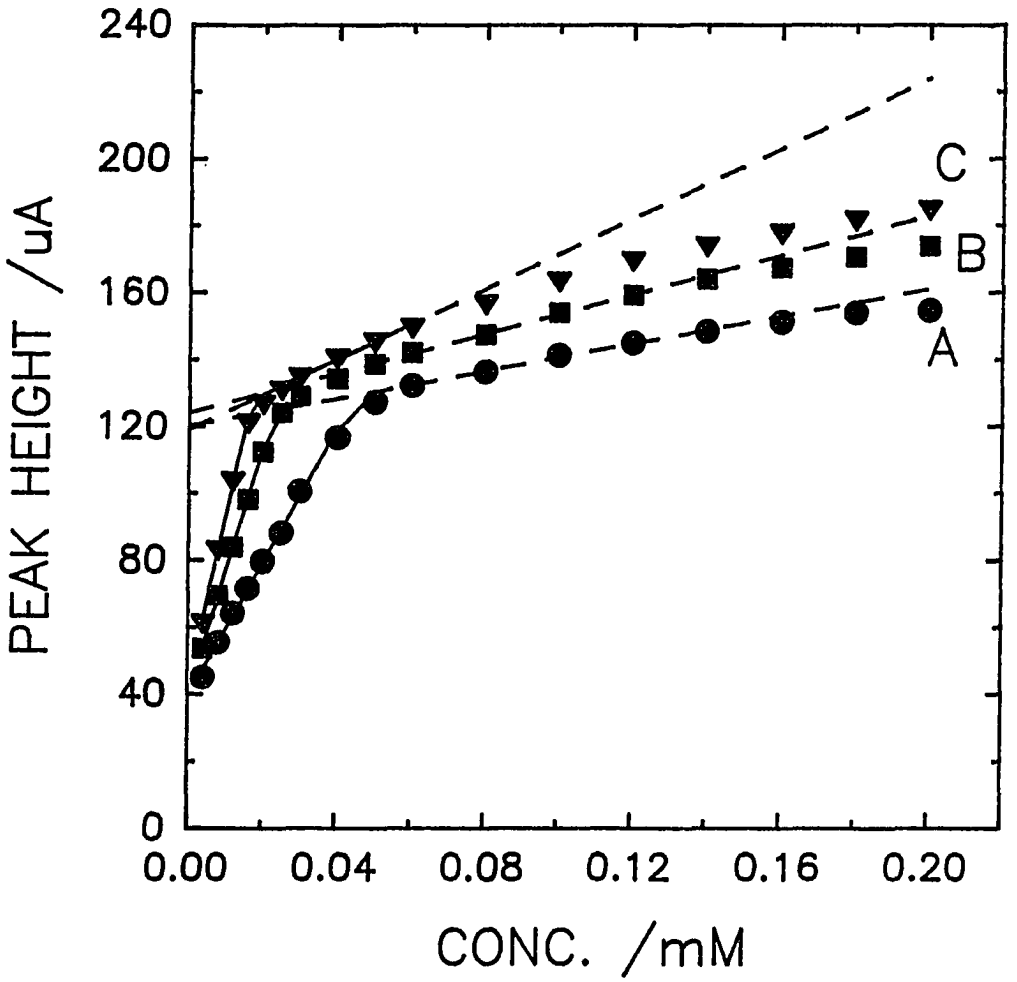

Figure 10. Peak current at +0.50 V for ethylenethiourea at the Au RDE as a function of concentration. Scan rate: 100 mV s^{-1}. Rotational velocity (rad s^{-1}): (A) 10.5, (B) 41.9, (C) 94.2.

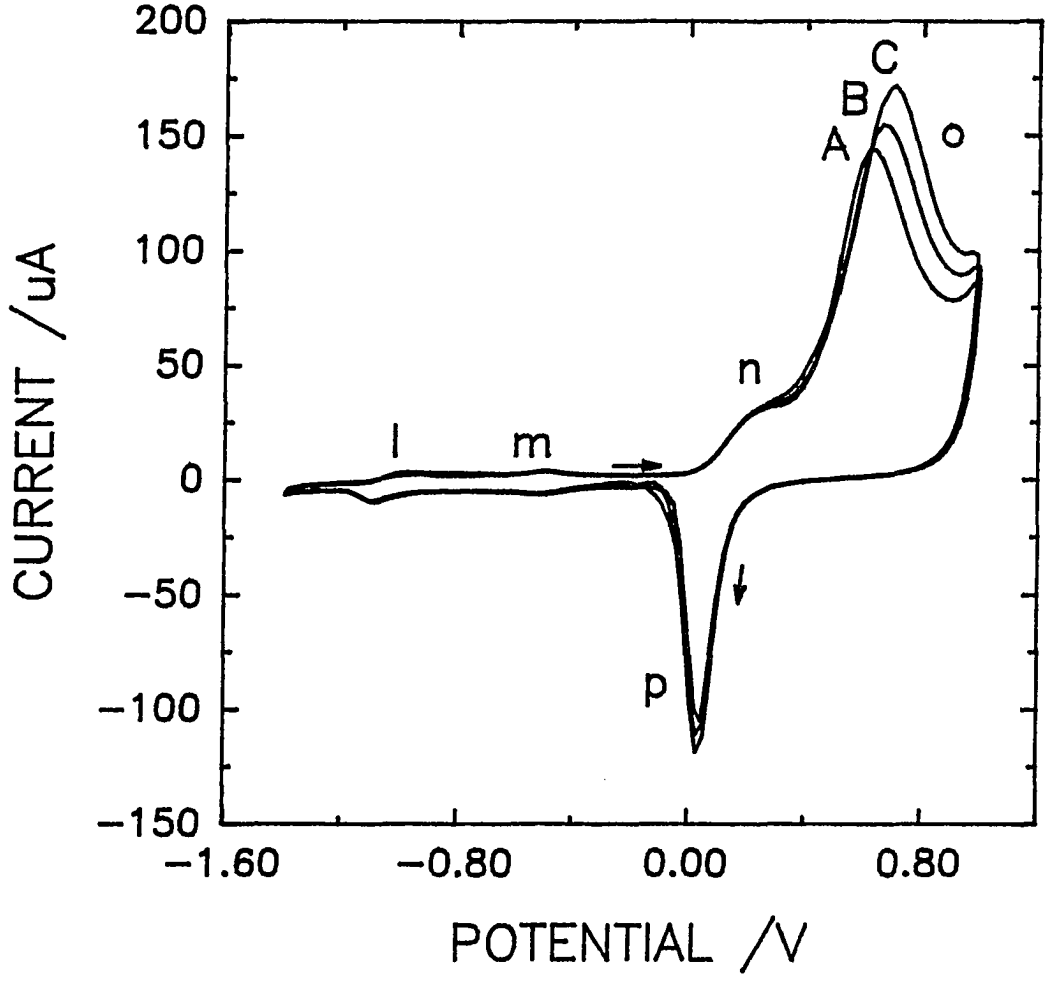

Figure 11. Voltammetric response of 0.10 mM ethylenethiourea at the Au RDE as a function of rotation speed. Scan rate: 100 mV s^{-1}. Rotational velocity (rad s^{-1}): (A) 10.5, (B) 41.9, (C) 167.6.

As expected for surface-controlled response, peak **o** is strongly dependent on ϕ, as is illustrated in Figure 12 for of 0.10 mM ETU, and a plot of i_{peak} vs. ϕ for 0.1 mM ETU is linear with a near-zero intercept. This evidence supports our conclusion of a surface-controlled mechanism for peak o.

Ring-disk study. The pulsed amperometric response at the ring of the RRDE is shown in Figure 13B for 0.050 mM ETU using E_{det} = 0.50 V in the PAD waveform. The response for 0.05 mM ETU at the disk of the RRDE is shown in Figure 13A for comparison. Shielding of the ETU flux at the ring electrode is apparent in the i_r-E_d curve (Fig. 13B) simultaneously with the occurrence of peaks **l** and **m** in the i_d-E_d curve during the positive scan (Fig. 13A). Whereas peaks **l** and **m** appear approximately equal in magnitude during the positive E_d scan, the corresponding shielding peaks demonstrate adsorption of a significantly greater amount of ETU during appearance of peak **l** than during peak **m**.

Significant shielding of the ETU flux at the ring (Fig. 13B) is also observed to correspond with onset of peak **n** at the disk electrode (Fig. 13A) during the positive E_d scan. Shielding begins gradually at ca. 0.0 V and increases to a maximum value corresponding to E_{peak} for peak **o** (ca. 0.6 V). Because the extent of shielding does not reach a plateau value, it is probable that oxidation of ETU transported to the disk during the appearance of peak **o** does not occur at a transport-limited rate.

With onset of the cathodic dissolution of surface oxide during the negative scan (peak **p**, Fig. 13A), shielding of the ETU flux at the ring appears to occur at a

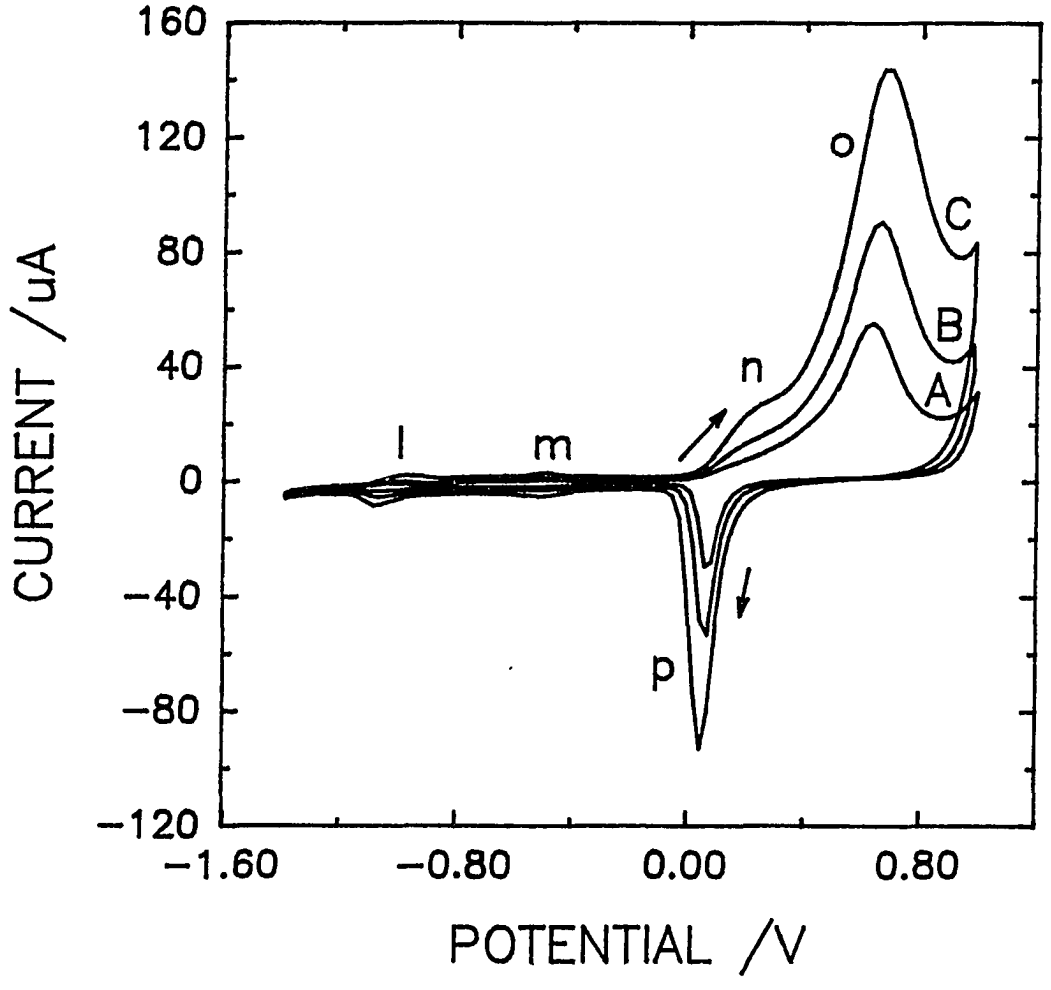

Figure 12. Voltammetric response for 0.10 mM ethylenethiourea at the Au RDE as a function of scan rate. Rotational velocity: 104.7 rad s^{-1}. Scan rate (mV s^{-1}): (A) 20, (B) 40, (C) 80.

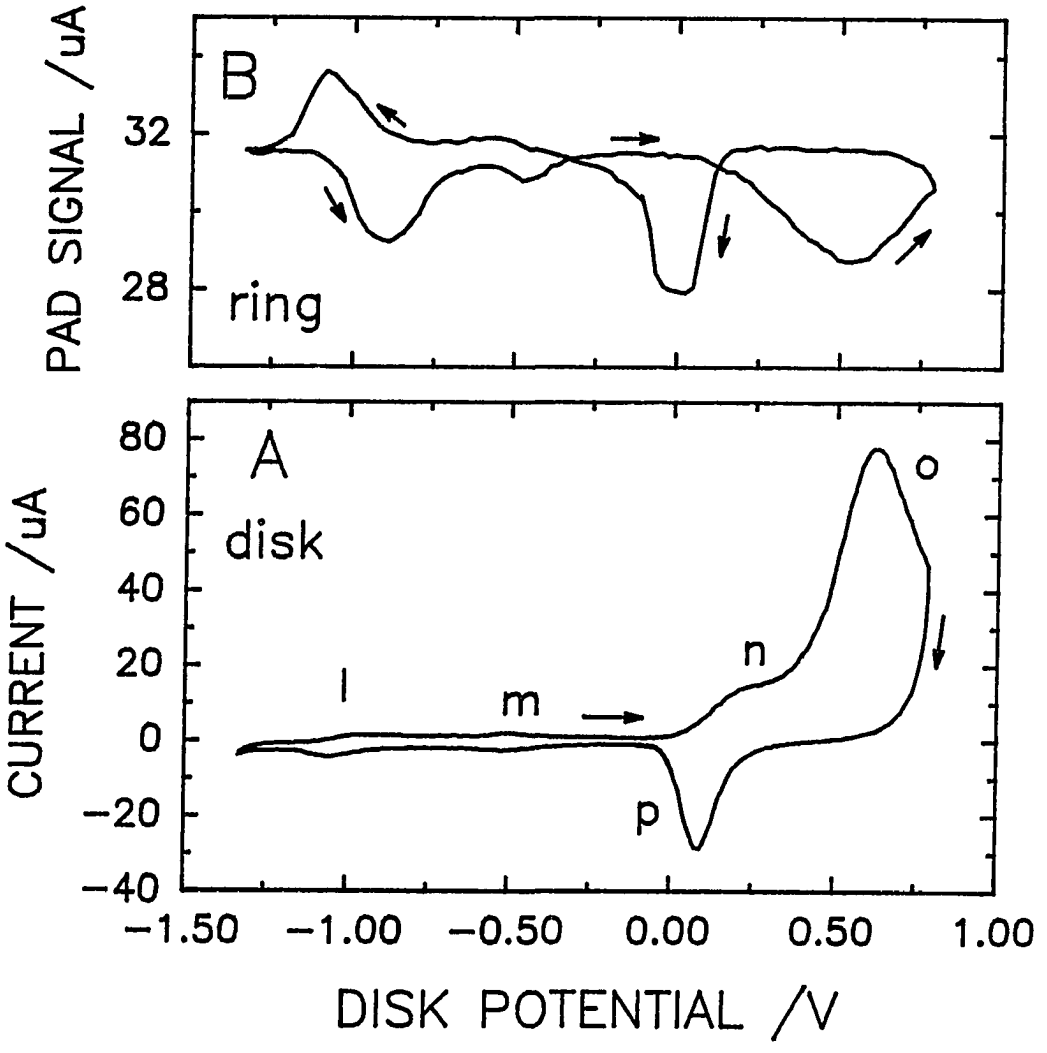

Figure 13. Voltammetric response for 0.050 mM ethylenethiourea at the disk (A) and ring (B) electrode of the Au-Au RRDE. Rotational velocity: 104.7 rad s^{-1}. E_d scan rate: 50 mV s^{-1}. PAD waveform at ring: E_{det} = +0.50 V, t_{det} = 300 ms (t_{del} = 200 ms, t_{samp} = 100 ms), E_2 = +0.80 V, t_2 = 60 ms, E_3 = -1.30 V, t_3 = 180 ms.

transport-limited rate, as indicated by the plateau in the i_r-E_d curve (Fig. 13B). The plateau value demonstrates a greater extent of shielding than observed to accompany peaks **n** and **o** (pos. scan) which confirms the conclusion that in this case adsorption and/or oxidation of ETU in the regions of peaks **n** and **o** do not occur at transport-limited rates. The ETU adsorbed during the negative scan, after cathodic stripping of surface oxide, is desorbed by processes corresponding to the small peaks **m** and **l** at the disk electrode (Curve A), as is indicated by the corresponding anodic collection signals at the ring electrode (Curve B). Whereas peaks **m** and **l** at the disk are comparable in size, the collection current at the ring corresponding to peak **l** is much larger than that corresponding to peak **m**.

CONCLUSIONS

The voltammetric response of TU and ETU at Au electrodes in alkaline media is complicated by accompanying adsorption and desorption processes. The largest anodic response is obtained during the positive potential scan concomitantly with formation of surface oxide for $E >$ ca. +0.5 V vs. SCE. The resulting anodic peaks correspond to the sum of contributions from formation of surface oxide (i_{ox}), oxidative desorption (i_{ads}) of TU or ETU which is adsorbed at $E << +0.5$ V, and oxidation of TU or ETU reaching the electrode by mass transport simultaneously with oxide formation (i_{mt}):

$$i_{peak} = i_{ox} + i_{ads} + i_{mt} \tag{9}$$

The relative magnitudes of these component signals at the RDE are strongly dependent on potential scan rate (ϕ), concentration (C^b), and rotational velocity (ω). Thus, as illustrated in Fig. 6 for TU, the response for small C^b values is dominated by $i_{ox} + i_{ads}$. Hence, the i_{peak}-C^b plot is linear with an intercept corresponding to i_{ox}. For large C^b values, the quantity of adsorbed TU is constant and, hence, the i_{peak}-C^b plot is linear with a slope significantly different than observed for small C^b values and an intercept corresponding to the sum $i_{ox} + i_{ads}$. These results are consistent with earlier observations for pulsed amperometric detection (PAD) of TU [5]. For ETU, as illustrated in Fig. 10, deviation from a linear i_{peak}-C^b plot can be severe for large C^b values at large ω values. Hence, quantitative determinations of TU and ETU based on their oxide-catalyzed detections at hydrodynamic electrodes require careful construction

of calibration curves for several standard values of C^b chosen to bracket the unknown value.

It is also significant that TU undergoes partial desulfurization to produce S° following adsorption in the region ca. -0.6 to -0.1 V. Hence, as shown previously for TU [5], it is important to periodically renew the electrode surface by cathodic desorption of adsorbed S° at E < -1.2 V. In contrast, there is no evidence that ETU nor its detection product(s) undergo a similar desulfurization reaction.

The voltammetric information gathered in this study will be of significance in the design of optimal potential-time waveforms to be applied for pulsed electrochemical detection (PED) of these organic sulfur compounds in liquid chromatography. To this application, the following observations have special significance: (i) The value of E_{peak} for maximum anodic response is observed to shift with increasing concentration. (ii) The PED technique must contend with a large background signal as a consequence of formation of surface oxide at potential values suitable for the detection. (iii) The calibration curve of response vs. concentration is likely to exhibit two linear segments.

ACKNOWLEDGMENTS

This work was supported by the National Science Foundation under contracts CHE-8914700 and CHE-9215963.

REFERENCES

1. D.C. Johnson and W.R. LaCourse, Electroanal., **4** (1992) 367.

2. W.R. LaCourse and D.C. Johnson, in C.A. Marsden (Ed.), Electrochemical Detection and Liquid Chromatography in the Biosciences, Royal Society of Chemistry, London, in press.

3. D.C. Johnson and W.R. LaCourse, Anal. Chem., **62** (1990) 589A.

4. T.Z. Polta and D.C. Johnson, J. Electroanal. Chem., **209** (1986) 159.

5. P.J. Vandeberg, J.L. Kawagoe and D.C. Johnson, Anal. Chim. Acta, **260** (1992) 1.

6. R.N. Adams, Electrochemistry at Solid Electrodes, Marcel Dekker, New York, (1969) chap. 10.

7. V.D. Parker, in M.M. Baizer (Ed.), Organic Electrochemistry, Marcel Dekker, New York, (1973) chap. XVI.

8. D.A. Dobberpuhl and D.C. Johnson, unpublished.

9. S.S. Dhaktode, R.G. Dhaneshwar and L.R. Zarapkar, Proc. Annu. Tech. Meet., Electrochem. Soc. India, (1984) 23.

10. T. Groenewald, J. Appl. Electrochem., **5** (1975) 71.

11. T. Groenewald, J. S. Afr. Inst. Min. Metallurgy, (1977) 217.

12. V.A. Zakharov, I.M. Bessarabova, O.A. Songina and M.A. Timoshkin, Elektrokhim., **7** (1971) 1215.

13. U.S. Department of Health and Human Service, Fourth Annual Report on Carcinogens, GPO, Washington, D.C. (1985).

14. S.N. Kumar, M.K. Srivastava and J.B. Morris, Natl. Acad. Sci. Lett. (India), **10** (1987) 13.

15. P. Bernstein and M.N. Hull, J. Electroanal. Chem., **28** (1970) App. 1.

16. V.G. Levich, Physiochemical Hydrodynamics, Prentice-Hall, Inc. Englewood Cliffs, New Jersey (1962), p. 69.

17. D.W. Kirk, F.R. Foulkes and W.F. Graydon, J. Electrochem. Soc., **127** (1980) 1069.

18. J.E. Vitt, L.A. Larew and D.C. Johnson, Electroanal., **2** (1990) 21.

19. L.D. Burke and V.J. Cunnane, J. Electrochem. Soc., **133** (1986) 1657.

20. L.D. Burke and V.J. Cunnane, J. Electroanal. Chem., **210** (1986) 69.

21. L.D. Burke and J.F. O'Sullivan, Electrochim. Acta, **37** (1992) 585.

22. L.D. Burke, M.M. McCarthy and M.B.C. Roche, J. Electroanal. Chem., **167** (1984) 291.

23. J. Kirchnerova and W.C. Purdy, Anal. Chim. Acta, **123** (1981) 83.

24. W.A. Jackson, W.R. LaCourse, D.A. Dobberpuhl and D.C. Johnson, Electoanal., **3** (1991) 1.

25. A.N. Buckley, I.C. Hamilton and R. Woods, J. Electroanal. Chem., **216** (1987) 213.

26. I.C. Hamilton and R. Woods, J. Appl. Electrochem., **13** (1983) 783.

27. D.G. Wierse, M.M. Lohrengel and J.W. Schultze, J. Electroanal. Chem., **92** (1978) 121.

28. P.W. Preisler and L. Berger, J. Am. Chem. Soc., **69** (1947) 322.

29. M. Iwamoto and R.A. Osteryoung, J. Electroanal. Chem., **169** (1984) 181.

30. R.V. Bucur and P. Mârginean, Electrochim. Acta, **29** (1984) 1297.

31. E.E. Reid, Organic Chemistry of Bivalent Sulfur, Vol V, Chemical Publishing Co., New York (1963), p. 36.

32. C.J. Miles and D.R. Doerge, J. Agric. Food Chem. **39** (1991) 214.

33. W.D. Marshall, J. Agric. Food Chem. **27** (1979) 295.

PAPER 3.

PULSED ELECTROCHEMICAL DETECTION OF CYSTEINE, CYSTINE, METHIONINE AND GLUTATHIONE AT GOLD ELECTRODES FOLLOWING THEIR SEPARATION BY LIQUID CHROMATOGRAPHY[3]

[3] Reprinted with permission from Vandeberg, P.J.; Johnson, D.C.; *Anal. Chem.* **1993**, *65*, 2713-2718.

ABSTRACT

A unique PED waveform is applied for detection of the sulfur-containing compounds of interest following their separation on a chromatographic column having both cation-exchange and reversed-phase properties. The mobile phase is 0.10 M $HClO_4$/0.15 M $NaClO_4$/5% MeCN which results in virtually no PED response for carbohydrates and non-sulfur containing amino acids. The PED waveform utilizes current integration throughout the period of a fast cyclic potential scan to eliminate the large background current normally observed for the conventional three-step PED waveform as a consequence of formation of surface oxide which is required by the detection mechanism. Limits of detection for the compounds of interest are at the picomolar level.

INTRODUCTION

Our laboratory has been instrumental in the development of so-called *pulsed electrochemical detection* (PED) at noble metal electrodes for applications to liquid chromatography (LC). PED is based on the application of multi-step potential-time (*E-t*) waveforms that manage the sequential processes of amperometric detection followed by oxidative cleaning and reductive reactivation of the electrode surface. PED has been demonstrated for the sensitive detection of numerous polar aliphatic organic compounds including alcohols, glycols and polyalcohols; monosaccharides, disaccharides and oligosaccharides; and amines, alkanolamines and amino acids. [1-3] Efforts to extend PED to organosulfur compounds have been challenging because these compounds are strongly adsorbed with the possibility of extensive fouling of noble metal electrodes. [4-7]

The mechanism for anodic detection of sulfur compounds at Au electrodes is believed to involve preadsorption on the oxide-free metal surface, undoubtedly *via* a non-bonded electron pair of the sulfur atom, followed by oxidative desorption concomitantly with the anodic formation of surface oxide. [4,8,9] Ultimately, however, the inert surface oxide effectively passivates the electrode surface and must be cathodically reduced to restore the reactivity of the pristine Au surface prior to the next detection cycle. A negative consequence of strong adsorption of sulfur compounds can come as a result of suppression of the oxide-formation process with the result that the potential for maximum analytical response is observed to shift positive as the concentration is

increased.[6] Furthermore, some organosulfur compounds are observed to undergo decomposition at the electrode surface with formation of a gold sulfide film which inhibits the cathodic regeneration of the Au surface.[6] A beneficial consequence of strong adsorption of sulfur compounds is that selective detection can be achieved in acidic media.[8,9] In view of the complexity of anodic reactions mechanisms for sulfur compounds, it is essential to obtain a good understanding of the voltammetric response of these compounds as the initial step in the design of successful PED waveforms.

A list of biologically significant sulfur compounds that are active under PED waveforms includes the amino acids methionine (Met), cysteine (Cys) and cystine (Cys_2), as well as simple peptides containing Met, Cys and/or Cys_2, *e.g.*, glutathione in its reduced (GSH) and oxidized (GSSG) forms. Traditionally, detection of amino acids separated by LC has been achieved *via* uv/vis absorbance or fluorescence photometry after derivatization with a suitable chromophoric or fluorophoric functional group.[10] However, determinations of Met and its derivatives in this manner are not always desirable because of the absence of the amine group necessary for the derivatization chemistry, *e.g.*, hydroxymethionine analogues.[11] Detection of GSH also is usually performed photometrically after derivatization; however, additional chemical steps are required for detection of GSSG.[12] In general, determinations of thiols are difficult because of their tendency to undergo oxidation in the presence of dissolved O_2. Thus, an abbreviated workup prior to detection would be considered advantageous.

Amperometric detection of thiols has been performed successfully based on anodic reactions at amalgam electrodes[13,14] which are now commercially available.

However, application of this procedure for Cys_2 and GSSG requires cathodic reduction at an upstream electrode prior to anodic detection as Cys and GSH. Anodic detection also has been performed at carbon electrodes modified with cobalt phthalocyanine [15] or ruthenium cyanide. [16,17] Applications of PED for organosulfur compounds at solid Au electrodes has the advantages of high sensitivity and selectivity, requires no prior chemical or electrochemical derivatization, and does not require special modification of the Au surfaces. In addition, PED instrumentation is available from various commercial sources.

General electrochemical studies have been described for Cys, [18] Cys_2, [19] GSH and GSSG [20] at Au electrodes. The anodic products were not identified in these earlier studies; however, a more recent study reported that adsorbed Cys is oxidized to the corresponding sulfinic acid at Au electrodes in 0.1 M $HClO_4$. [21] The sulfinic acid can undergo further oxidation to the sulfonic acid and, furthermore, cleavage of the C-S bond can occur to yield sulfite and alanine. Oxidation of Met at Au electrodes has been speculated to occur with cleavage of the C-S bond to yield methanesulfonic acid and an adsorbed amino acid fragment. [22] There is no speculation as to the nature of the amino acid fragment, nor regarding its fate during subsequent voltammetric scans. Oxidation at a mixed-valence ruthenium cyanide-modified electrodes has been reported to result in a four-electron oxidation of Met to the corresponding sulfone. [23]

Here, we describe the voltammetric basis of PED for Cys, Cys_2 and Met, and present LC-PED results for mixtures of various biologically-significant sulfur-containing compounds.

EXPERIMENTAL SECTION

Reagents. All solutions were prepared from reagent grade chemicals that were used as received. Reduced glutathione (96%) and *l*-cysteine were from Aldrich. Oxidized glutathione (98%) and glycine were from Sigma. All other chemicals were from Fisher Scientific. Tap water was treated in a serial fashion by passage through ion-exchange cartridges (Culligan) and a Milli-Q water purification system (Millipore).

Stock solutions of chemical reagents were made fresh weekly and stored at 5°C. Chromatographic results indicated that oxidation of the thiols to the corresponding disulfides was not a problem. Test solutions were prepared just prior to use by dilution of the appropriate aliquots of stock solutions with the desired electrolyte solution.

Blood samples was prepared as follows: a 100-μL aliquot of human blood was diluted to 2.00 mL with the acidic LC mobile phase which caused the red blood cells to lyse. The samples then were centrifuged for 5 min at 5000 rev min^{-1} to separate the precipitated proteins and other non-soluble matter. Samples were injected into the LC system through a 0.22-μm syringe filter. For the determination of GSH in blood, a further 5-fold dilution was required to achieve a concentration within the range of linear response of PED.

Voltammetry. Voltammetric studies were conducted using a Au rotated disk electrode (RDE; 0.178 cm^2), a MSR rotator and speed controller, and a Model RDE-4 potentiostat (Pine Instrument Co.) The RDE was polished daily with 0.05-μM alumina (Buehler) on microcloth with water as the lubricant. The electrochemical cell

(150 mL) was constructed from Pyrex glass with two side arms (5 mL) joined to the cell via fritted glass disks (medium porosity) to accommodate the reference and counter electrodes. The reference potential in voltammetric studies was provided by a saturated calomel electrode (SCE, 0.24 V *vs.* NHE; Fisher Scientific) and all potentials are reported with respect to the SCE. The counter electrode was a coiled Pt wire. Supporting electrolyte solutions contained 0.10 M NaOH or 0.10 M $HClO_4$ containing 5% acetonitrile. Dissolved O_2 was removed by dispersion of N_2 (99.99%) through a fritted-glass disk (medium) and a N_2 atmosphere was maintained over the test solutions during experimentation. Voltammetric data were recorded with a 386 IBM-compatible PC using a DAS-1602 interface and Asyst 4.0 software (Keithley-Metrabyte-Asyst).

Slow cyclic analog waveforms (100 mV s^{-1}) were generated internal to the RDE4 potentiostat. Fast cyclic staircase waveforms (4000 mV s^{-1}) were generated at the RDE4 potentiostat using the PC and Asyst software. The staircase waveform consisted of 50-mV steps having a duration of 12.5 ms. The electrode current was sampled at each potential step after a 4.17-ms delay.

Chromatography. The LC system consisted of a GPM-2 gradient pump and programmable PED (Dionex). The detector cell was of the thin-layer design with a Au working electrode (1.5 mm^2), a 50-μm spacer, a Ag/AgCl reference electrode (0.20 V *vs.* NHE) and a stainless steel counter electrode. The cutout in the spacer defined the cell volume as *ca.* 1.5 μL. Separations were performed using OmniPac PCX-500 guard (4 x 50 mm) or analytical (4 x 250 mm) columns (Dionex). The PCX-500

columns exhibit both reversed-phase and cation-exchange character. The injection valve was a model 7010 (Rheodyne) with a 50-μL sample loop.

The chromatographic mobile phase consisted of 0.10 M $HClO_4$ containing 0.15 M $NaClO_4$ and 5% acetonitrile (MeCN), and was filtered through a 0.22-μm nylon 66 membrane (MSI) prior to use. The mobile phase was not deaerated.

Design of the PED waveform is discussed below.

RESULTS AND DISCUSSION

Voltammetric Response in Alkaline Solutions. It has been our general observation that PED response for polar aliphatic compounds is most favorable under alkaline conditions.[1-3] Hence, pH ≥ *ca.* 12 has been prescribed commonly for amines and carbohydrates at Au electrodes.[1-3] Thus, 0.10 M NaOH was chosen for the initial voltammetric studies of organosulfur compounds.

The residual voltammetric *i-E* response for the Au RDE in 0.10 M NaOH is shown by in Figure 1 by Curve **a**. The residual response has been discussed[7,24-29] and only the most significant features are mentioned here. These include: (i) the so-called double-layer region (-1.4 to 0.0 V), (ii) a small anodic wave (*ca.* +0.05 V, pos. scan) believed to correspond to formation of a small amount of surface oxide having unknown stoichiometry, (iii) a large anodic wave (*ca.* +0.15 to +0.6 V, pos. scan) commonly associated with formation of a monolayer of surface oxide (AuO), (iv) anodic evolution of O_2 (> 0.6 V), and (v) cathodic reduction of surface oxide (*ca.* +0.2 to -0.2 V, neg. scan).

The voltammetric response of sulfur compounds in 0.10 M NaOH is illustrated in Figure 1 by Curve **b** for 0.50 mM Cys. The most prominent feature of this response is the large anodic peak (*ca.* +0.1 to 0.6 V, pos. scan) which occurs concomitantly with formation of surface oxide. The height of the anodic peak for Cys in this solution was determined to be virtually independent of variations in rotation rate of the RDE and virtually a linear function of the scan rate. These characteristics

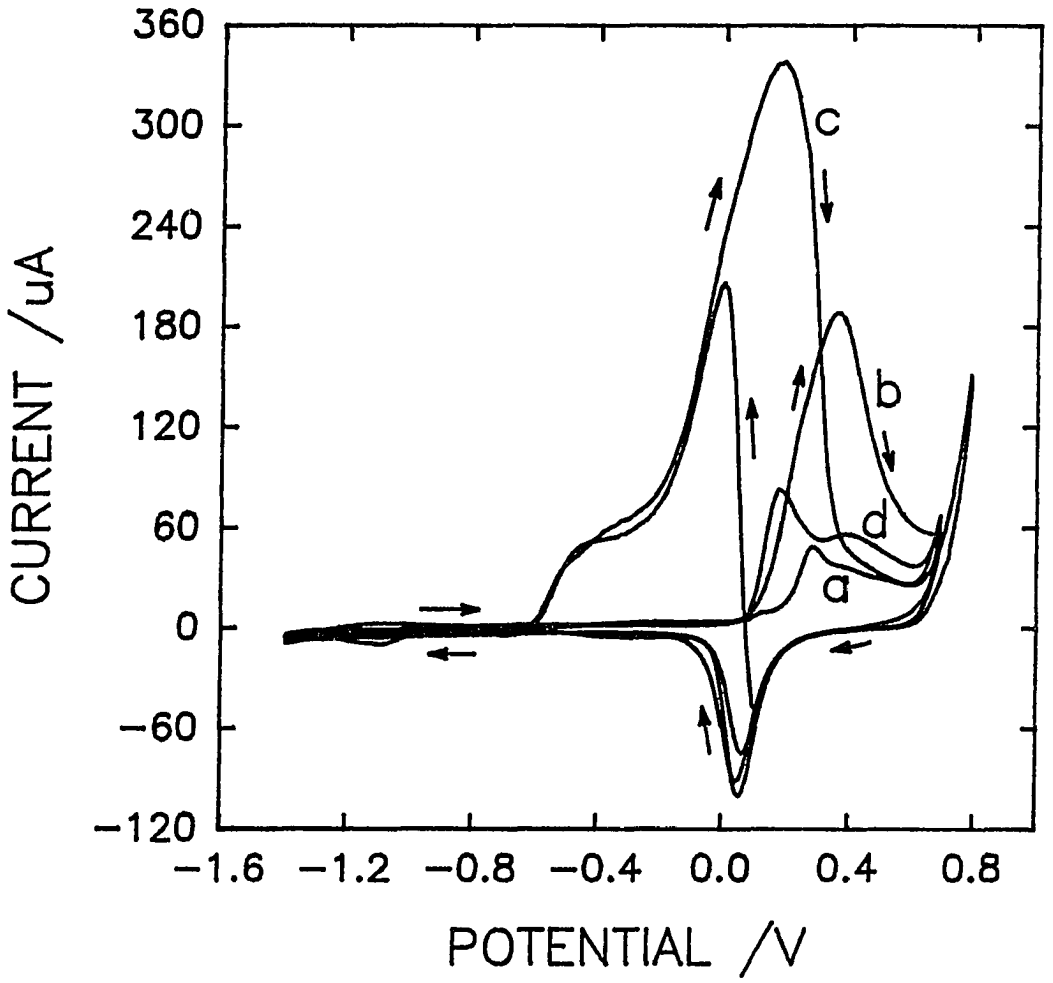

Figure 1. Voltammetric response at Au RDE in 0.10 M NaOH. Rotation rate: 1000 rev min^{-1}. Scan rate: 100 mV s^{-1}. Curves: (a) residual response, (b) 0.50 mM cysteine, (c) 0.50 mM glucose, (d) 0.50 mM glycine.

indicate that the predominate contribution to the anodic signal for Cys in Curve **b** comes from oxidative desorption of Cys previously adsorbed at the oxide-free Au surface in the region $E <$ *ca.* 0.0 V. It is also significant in Curve **b** that the anodic response for Cys (pos. scan) is severely attenuated by surface oxide with the result that the electrode current quickly goes to zero following scan reversal at +0.6 V. A consequence of the surface passivation by oxide is the observation, in general, that sulfur compounds are not detectable at Au electrodes under conditions of constant (dc) applied potential. It appears from a comparison of the cathodic peaks for oxide reduction in Curves **a** and **b** that the presence of adsorbed Cys suppresses slightly the quantity of oxide formed during the positive scan. The final feature of merit for Cys in Curve **b** is the pair of small quasi-reversible peaks at *ca.* -1.2 V. These are believed to correspond to anodic adsorption and cathodic desorption of Cys at the oxide-free Au surface. [6,21]

Shown also in Figure 1 for purposes of comparison are the *i-E* curves for 0.50 mM glucose (Glu, Curve **c**) and 0.50 mM glycine (Gly, Curve (**d**). Adequate discussions have been presented for the response of carbohydrates [30] and amino acids [31] at Au in alkaline media. Of significance to this discussion is the fact that there is significant overlap between the response peaks (pos. scan) for carbohydrates and amines with that of sulfur compounds at Au electrodes in alkaline media. Hence, application of LC-PED for determinations of Cys, Cys_2, Met and their derivatives in biological samples, with detection in alkaline mobile phases, will undoubtedly require

very careful choice of both chromatographic conditions and PED waveforms to prevent interference from carbohydrates and other amino acids.

Voltammetric Response in Acidic Solutions. The voltammetric responses of Cys, Glu and Gly were examined as a function of pH. To summarize, the anodic response for Glu and Gly was attenuated severely in neutral and acidic media, whereas a strong anodic signal persisted for Cys under all conditions. As for the case in alkaline media (see Fig. 1), an anodic peak is observed for Cys in acidic media during the positive scan concomitantly with formation of AuO. The most significant effect of changing from alkaline to acidic media is a positive shift in the potential for onset of AuO formation. As a direct consequence, the peak response for Cys is shifted from *ca.* +0.4 V *vs.* SCE in 0.10 M NaOH to *ca.* 1.2 V *vs.* SCE for 0.10 M $HClO_4$. The addition of acetonitrile (MeCN) to the acidic solutions was observed to further diminish the already weak responses of Glu and Gly, presumably because adsorption of MeCN at the Au surface blocks the anodic mechanisms of the more weakly adsorbed carbohydrate and amino acid. In contrast, addition of MeCN had virtually no effect on the anodic response of the more strongly adsorbed Cys.

Figure 2 shows the voltammetric response for 0.0050 mM Cys (Curve **d**), Cys_2 (Curve **c**) and Met (Curve **b**) in comparison to the residual response (Curve **a**) for 0.10 M $HClO_4$ containing 5% MeCN. The response for Glu and Gly were virtually identical to the residual response (Curve **a**) and, therefore, are not shown in Figure 2. A further increase in MeCN concentration to 50% resulted in no change in the

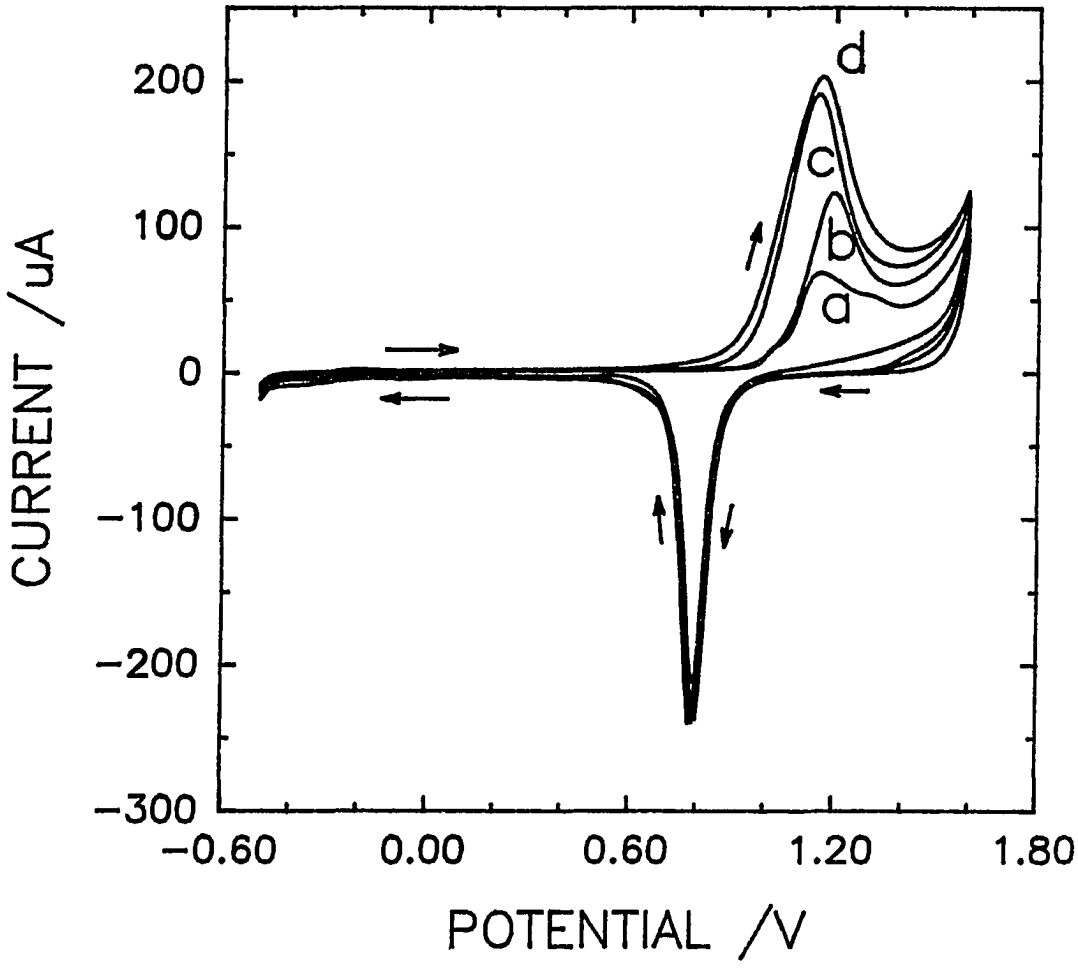

Figure 2. Voltammetric response for sulfur-containing amino acids at Au RDE in 0.10 M $HClO_4$ with 5% MeCN. Rotation rate: 1000 rev min^{-1}. Scan rate: 100 mV s^{-1}. Curves: (a) residual response, (b) 0.0050 mM Met, (c) 0.0050 mM Cys_2, (d) 0.0050 mM Cys.

voltammetric response for Cys, Cys_2 and Met from that shown in Figure 2. This observation indicates that MeCN is not electroactive and, furthermore, does not interfere in the detection mechanisms for these sulfur compounds.

The *i-E* response for Cys (Curve **d**, Fig. 2) is very similar to that for Cys_2 (Curve **c**) with no evidence of a separate wave corresponding to oxidation of Cys to Cys_2 (1 eq mol^{-1}). These observations are consistent with speculations that the response mechanisms involve preadsorption on the oxide-free Au surface so that the voltammetric response for both Cys and Cys_2 corresponds to that of adsorbed thiol radicals (RS·). [19,20] Furthermore, for the solutions used to obtain Curves **c** and **d** (Fig. 2), the peak responses for Cys and Cys_2 at *ca.* 1.15 V were determined to be virtually independent of the rotational velocity of the Au RDE and were approximately linear functions of the potential scan rate. These characteristics are consistent with voltammetric response dominated by the contribution from oxidative desorption of adsorbed species.

Whereas we are convinced that the anodic response for Cys, Cys_2 and Met is the direct result of mechanisms catalyzed by the process of oxide formation (AuOH and AuO), we note that the potential for onset of the Met response is slightly more positive than that for the Cys and Cys_2 response. We are unable at this time to offer a convincing explanation for this difference; however, we note from voltammetric studies as a function of concentration that the onset of the oxide-formation wave during the positive scan is shifted slightly more positive by adsorbed Met than by adsorbed Cys. This result is consistent with a greater inhibition of the oxide-formation reaction by

adsorbed Met. We speculate, but without proof, that this might reflect a greater hydrophobic nature of Met in comparison to Cys with the result that the activity of H_2O contacting the electrode surface is smaller when Met is adsorbed.

It will become significant to the development of the PED waveform for organosulfur compounds that the electronic integral of anodic current for oxide formation during the positive scan is virtually the same, but with opposite sign, as the integral of the cathodic current for oxide dissolution during the subsequent negative scan (see Fig. 2, Curve a).[8] More specifically, under typical conditions, the net charge remaining on the integrator following a cyclic potential scan can $< 5\%$ of the anodic charge for the positive scan, provided scan reversal occurs at a potential value below that for onset of O_2 evolution.

Selection of PED Waveform Parameters. Application of the traditional three-step PED waveforms for detection of sulfur compounds using a value for the detection potential (E_{det}) chosen in the region of anodic response (*i.e.*, *ca.* 1.1 to 1.6 V) results in a large background signal as a consequence of oxide formation. This problem can be diminished substantially by the use of the waveform described in Table I. This waveform computes the total electronic integral of electrode current during a rapid cyclic scan throughout the potential region for anodic formation and cathodic dissolution of surface oxide.[8] Hence, the anodic charge for oxide formation is substantially offset by the cathodic charge for oxide reduction and the net charge on the integrator corresponds to the anodic signal for detection of the electroactive component

Table I. Description of *E-t* Waveforms.

time (ms)	potential (V vs. Ag/AgCl)
0	0.00
400	1.60
800	0.00
810	1.90
840	1.90
850	-0.60
980	-0.60
sample integration: 10 to 800 ms	

of the solution. [8,31] Additional benefits of using this waveform include negation of the consequences of small shifts in the potential for maximum analytical response as well as variation in the amount of oxide formed, both of which occur as a consequence of adsorbed analyte and are, therefore, functions of concentration. Following execution of the cyclic scan with current integration, positive and negative potential pulses are applied to insure complete oxidative cleaning and reductive reactivation of the electrode surface.

The cyclic potential scan in the PED waveform shown in Table I is applied at relatively fast scan rates (*e.g.*, > 1000 mV s^{-1}) to permit a useful waveform frequency (*ca.* 1 Hz). Therefore, the designation of the potential range for this cyclic scan must be based on review of the voltammetric response observed for the scan rate to be used

in the waveform. Figure 3 contains *i-E* curves obtained using a cyclic staircase waveform at a scan rate of 4000 mV s^{-1} applied at the Au RDE in 0.10 M $HClO_4$. Curve **a** corresponds to the residual response and Curve **b** was obtained following addition of 50 μM Cys. It is apparent that the oxide reduction peak (neg. scan) is substantially broadened in comparison to that shown in Figure 2 for a scan rate of 100 mV s^{-1}. More specifically, the peak width at half peak height ($\Delta E_{p,1/2}$) is 230 mV at 4000 mV s^{-1} (Fig. 3) as compared to 74 mV at 100 mV s^{-1} (Fig. 2). It is apparent also that the peak potential for Cys oxidation (pos. scan) in Figure 3 is shifted *ca.* 200 mV positive from that in Figure 2. Both phenomena are consequences of finite values for the heterogeneous rate constants of the corresponding surface reactions and the fact that the potential axis in voltammetry is also a time axis. [32]

On the basis of the *i-E* curves in Figure 3, the negative and positive limits for the cyclic scan in the PED waveform were chosen as 0.0 and 1.6 V, respectively. The value 0.0 V is suitable to allow complete reduction of the surface oxide during the negative potential scan without causing the cathodic detection of dissolved O_2. The value 1.6 V results in near maximal surface coverage by oxide without excessive evolution of O_2. Values for the anodic cleaning pulse and a cathodic regeneration pulse were chosen to be 1.9 and -0.6 V, respectively. Because the $E^{o'}$ values for the SCE and Ag/AgCl references are very similar, the potential values specified above on the basis of voltammetry data recorded with the SCE reference were applied without adjustment in the flow-through PED cell (see Table I).

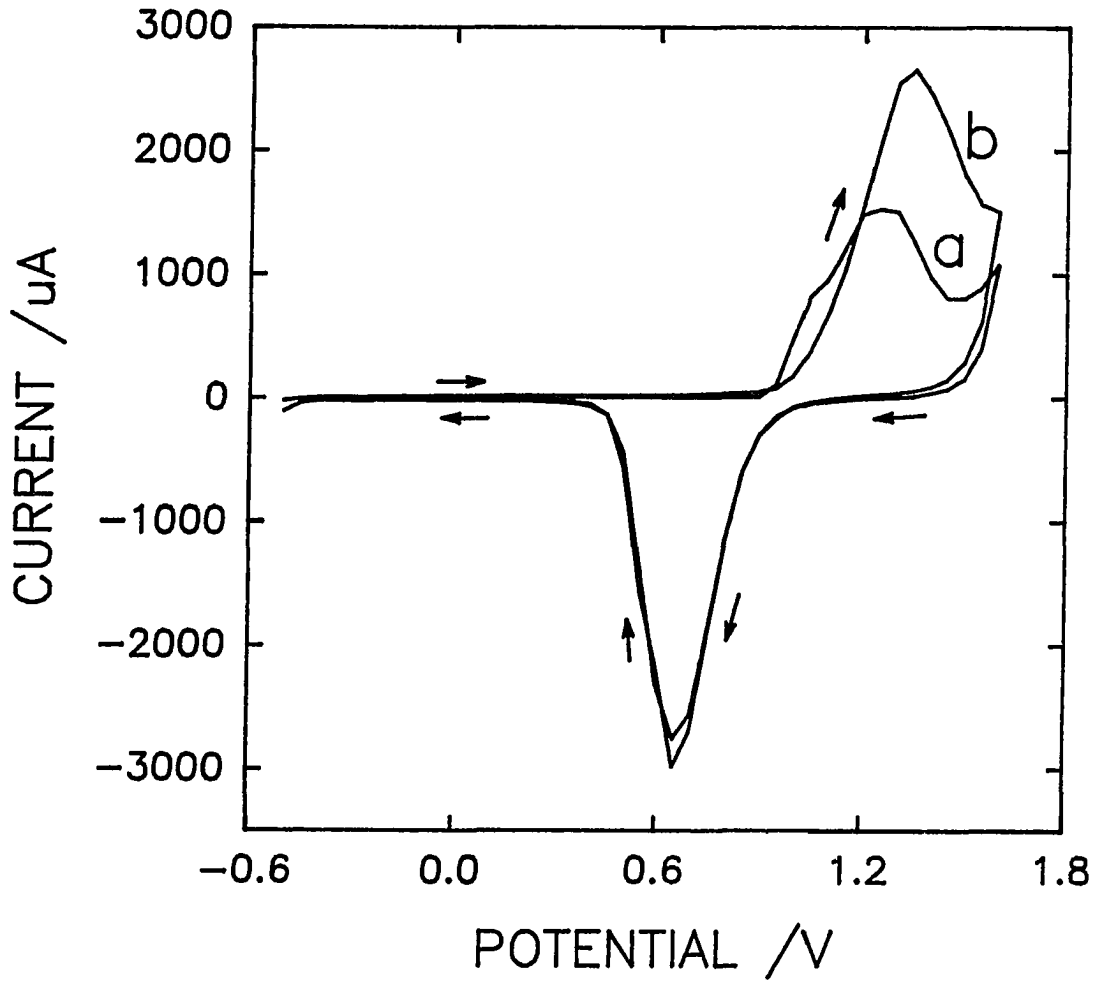

Figure 3. Rapid-scan staircase voltammetric response of Cys at Au RDE in 0.10 M $HClO_4$. Scan rate: 4000 mV s^{-1}. Potential step: 50 mV. Step duration: 12.5 ms. Delay prior to current measurement: 4.2 ms. Curves: (a) residual response, (b) 50 μM Cys.

LC-PED results. Preliminary data were obtained with separation on the OmniPac PCX-500 guard column (4 x 50 mm) and detection under control of the waveform described in Table I. The aqueous mobile phase contained 0.10 M $HClO_4$, 0.15 M $NaClO_4$ and 5% MeCN. The presence of Na^+ from $NaClO_4$ minimized the retention times (t_r) of Cys_2, GSH and GSSG. For example, t_r for Cys_2 decreased from *ca.* 18 min to *ca.* 6 min following addition of the 0.15 M $NaClO_4$. The addition of $NaClO_4$ had minimal effect on t_r values for Cys and Met. Hence, we speculate for the PCX-500 column that the retention mechanisms of Cys_2, GSH and GSSG have a strong cation-exchange component whereas the retention mechanisms of Cys and Met have a strong reversed-phase component. There was no noticeable effect on the voltammetric or PED response for any of the compounds caused by addition of $NaClO_4$.

Figure 4 shows the LC-PED response for ten consecutive 50-μL injections of 5.0 μM Cys onto the PCX-500 guard column (4 x 50 mm). Statistical evaluation of the peak heights revealed excellent reproducibility with an average peak height of 361.8 nC and a relative standard deviation (rsd) of 0.9%. Problems of drifting baseline were observed when the Au electrode was not used for extended periods (several days) or was mechanically polished prior to use. In both situations, several hours of operation were required to achieve a stable baseline. These observations undoubtedly reflect the beneficial effect of surface reconstruction that occurs during application of the PED waveform. It is recommended as standard procedure that the PED waveform be applied for 1 hr prior to the start of LC-PED experiments. Following this protocol, a

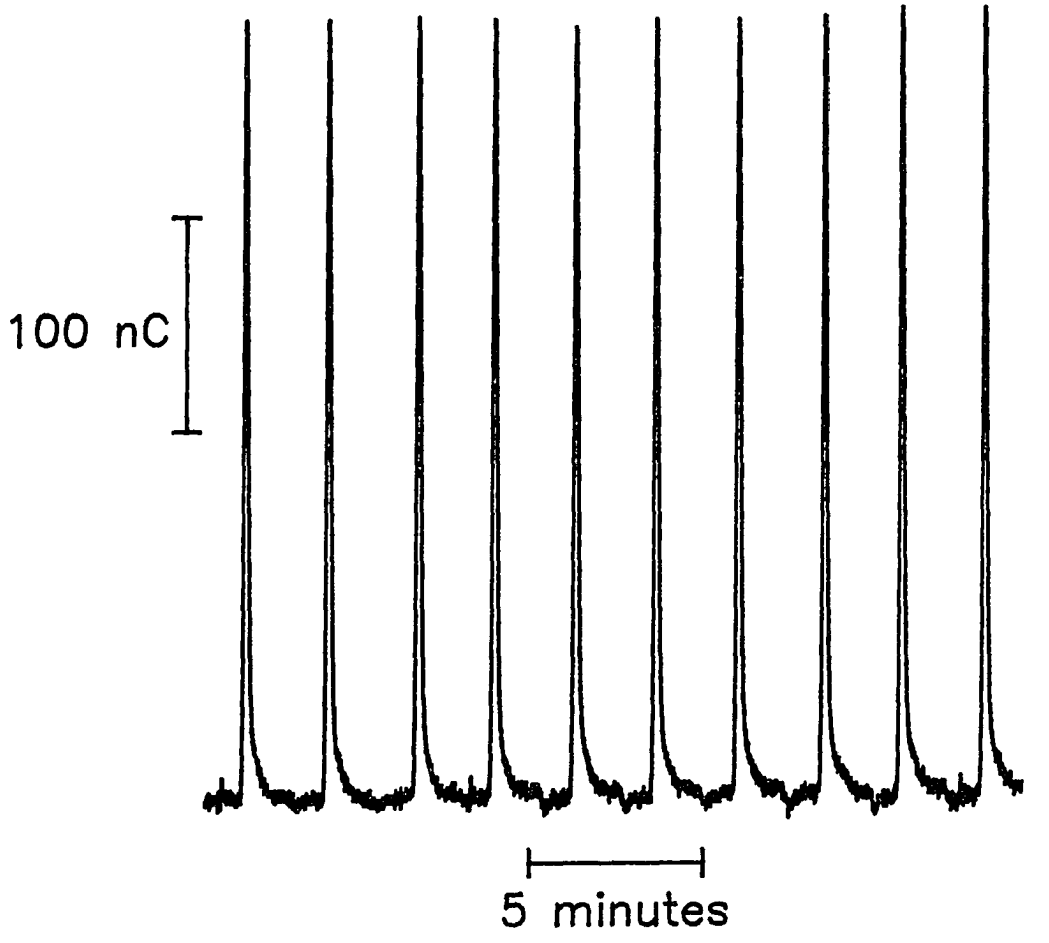

Figure 4. LC-PED response for 10 consecutive injections of 5.0 μM Cys. Mobile phase: 0.10 M $HClO_4$/0.15 mM $NaClO_4$/5% MeCN at 0.80 mL min^{-1}. Column: Dionex OmniPac PCX-500 (4 x 50 mm). PED waveform: see Table I.

test of reproducibility over a six-day period, with 1-2 hours of daily operation, yielded an rsd value of 1.1% for peak heights from injections of 5.0 μM Cys.

The slopes of calibration curves for Cys, Cys_2, Met and GSH ($\geq$ 24 injections each) were calculated by linear regression and are given in Table II. The correlation coefficients (R^2) for these data were $\geq$ 0.994. The difference in these slopes is thought to reflect differences in the prevailing adsorption isotherms for the various compounds. Also given in Table II are limits of detection (LODs) corresponding to the concentrations for which S/N = 3 (50-μL injection). These LODs are 0.90, 1.6, 3.1 and 1.8 pmoles for Cys, Cys_2, Met and GSH, respectively. The calibration study for Cys was repeated over the range 0.1 to 10 μM (n = 54 injections) with the following linear regression statistics: slope = 70.7 nC μM^{-1}, intercept = 6.3 nC, and R^2 = 0.9995. Negative deviations from the linear calibration curve were observed to occur for concentrations above 10 μM. We speculate this is a consequence of a transformation in the response mechanism from that of surface control, which exists at low concentrations, to mass-transport control, at higher concentrations.[7] However, no linearity was observed in the calibration curve for concentrations » 10 μM.

Figure 5 illustrates an application of the LC-PED system to a sample containing 1.0 μM each of Cys, Cys_2, Met, GSH and GSSG. These six compounds are easily separated under these conditions within a 6-min period. It is especially noteworthy that both the reduced and oxidized forms of Cys and GSH are detected with comparable sensitivity. This is expected to be useful for analyses in which quantitative

Table II. Least-squares regression statistics for Cys, Cys_2, Met and GSH [a]

Compound	Range (μM)	Slope (nC μM^{-1})	LOD [b] (pmol)	LOD [b] (nM)
Cys	0.1 to 100	67	0.90	18
Cys_2	0.5 to 100	31	1.6	32
Met	0.5 to 20	20	3.1	62
GSH	0.5 to 20	33	1.8	36

[a] $n \geq 24$ injections; $R^2 \geq 0.994$.
[b] LOD estimated for 50-μL injections at S/N = 3.

determinations of both the thiols and their disulfide metabolites are required.

Figure 6 contains typical results for application of the LC-PED system for determination of GSH in a human whole-blood sample following 1:100 dilution. Because of the selectivity of PED detection at Au for sulfur compounds, an extensive sample clean-up was not performed. In fact, detector selectivity allowed for very simple and rapid chromatography with the Dionex PCX-500 guard column (4 x 50 mm), despite the complicated nature of the sample matrix. Elution of the GSH occurs at *ca.* 2 min following sample injection. The GSH concentration of this blood sample was determined to be 0.99 mM, which is good agreement with reported values. [13,33]

Figure 7 contains typical LC-PED results for a blood sample following 1:20 dilution. This separation utilized the Dionex PCX-500 analytical column (4 x 250 mm)

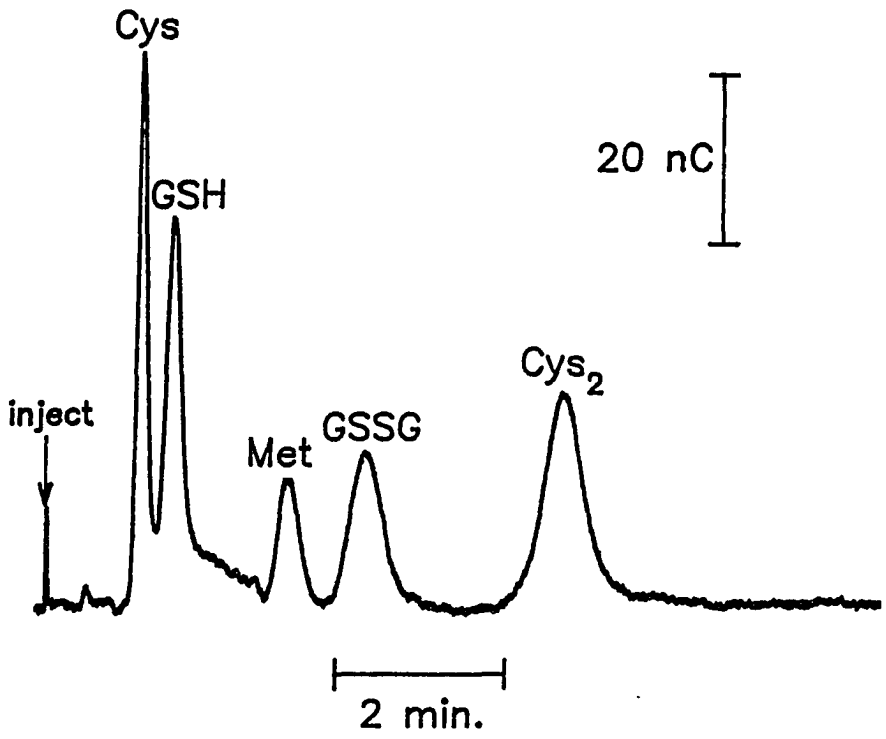

Figure 5. LC-PED results for sample containing 1.0 μM each of Cys, GSH, Met, GSSG and Cys_2. Mobile phase: 0.10 M $HClO_4$/0.15 mM $NaClO_4$/5% MeCN at 0.80 mL min^{-1}. Column: Dionex OmniPac PCX-500 (4 x 50 mm). PED waveform: see Table I.

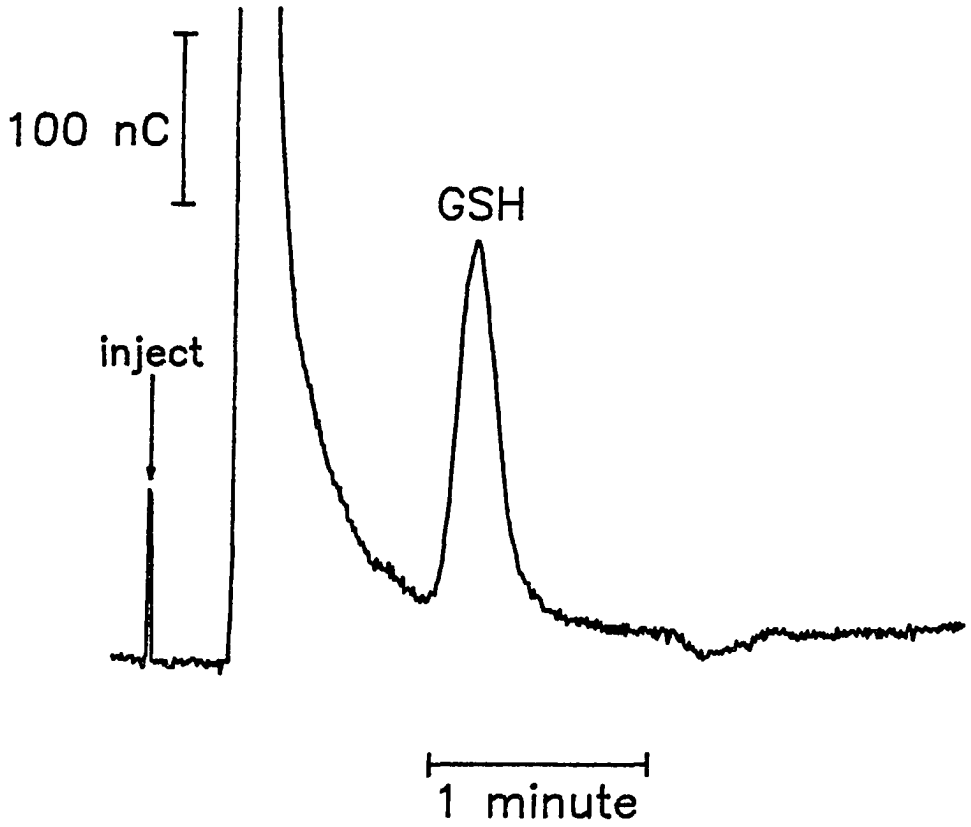

Figure 6. LC-PED results for human whole-blood sample (1:100 dilution) showing peaks for GSH. Mobile phase: 0.10 M $HClO_4$/0.15 mM $NaClO_4$/5% MeCN at 0.80 mL min^{-1}. Column: Dionex OmniPac PCX-500 (4 x 50 mm). PED waveform: see Table I.

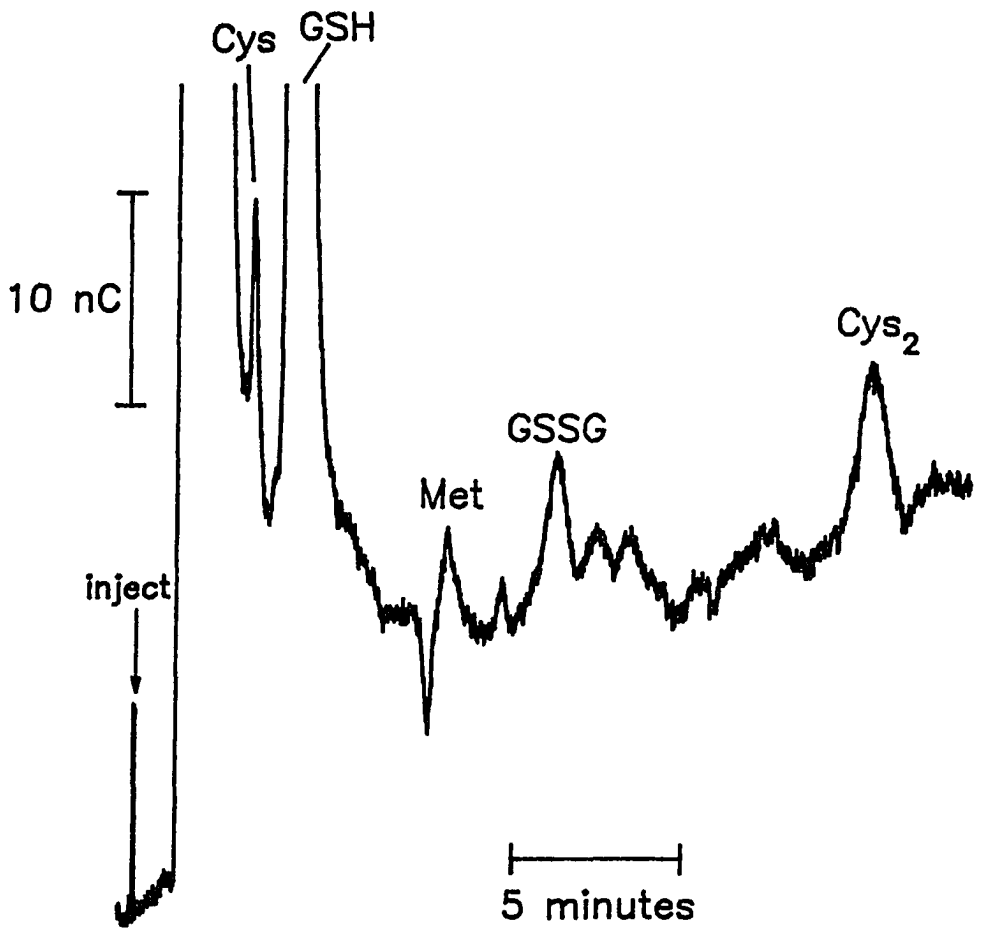

Figure 7. LC-PED results for human whole-blood sample (1:20 dilution) showing peaks for Cys, GSH, Met, GSSG and Cys_2. Mobile phase: 0.10 M $HClO_4$/0.15 mM $NaClO_4$/5% MeCN at 1.2 mL min^{-1}. Column: Dionex OmniPac PCX-500 (4 x 250 mm). PED waveform: see Table I.

to achieve resolution of the small Cys peak from the large GSH peak and the large response corresponding to elution of the column void volume. An increased PED sensitivity, as compared to Figure 6, permitted visualization of the peaks for Cys, Cys_2, Met and GSSG in the blood sample. GSH occurs in human blood at a concentration *ca.* 500X greater than that of GSSG [13] and, as a result, the GSH peak is off-scale at the sensitivity required to visualize the peaks for the other components of the sample. The identities of the peaks were confirmed by comparison to t_r values for standards. The detection of Met (*ca.* 10 min) is slightly hampered by a baseline disturbance which is observed whenever MeCN is present in the mobile phase. Whereas this disturbance can be greatly decreased by carefully matching the sample diluent with the mobile phase, efforts to completely eliminate it have proved elusive. The greater peak dispersion associated with use of the longer column (Figure 7) resulted in somewhat poorer detectability as compared with that of the shorter column (Figures 4 to 6). In addition to the large peaks for known compounds in Figure 7, several smaller albeit reproducible peaks are seen. These peaks probably are the result of other sulfur-containing compounds, *e.g.*, the glutathione fragments cysteinylglycine and glutamylcysteine, or possibly mixed disulfides such as GSH-Cys.

CONCLUSIONS

The separation of several sulfur-containing amino acids and related small peptides can be achieved using a Dionex PCX-500 column with an aqueous mobile phase containing 0.10 M $HClO_4$, 0.15 M $NaClO_4$ and 5% MeCN. Interference from carbohydrates and amino acids without sulfur is virtually nonexistent using the prescribed PED waveform applied at Au electrodes in this mobile phase.

A large background signal would be obtained if the conventional three-step PED waveform is applied for sulfur compounds. This is the result of the oxide-formation reaction at Au electrodes which is required for the oxidative detection mechanism. However, the large background is circumvented by a unique waveform in which a fast cyclic scan is applied during electronic integration of the electrode current. This operation effectively subtracts the charge for oxide reduction from that for oxide formation with the result of a near-zero value for the net background signal. Parameters are suggested for a useful waveform; however, careful optimization of the waveform has not attempted. For example, we anticipate that the PED sensitivity for sulfur-containing compounds might be increased by optimization of the value and duration of the reductive step in the waveform to maximize the quantity of the adsorbed analyte.

ACKNOWLEDGEMENTS

This research is supported by grants CHE-8914700 and CHE-9215963 from the U.S. National Science Foundation.

REFERENCES

1. Johnson, D.C.; LaCourse, W.R. *Anal. Chem.* **1990**, *62*, 589A-597A.

2. Johnson, D.C.; LaCourse, W.R. *Electroanal.* **1992**, *4*, 367-380.

3. Johnson, D.C.; Dobberpuhl, D.A.; Roberts, R.A.; Vandeberg, P.J. *J. Chromatogr.* accepted.

4. Polta, T.Z.; Johnson, D.C. *J. Electroanal. Chem.* **1986**, *209*, 159-169.

5. Polta, T.Z.; Johnson, D.C.; Luecke, G.R. *J. Electroanal. Chem.* **1986**, *209*, 171-181.

6. Vandeberg, P.J.; Kawagoe, J.L.; Johnson, D.C. *Anal. Chim. Acta* **1992**, *260*, 1-11.

7. Vandeberg, P.J.; Johnson, D.C. *J. Electroanal. Chem.*, accepted.

8. Neuburger, G.G.; Johnson, D.C. *Anal. Chem.* **1988**, *60*, 2288-2293.

9. Ngoviwatchai, A.; Johnson, D.C. *Anal. Chim. Acta* **1988**, *215*, 1-12.

10. Stryer, L. *Biochemistry* 3rd. ed.; Freeman, W.H.: New York, 1988; chapt. 3.

11. Wauters, D.: De Mol, J.; De Temmerman, L. *J. Chromatogr.* **1990**, *516*, 375-382.

12. Reed, D.J.; Babson, J.R.; Beatty, P.W.; Brodie, A.E.; Ellis, W.W.; Potter, D.W. *Anal. Biochem.* **1980**, *106*, 55-62.

13. Allison, L.A.; Shoup, R.E. *Anal. Chem.* **1983**, *55*, 8-12.

14. Sun, Y.; Smith, D.L.; Shoup, R.E. *Anal. Biochem.* **1991**, *197*, 69-76.

15. Halbert, M.K.; Baldwin, R.P. *Anal. Chem.* **1985**, *57*, 591-595.

16. Cox, J.A.; Gray, T.J. *Electroanal.* **1990**, *2*, 107-111.

17. Cox, J.A.; Dabek-Zlotorzynska, E. *J. Chromatogr.* **1991**, *543*, 226-232.

18. Koryta, J.; Pradac, J. *J. Electroanal. Chem.* **1968**, *17*, 185-189.

19. Koryta, J.; Pradac, J. *J. Electroanal. Chem.* **1968**, *17*, 177-183.

20. Ossendorfova, N.; Pradac, J.; Koryta, J. *J. Electroanal. Chem.* **1970**, *28*, 311-316.

21. Fawcett, W.R.; Fedurco, M.; Kovacova, Z.; Borkowska, Z. *J. Electroanal. Chem.*, in review.

22. Reynaud, J.A.; Malfoy, B.; Canesson, P. *J. Electroanal. Chem.* **1980**, *114*, 195-211.

23. Cox, J.A.; Gray, T.J. *Anal. Chem.* **1990**, *62*, 2742-2744.

24. Kirk, D.W.; Foulkes, F.R.; Graydon, W.F. *J. Electrochem. Soc.* **1980**, *127*, 1069- 1075.

25. Burke, L.D.; McCarthy, M.M.; Roche, M.B.C. *J. Electroanal. Chem.* **1984**, *167*, 291- 296.

26. Burke, L.D.; Cunnane, V.J. *J. Electrochem. Soc.* **1986**, *133*, 1657-1662.

27. Burke, L.D.; Cunnane, V.J. *J. Electroanal. Chem.* **1986**, *210*, 69-94.

28. Vitt, J.E.; Larew, L.A.; Johnson, D.C. *Electroanal.* **1990**, *2*, 21-30.

29. Burke, L.D.; O'Sullivan, J.F. *Electrochim. Acta* **1992**, *37*, 585-594.

30. Larew, L.A.; Johnson, D.C. *J. Electroanal. Chem.* **1989**, *262*, 167-182.

31. Welch, L.E.; LaCourse, W.R.; Mead, D.A.; Johnson, D.C. *Anal. Chem.* **1989**, *61*, 555-559.

32. Roberts, R.A.; Johnson, D.C. *Electroanal.* **1992**, *4*, 741-749.

33. Lin Ling, B.; Baeyens, W.R.G.; Marysael, H. *Anal. Chim. Acta* **1989**, *227*, 203-209.

PAPER 4.

COMPARISON OF PULSED AMPEROMETRIC DETECTION AND INTEGRATED VOLTAMMETRIC DETECTION OF ORGANIC SULFUR COMPOUNDS IN LIQUID CHROMATOGRAPHY[4]

[4] Vandeberg, P.J.; Johnson, D.C., submitted to *Anal. Chim. Acta.*

ABSTRACT

A variety of potential-time waveforms are applicable in Pulsed Electrochemical Detection (PED) of numerous polar organic compounds separated by liquid chromatography (LC). Here, we compare the waveforms for Pulsed Amperometric Detection (PAD) and Integrated Voltammetric Detection (IVD) applied to organosulfur compounds at Au electrodes in acidic media. In PAD waveforms, electrode response is measured at a constant detection potential. In IVD waveforms, electrode current is integrated throughout a fast cyclic scan of potential. As a consequence of this difference in detection strategy, the baseline for IVD is significantly smaller than for PAD in the detection of organosulfur compounds whose response mechanisms require the concomitant formation of surface oxides on the Au electrodes. Furthermore, in comparison to PAD, IVD has a larger sensitivity and a diminished system peak from O_2 dissolved in the sample. Use of a preadsorption step is found to increase detection sensitivity in both the PAD and IVD. The limit of detection (S/N = 3) for cysteine in LC-IVD is 10 nM per 50-μl injection (i.e., 1.1 pmol, 130 pg) using a detection waveform that includes a 1000-ms preadsorption period.

INTRODUCTION

A considerable effort has been expended in our laboratory related to the development of Pulsed Electrochemical Detection (PED) for application to polar aliphatic compounds separated by liquid chromatography (LC) [1-3]. In these applications of PED, multi-step potential-time (*E-t*) waveforms are applied at noble metal electrodes (Au and Pt) to obtain a sensitive and reproducible anodic response based on electrocatalytic mechanisms. The analytical significance of PED comes as the result of capability for direct detection of numerous aliphatic compounds that do not possess strong chromophoric and/or fluorophoric functional groups, including carbohydrates, alcohols, and amines [1-3]. The success of the PED technology has resulted in the commercial production of LC-PED systems by several instrument companies.

Efforts have been successful to extend PED at Au electrodes to a variety of organosulfur compounds, including thiocarbamates, thiophosphates, thiones, thiols, sulfides, and disulfides [4-9]. Whereas some problems can occur as a result of strong adsorption of these compounds and/or their decomposition products, with consequential loss of detector sensitivity and distortion of LC-PED peak shapes, these problems can be alleviated by careful design of the PED waveforms [8]. The most common PED waveform is shown in Figure 1A and consists of three distinct potential steps to achieve the sequential operations of anodic detection (E_{det}), oxidative cleaning of the electrode (E_{oxd}), and reductive reactivation of a clean and oxide-free surface (E_{red}). The detection

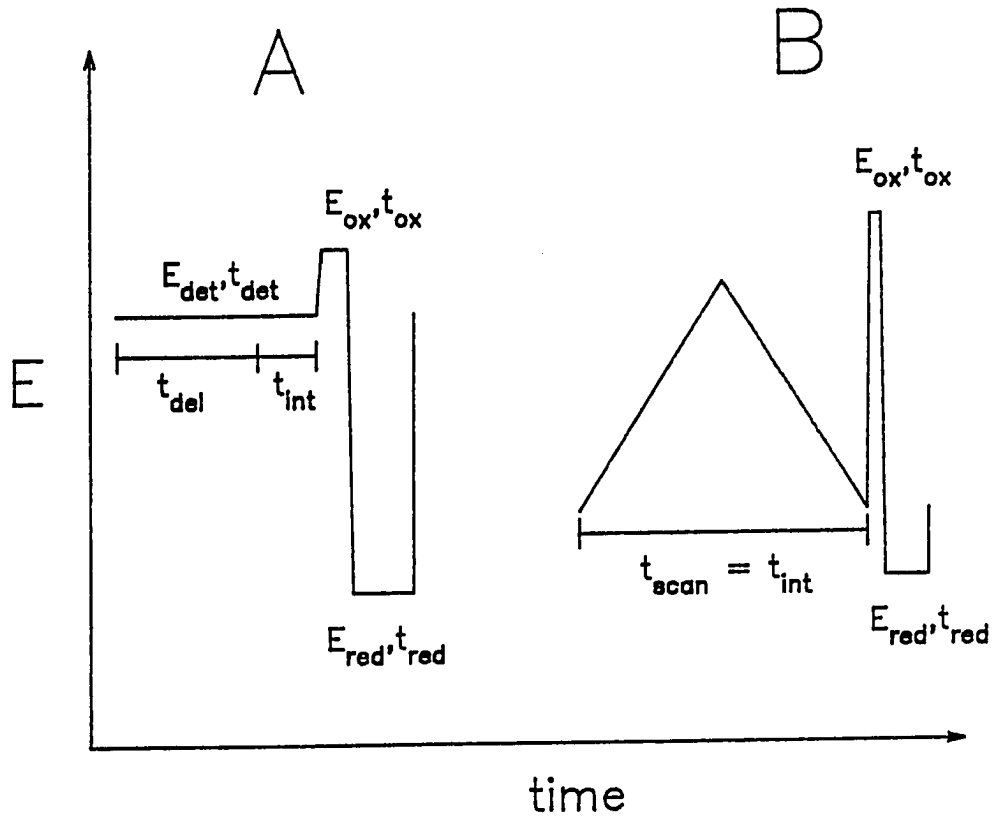

Figure 1. Potential-time (*E-t*) waveforms. (A) Pulsed amperometric detection (PAD): E_{det} = detection potential; t_{det} = detection time; t_{del} = delay time; t_{int} = integration time; E_{oxd} = oxidation potential; t_{oxd} = oxidation time; E_{red} = reduction potential; t_{red} = reduction time. (B) Integrated voltammetric detection (IVD): t_{scan} = scan time; t_{int} = integration time. See Table I for detailed description of IVD waveforms.

period (t_{det}) consists of a brief delay (t_{del}) to allow decay of background signals, e.g., double-layer charging current, followed by electronic integration of the electrode current (t_{int}). This detection scheme is known commonly as Pulsed Amperometric Detection (PAD) because the output voltage is commonly proportional to the estimated average electrode current for the period t_{int}. Alternately, the output signal can be proportional to the current integral.

Anodic detection of organosulfur compounds at Au electrodes occurs by an electrocatalytic mechanism requiring the concomitant formation of the intermediate surface oxide (AuOH) for the formation of the inert oxide (AuO) [4,8-9]. Thus, the total electrode signal in PAD applied for organosulfur compounds includes a very large background component from oxide formation. One approach suggested for minimizing this background current utilizes a so-called Activated-PAD waveform (APAD) in which a step to $E_{act} > E_{det}$ is applied briefly before the detection process to activate the electrode surface by generation of the active oxide (AuOH). The subsequent negative step from E_{act} to E_{det} greatly diminishes the background current from conversion of AuOH to AuO during the detection process [10]. Whereas APAD waveforms have been demonstrated to decrease the background signal, there is risk for very large values of E_{act} and/or long t_{act} that the active AuOH will be converted to the inert AuO prior to the detection step with a consequential loss in analytical response.

Another approach to decrease the background signal from oxide formation is illustrated by the waveform in Figure 1B. Accordingly, the total electrode current is electronically integrated throughout a rapid, cyclic staircase-scan of the detection

potential ($t_{int} = t_{scan}$) to achieve oxide formation with concurrent oxidative detection (pos. scan) followed by cathodic reduction of the surface oxide (neg. scan) [11-12]. Hence, the contribution to the total current integral from the anodic charge for oxide formation (pos. scan) is compensated by the cathodic charge for oxide reduction (neg. scan). Thereafter follows the usual positive and negative steps to achieve oxidative (E_{oxd}) and reductive (E_{red}) cleaning and reactivation, respectively, of the electrode surface. This procedure (Fig. 1B) was originally called Potential-Sweep Pulsed Coulometric Detection (PS-PCD); however, we prefer the shorter name Integrated Voltammetric Detection (IVD) to emphasize the nature of the process applied for signal measurement. In comparison to PAD, this waveform has been demonstrated to yield smaller baseline shifts associated with application of organic modifier gradients and small changes in pH [11-12].

Recently, we reported on the application of IVD for organic thiols, sulfides, and disulfides using a commercial instrument (Dionex Corp.) [9]. This instrument is also capable of performing PAD with an output signal that is proportional to the integral of electrode current for the period t_{int}. Hence, with this instrument, we are able to make a direct comparison of the response from PAD and IVD waveforms. Here, we discuss the selection of waveform parameters designs of PAD and IVD waveforms for application to organosulfur compounds, and compare linearity of response, detection limits, baseline stability, interference from O_2 in the samples, and the effect of an adsorption step inserted in the waveforms. Finally, LC-PED results are shown for mixture of several biologically important organosulfur compounds.

EXPERIMENTAL SECTION

Reagents. Solutions were prepared from reagent grade chemicals as received. L-cysteine and glutathione (reduced form) were from Aldrich; N-acetyl-L-cysteine, DL-homocysteine and glutathione (oxidized form) were from Sigma; and other chemicals were from Fisher Scientific. Tap water was treated in a serial fashion by passage through ion-exchange cartridges (Culligan) and a Milli-Q water purification system (Millipore). Chromatographic eluents were aspirated through a 0.20-μm filter prior to use to remove particulate matter. Stock aqueous solutions of cysteine and captopril were made fresh weekly and stored at 5°C. Chromatographic results indicated that oxidation of these thiols to the corresponding disulfides did not occur in the stock solutions. Test solutions were prepared immediately prior to use by dilution of appropriate aliquots of stock solutions.

Voltammetry. Voltammetric data were obtained using a Au rotated disk electrode (RDE, 0.178 cm^2), a MSR rotator and speed controller, and a RDE4 potentiostat (Pine Instrument). The RDE was polished daily with 0.05-μm alumina on microcloth (Buehler). The voltammetric cell (150 ml) was constructed from Pyrex with two side arms (5 ml) joined to the cell via fritted glass disks (medium porosity) to accommodate the reference and counter electrodes. The reference electrode in voltammetric studies was a saturated calomel electrode (SCE, 0.24 V vs. NHE; Fisher Scientific) and all potentials are reported with respect to the SCE. The counter electrode was a coiled Pt wire. The supporting electrolyte was 0.1 M $HClO_4$.

Dissolved O_2 was removed by dispersed N_2 (99.99%) and a N_2 atmosphere was maintained over test solutions during experimentation. Voltammetric data were recorded with a 386 IBM-compatible PC using a DAS-1602 interface and Asyst 4.0 software (Keithley-Metrabyte-Asyst).

Slow cyclic analog waveforms (100 mV s^{-1}) were generated within the RDE4 potentiostat. Pulsed waveforms were generated at the RDE4 potentiostat using the PC and Asyst software. Pulsed voltammetry consisted of a three-step PAD waveform applied to the RDE in which E_{det} (t_{det} = 360 ms) was scanned by 50-mV increments across the potential range of interest. Other parameters of the pulsed voltammetric waveform were as follows: E_{oxd} = 1.80 V (t_{ox} = 30 ms) and E_{red} = -0.40 V (t_{red} = 180 ms). The amperometric response for E_{det} was the average of 10 samples taken at 0.1-ms intervals following a delay of t_{del} = 300 ms. Fast cyclic staircase waveforms (4000 mV s^{-1}) were generated at the RDE4 potentiostat using the PC and Asyst software. The staircase consisted of 50-mV steps each having a duration of 12.5 ms with current sampling after a 3.75-ms delay.

Chromatography. The LC system consisted of a GPM-2 gradient pump and programmable PED system (Dionex). The detector cell was of the thin-layer design with a Au working electrode (1.5 mm^2), a 50-μm spacer, a Ag-AgCl reference electrode (0.20 V vs. NHE) and a stainless steel counter electrode. The cutout in the spacer defined the cell volume as *ca.* 1.5 μL. Separations were performed using OmniPac PCX-500 guard (4 x 50 mm) and analytical (4 x 250 mm) columns (Dionex).

These are so-called "mixed-mode" columns with both reverse-phase and cation-exchange characteristics. The injection valve was a model 7010 (Rheodyne) with a 50-μl sample loop. Eluent reservoirs were pressurized (ca. 5 psi) with N_2. LC-PED data were recorded by the PC using Snapshot software (HEM Data Corp.). Baseline noise (N) was estimated as the standard deviation of baseline fluctuations over 1-min intervals.

RESULTS AND DISCUSSION

Voltammetric Response for Cysteine in 0.1 M $HClO_4$. Acidic media were chosen for this study because of the selectivity of detection observed for PED at Au electrodes applied to organosulfur compounds at low pH [9]. Other classes of compounds known to be detected by PED at Au electrodes, including amines and carbohydrates, show little or no response at pH < *ca.* 9. Perchloric acid in particular was chosen because of its inertness at Au electrodes [13] and because of its use in prior studies involving PED of organosulfur compounds [9]. Cysteine (CYS) was chosen as the primary model compound for this study because it displays electrochemical character representative of that for thiols, sulfides and disulfides at Au electrodes [9].

The residual voltammetric (*i-E*) response for the Au RDE in 0.1 M $HClO_4$ is shown in Figure 2 by Curve a. This residual response has been discussed previously [9,13] and only a brief explanation of prominent features is given here. The region ca. -0.40 V to 0.80 V is the so-called "double-layer region". The region ca. 0.9 to 1.5 V (pos. scan) corresponds to formation of surface oxides (AuOH and AuO). Anodic evolution of O_2 occurs for E > ca. 1.5 V. The surface oxides are reduced during the negative scan to produce the cathodic peak in the region *ca.* 1.0 to 0.7 V. Cathodic detection of O_2, if present, occurs for E < ca. +0.2 V and cathodic evolution of H_2 occurs at E < ca. -0.5 V.

The voltammetric response for 20 μM CYS is shown in Figure 2 by Curve b. The most prominent feature of this response is the large anodic peak observed during

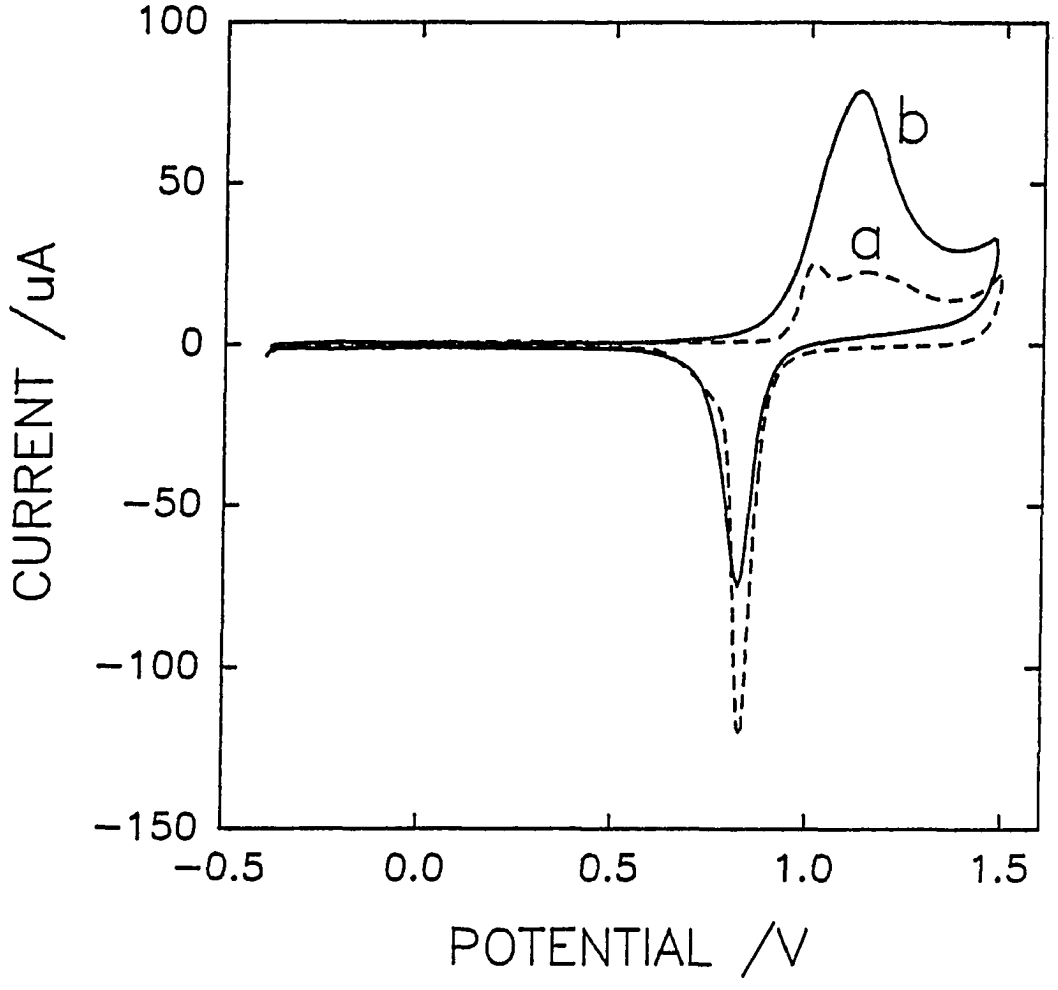

Figure 2. Voltammetric response at Au RDE in 0.1 M $HClO_4$. Rotation rate: 400 rev min^{-1}. Scan rate: 100 mV s^{-1}. Curves: (a) residual response, (b) 20 μM cysteine.

the positive scan concomitantly with formation of surface oxides (*ca.* 0.9 to 1.5 V). The height of this anodic peak signal, which has components from both the oxidation of CYS and formation of AuOH and AuO, exhibits small increases with increased rotation rate of the RDE and a linear dependence on changes in potential scan rate. This behavior is characteristic of reaction mechanism under mixed transport-surface control. It has been concluded [9,14] that the analytical signal for CYS at Au electrodes corresponds both to the oxidation of CYS that has been adsorbed during the potential scan throughout the region ca. 0.0 - 0.9 V as well as the oxidation of some CYS transported to the electrode surface simultaneously with oxide formation. The anodic response of CYS is severely diminished by formation of the inert surface oxide (AuO) and nearly ceases upon reversal of the scan direction at 1.5 V. Because Au electrodes quickly become passivated by AuO formed in the region 1.0 - 1.5 V, organosulfur compounds are generally not detectable at Au electrodes under conditions of constant (dc) potential. The cathodic peak area for oxide reduction (neg. scan) obtained in the presence of CYS (Fig. 2, curve b) is smaller than that for the absence of CYS (curve a). This is interpreted to be an indication that the presence of CYS has a slight inhibiting effect on the rate and/or extent of oxide formation.

It is important to note, when constructing PED waveform, that careful consideration must be made of the control of solution pH. The detection of organosulfur compounds at Au electrodes requires concomitant the formation of surface oxides, which is dependent on pH. Thus, the potential values specified here for PAD and IVD waveforms are optimal only for 0.1 M $HClO_4$.

Selection of PAD Waveform Parameters. The voltammetric response obtained at slow scan rates for any particular compound can be helpful in selection of the appropriate values for E_{det} in PAD waveforms to be applied for that compound. For example, based on Figure 2 (Curve b), it is anticipated that E_{det} = 1.15 V is appropriate in PAD waveforms applied to organosulfur compounds in 0.1 M $HClO_4$. However, optimal values of E_{oxd} and E_{red}, as well as all timing parameters in PAD waveforms, cannot be selected merely on the basis of the voltammetric response obtained with relatively slow scan rates. Hence, it is recommended that further optimization of PAD waveforms must be based on pulsed voltammetric response as described previously [8,10,15]. For example, Figure 3 contains the pulsed voltammetric response obtained in the absence (Curve a) and presence (Curve b) of 20 μM CYS. These data were obtained using a three-step PAD waveform (Fig. 1A) in which E_{det} was caused to scan according to a staircase waveform through the region -0.2 to 1.5 V. Hence, these data show exactly the PAD response at the Au RDE as a function of E_{det} for the fixed values of the remaining waveform parameters as listed in the figure caption. This pulse voltammetric response clearly shows that surface oxide formation occurs for E_{det} > 1.0 V with concomitant anodic response for CYS. Hence, useful values of E_{det} are in the range ca. 1.1 to 1.3 V and we have selected 1.30 V for this study. Based on additional data (not shown) obtained by pulsed voltammetry, the following values were selected for the remaining parameters of the PAD waveform: t_{del} = 300 ms and t_{int} = 100 ms, i.e., t_{det} = 400 ms; E_{oxd} = 1.50 V (t_{oxd} = 50 ms); and E_{red} = -0.40 V (t_{red} = 120 ms). The t_{int} chosen is consistent with that used in the

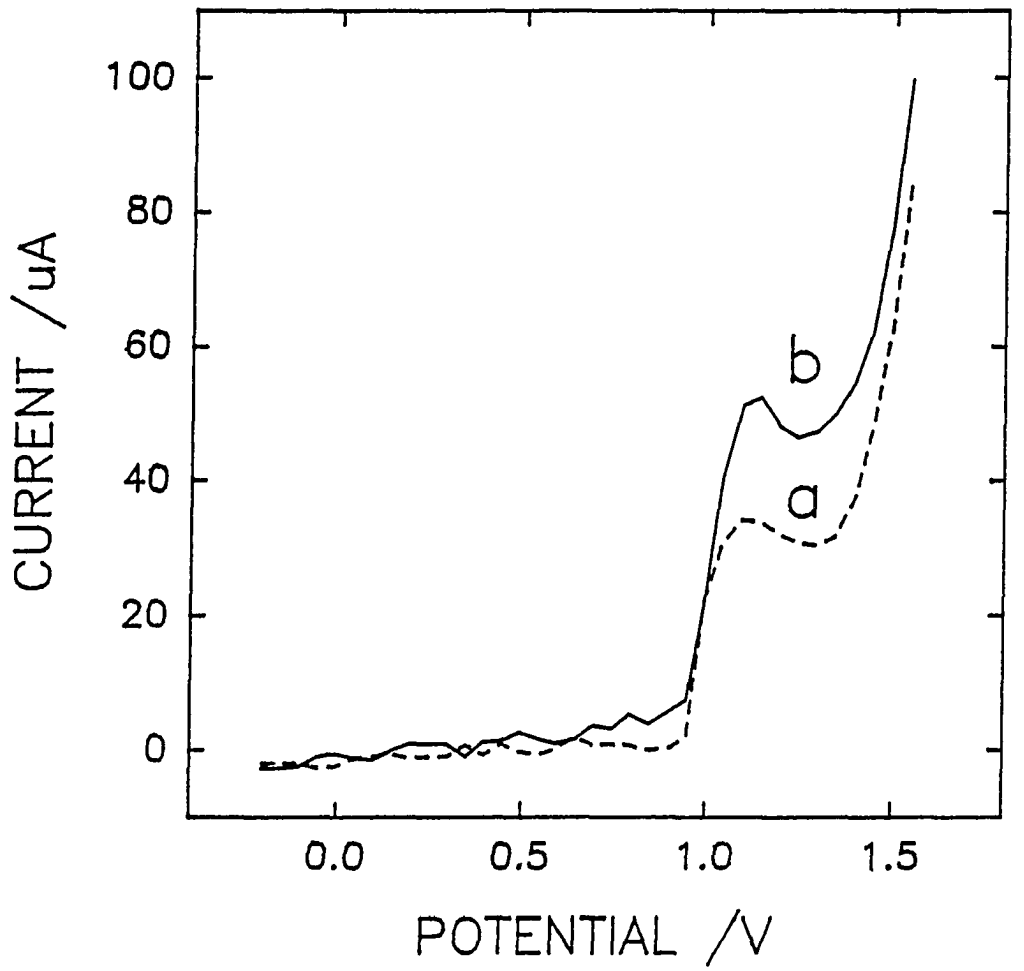

Figure 3. Pulsed voltammetric response for 20 μM cysteine at Au RDE in 0.1 M $HClO_4$. Rotation rate: 900 rev min^{-1}. PAD waveform: E_{det} = varied, t_{det} = 360 ms, t_{del} = 300 ms, t_{int} = 60 ms; E_{oxd} = 1.80 V, t_{oxd} = 30 ms; E_{red} = -0.40 V, t_{red} = 180 ms; ΔE_{det} = 50 mV. Curves: (a) residual response, (b) 20 μM cysteine.

Dionex PAD-2 system which was used in earlier work with organosulfur compounds [8]. The value chosen for t_{del} allows for significant decay of current from oxide formation prior to sampling the analytical response. Shorter values of t_{del} resulted in high background signals and longer values resulted in significant loss of signal strength because of electrode passivation by inert oxide (AuO). Because AuO is formed during the detection step in waveforms applied to organosulfur compounds, choice of E_{oxd} and t_{oxd} are not critical [11]. Indeed, E_{oxd} can be varied in increases in the range 1.5 to 1.9 V with little negative effect on the CYS signal; however, choice of $E_{oxd} > 1.9$ V resulted in excessive baseline noise in LC-PAD, probably because of the accumulation of small O_2 bubbles on the electrode surface. The optimal value indicated for E_{red} was chosen to achieve cathodic desorption of decomposition productions observed for some organosulfur compounds [8,9] with negligible evolution of H_2.

Selection of IVD Waveform Parameters. In produce an IVD waveform having a frequency of ca. 1 Hz, which is necessary for accurate description of LC-IVD peak shapes, the value of E_{det} must be scanned very fast (ca. 3000 - 5000 mV s^{-1}). This scan rate is considerably faster than used in conventional voltammetry, such as that shown in Figure 2 (100 mV s^{-1}). Hence, selection of the optimal range for the cyclic scan of E_{det} in IVD requires examination of the voltammetric response obtained at scan rates to be applied in IVD. The results of fast-scan cyclic staircase voltammetry are shown in Figure 4A for the absence (Curve a) and presence (Curve b) of 40 μM CYS. It is apparent from a comparison of these *i-E* curves with those in

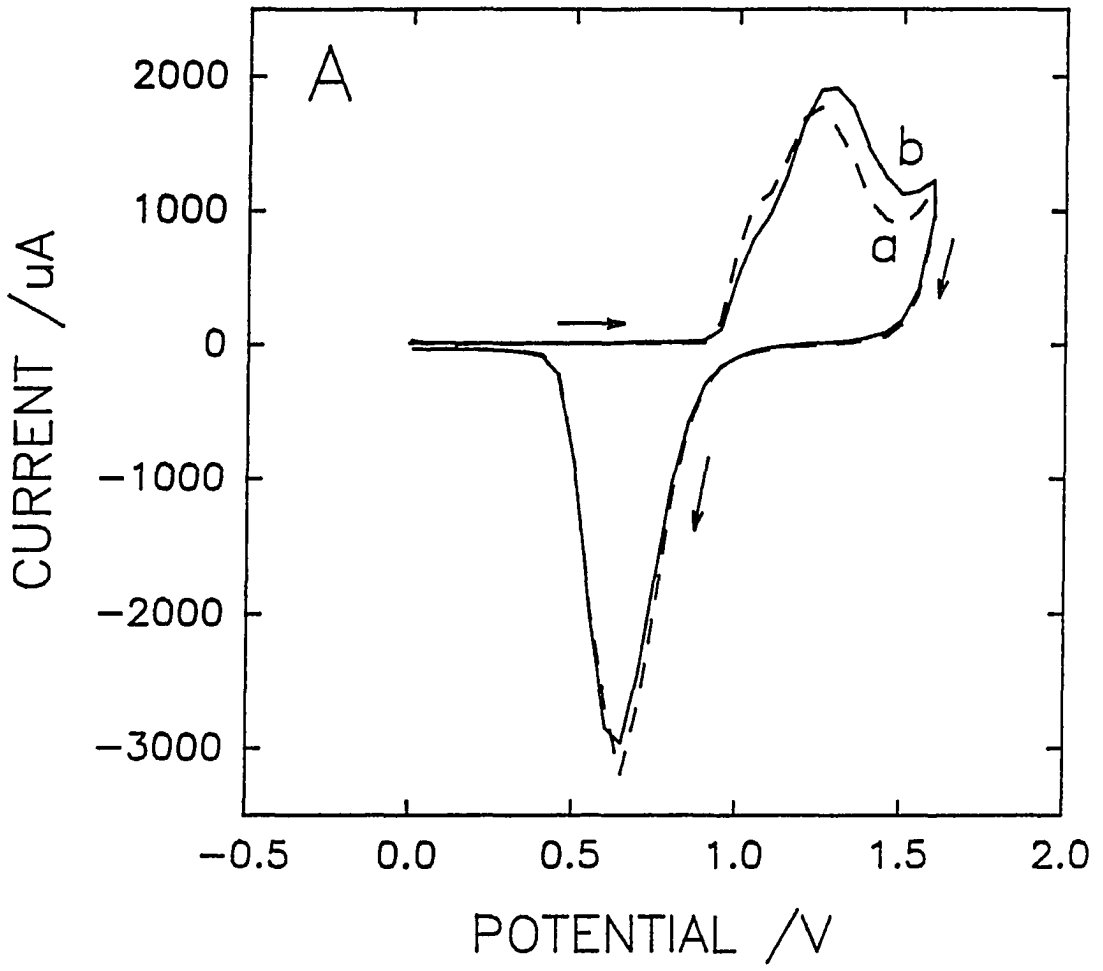

Figure 4A. Voltammetric response using a rapid-scan staircase waveform for cysteine at Au RDE in 0.1 M $HClO_4$. Rotation rate: 900 rev min^{-1}. Scan rate: 4000 mV s^{-1}. Potential step: 50 mV. Step duration: 12.5 ms. Delay prior to current measurement: 3.75 ms. Curves: (a) residual, (b) 40 μM cysteine.

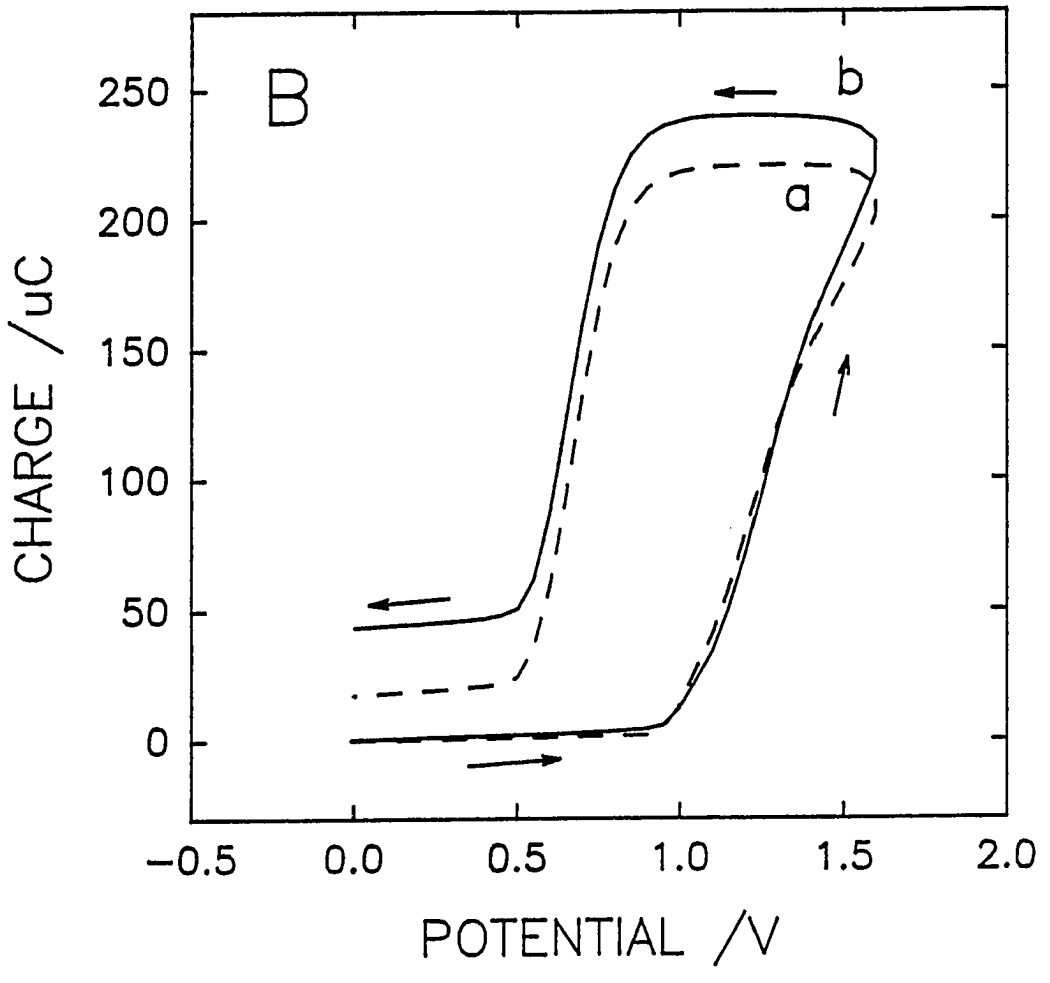

Figure 4B. Integrated voltammetric response using a rapid-scan staircase waveform for cysteine at Au RDE in 0.1 M $HClO_4$. Rotation rate: 900 rev min^{-1}. Scan rate: 4000 mV s^{-1}. Potential step: 50 mV. Step duration: 12.5 ms. Delay prior to current measurement: 3.75 ms. Curves: (a) residual, (b) 40 μM cysteine.

Figure 2 that the maximum rate of oxide formation is shifted from ca. 1.0 for the slow scan (Fig. 2) to ca. 1.3 V for the fast scan (Fig. 4). Furthermore, for the fast scan (Fig. 4), oxide reduction (neg. scan) continues to ca. 0.3 V whereas for the slow scan (Fig. 2) oxide reduction was complete at ca. 0.6 V. It is also apparent that the anodic response for CYS represents a much smaller fraction of the total signal for the fast scan in comparison to the slow scan. This is believed to be the consequence of the shorter time spent in the region of CYS adsorption for the fast scan rate prior to the oxidative detection process.

The large contribution from the charge for oxide formation to the total anodic signal can be virtually eliminated in IVD by electronic integration of the electrode current during the cyclic scan of potential throughout the range for oxide formation (pos. scan) and subsequent oxide reduction (neg. scan). This technique is illustrated by the curves in Figure 4B obtained in the absence (Curve a) and presence (Curve b) of 40 μM CYS. Whereas a very large anodic charge is accumulated from oxide formation (ca. 200 μC) during the positive scan in Curve a, the net signal is only ca. 15 μC at the conclusion of the negative scan. The majority of this remaining signal is the result of O_2 evolution at $E >$ ca. 1.5 V and can be virtually eliminated by decreasing the positive scan limit from 1.6 V to 1.4 V. Based primarily on these results, IVD waveform A was developed (see Table I), which consisted of a fast cyclic scan of E_{det} from 0.00 to 1.40 V and back to 0.00 V, during an 800-ms period, with simultaneous current integration ($t_{int} = t_{scan} = t_{det}$). This cyclic scan was followed by oxidative cleaning at E_{oxd} = 1.80 V (t_{oxd} = 30 ms) and reductive reactivation at E_{red} = -0.40 V

Table I. Description of IVD waveforms.

IVD Waveform A		IVD Waveform B	
time (ms)	potential (V vs. SCE)	time (ms)	potential (V vs. SCE)
0	0.00	0	0.30
400	1.40	400	1.40
800	0.00	800	0.30
810	1.80	810	1.80
840	1.80	840	1.80
850	-0.40	850	-0.40
970	-0.40	970	-0.40
integration: 10 - 800 ms		integration: 10 - 800 ms	

(t_{red} = 120 ms). Application of this waveform to the Au electrode in the flow-through cell yielded a total residual charge of ca. 20 μC for the positive scan; however, the net charge remaining for integration over the entire cyclic scan was routinely only in the range 300 - 600 nC.

Linearity of Response and Limits of Detection. In order to compare limits of detection and linear dynamic range, calibration curves were constructed from LC-PED data for CYS obtained with the PCX-500 guard column (4 x 50 mm) using the PAD waveform described above and the IVD waveform A in Table I. The eluent was 0.1 M $HClO_4$ at a flow rate of 0.8 mL min^{-1}. The CYS concentrations spanned the range 0.10

- 1000 μM. Linear regression analysis of LC-PAD data revealed a linear response in the range 0.10 - 100 μM with a sensitivity of 7.50 nC μM^{-1} (N = 30, R^2 = 0.9993). The LOD for LC-PAD (S/N = 3) was estimated to be 77 nM (3.9 pmol, 470 ng). Similarly, linear regression analysis of LC-IVD data revealed a linear response for CYS in the range of 0.10 - 100 μM with a sensitivity of 58.35 nC μM^{-1} (N = 30, R^2 = 0.9975). The limit of detection (LOD) for LC-IVD was estimated for S/N = 3 to be 21 nM CYS (1.1 pmol, 130 pg). Hence, the sensitivity of IVD in this study was ca. 7.8X greater than that of PAD. Negative deviation from linearity occurred for both the IVD and PAD waveforms at concentrations above 100 μM CYS.

Baseline Drift. Neuburger and Johnson [11] observed for oxide-catalyzed detection mechanisms that the baseline signal for IVD equilibrated more rapidly than for PAD following the polishing of the electrode surfaces. Because of the larger background signals in PAD applied for oxide-catalyzed detection mechanisms, any factors that alter the amount of oxide formed will result in significant change to baseline response in LC-PAD. Thus, the large background signal produced by PAD applied to a freshly polished electrode is expected to drift until the surface area has reached an equilibrium value and no longer changes as a result of surface reconstruction due to the oxide formation-dissolution cycles. Conversely, the IVD waveform provides automatic compensation for oxide formation and, therefore, baseline drift is expected to be less of a problem [11]. Furthermore, the larger sensitivity of IVD in comparison to PAD will decrease the relative significance of

baseline changes in the IVD.

The expectations enumerated above are verified by LC-PAD and LC-IVD data shown in Figure 5 for injection of 10 μM CYS and obtained immediately after polishing the Au electrode in the flow-through cell. The scaling of the response axes in Figure 5 was selected to give comparable peak heights for CYS. Clearly, the initial extent of baseline drift relative to the peak signal for CYS is much greater for the PAD waveform (Fig. 5A) than for the IVD waveform (Fig. 5B). Furthermore, the PAD baseline was observed to drift for several hours whereas the IVD baseline was steady after ca. 10 min.

Elimination of System Peak for O_2 in the Sample. Several workers have noted the appearance of a peak resulting from O_2 dissolved in the sample injected into a LC-PAD system [9,15-17]. This peak generally appears several minutes after elution of the column void volume and can interfere with quantitation of co-eluting analytes. The O_2 peak is particularly troublesome for the presence of acetonitrile (MeCN) in the mobile phase because of the increased solubility of O_2 is these modified phases. Reduction of the O_2 peak has been achieved by careful matching of the O_2 content in the sample diluent and the mobile phase; however, total elimination of the peak is difficult [9]. An effort was made to better understand the effect of O_2 dissolved in the injected sample by examining the O_2 peak as a function of sample treatment using an eluent of 0.1 M $HClO_4$ containing 5% MeCN. Blank injections of O_2-saturated H_2O were made to confirm that the peak was indeed caused by O_2. In

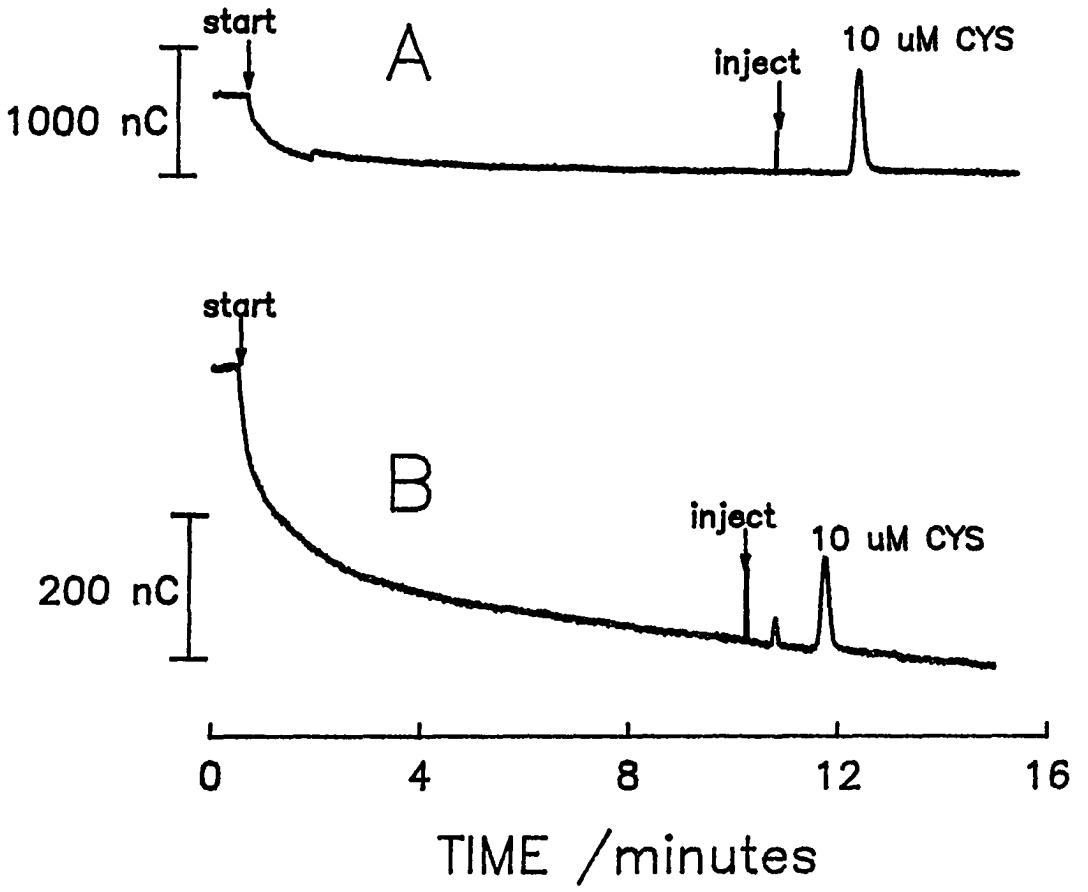

Fig. 5. LC-PED baseline response after polishing electrode. Column: Dionex PCX-500 guard. Eluent: 0.1 M $HClO_4$. Flow Rate: 0.8 mL min^{-1}. Curves: (A) Response for IVD waveform. (see Table I., Waveform B). (B) Response for PAD waveform. E_{det} = 1.30 V, t_{det} = 400 ms, t_{del} = 300 ms, t_{det} = 100 ms; E_{ox} = 1.50 V, t_{ox} = 50 ms; E_{red} = -0.40 V, t_{red} = 120 ms.

contrast, blank injections of vacuum-degassed H_2O resulted in large reduction, if not total elimination, of this peak. Based on results of these experiments, we are in agreement with Rocklin [17] that the O_2 peak obtained for LC-PAD is the result of the anodic detection at E_{det} of H_2O_2 produced by reduction of O_2 simultaneously with surface reactivation at E_{red}.

Samples of air-saturated 0.1 M $HClO_4$ containing 1.0 μM CYS were injected into the LC system used to obtain data in Figure 5 and the relative sizes of the O_2 peaks were compared for the PAD and IVD waveforms. These results are shown in Figure 6. The LC-PAD data (Fig. 6A) exhibit a typical O_2 peak. The LC-IVD data (Fig. 6B) were obtained using Waveform A (Table I) in which the lower scan limit of E_{det} was 0.00 V. This potential is sufficiently negative to cause reduction of O_2 and, therefore, a large cathodic peak is obtained. When the lower scan limit in the IVD waveform was increased from 0.00 V to 0.30 V (Waveform B, Table I), O_2 was not detected and the peak was virtually eliminated with little effect on the CYS peak (Fig. 6C). Based on these data, we recommend Waveform B for IVD if interference from dissolved O_2 is a problem. However, raising the lower scan limit from 0.00 to 0.30 V resulted in a slight increase in the total background signal from about 500 to 1200 nC. This occurred because the surface oxide is not completely reduced during the negative scan to 0.30 V (see Fig. 4).

Effect of a Preadsorption Step in PAD and IVD Waveforms. In earlier studies of thiourea response at Au electrodes in alkaline media, we determined that

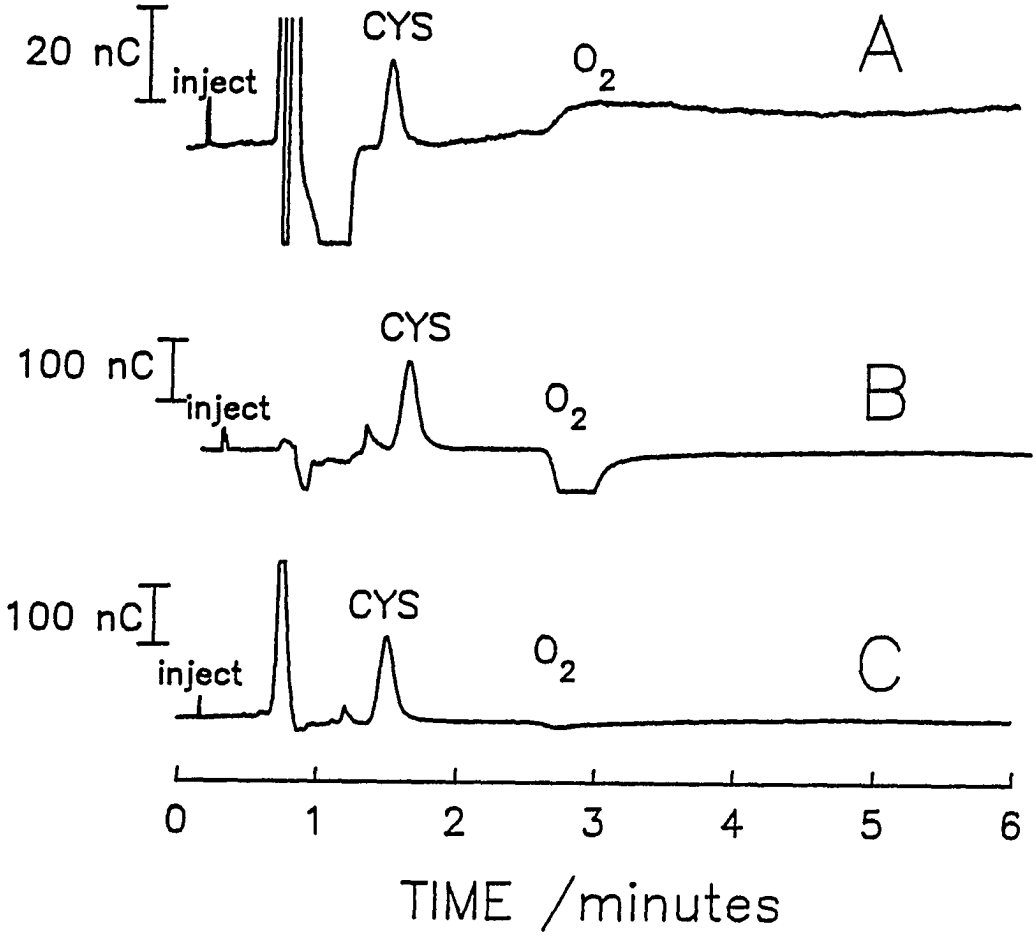

Figure 6. Response from O_2 in injection sample. Column: Dionex PCX-500 guard. Eluent: 0.1 M $HClO_4$ with 5% acetonitrile. Flow rate: 0.8 mL min^{-1}. Sample: 1.0 μM cysteine in H_2O. Curves: (A) PAD waveform, (B) IVD Waveform A, (C) IVD Waveform B.

PAD response could be increased slightly by addition of a potential step in the waveform to permit adsorption of the analyte after reductive reactivation and prior to detection ($E_{rcd} < E_{ads} < E_{det}$) [8]. The PAD and IVD waveforms used to obtained data shown in Figures 6A and 6C, respectively, were modified to incorporate an adsorption step prior to the detection step. In the PAD waveform, adsorption was permitted to occur at E_{ads} = 0.20 V (variable t_{ads}). In the IVD Waveform B, adsorption was permitted to occur at E_{ads} = 0.30 V (variable t_{ads}) prior to the fast cyclic scan of E_{det} originating from 0.30 V. LC-PAD and LC-IVD data were obtained for solutions containing 1.0 μM CYS as a function of t_{ads} in the range 0 - 1000 ms and the peak signals are shown plotted vs. t_{ads} in Figure 7 where the linear regression statistics are represented by the dashed lines. Clearly, the peak responses for both waveform increase as a virtually linear function of t_{ads}. This behavior suggests that full surface coverage by CYS has not yet been reached even at t_{ads} = 1000 ms for 1.0 μM CYS and, therefore, the peak signals are expected to be increased more by use of t_{ads} > 1000 ms. Ratios of the peak signals for IVD and PAD (S_{IVD}/S_{PAD}) decreased from ca. 8.5 at t_{ads} = 0 ms to ca. 6.4 for t_{ads} = 1000 ms. Based on the increased signal that resulted from inclusion of the preadsorption step (t_{ads} = 1000 ms) for 1.0 μM CYS, limits of detection for CYS are decreased to ca. 10 nM (0.50 pmol, 60 pg) for LC-IVD and 29 nM (1.5 pmol, 180 pg) for LC-PAD.

Previously, it was speculated for PAD that a large percentage of the adsorbed sulfur compound is oxidatively desorbed from the Au surface during the delay period following application of E_{det} with a consequential loss of anodic signal [8]. Conversely,

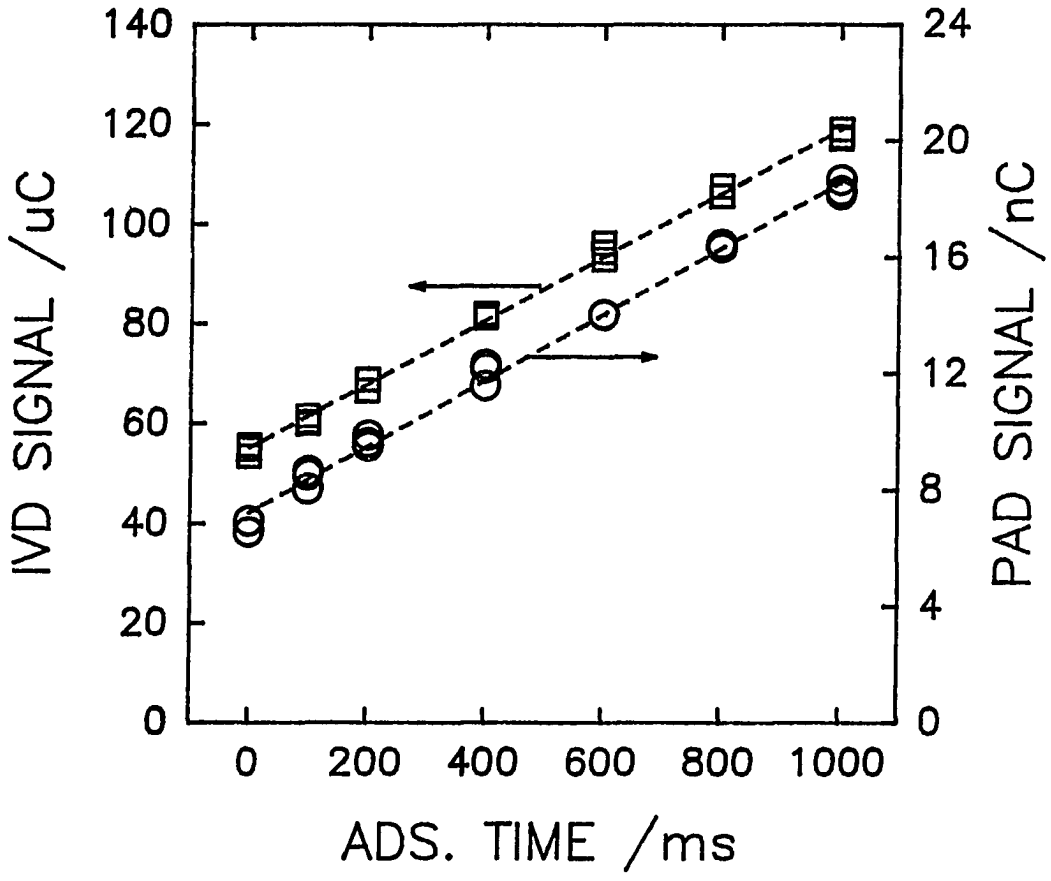

Figure 7. LC-PED Peak height for 1.0 μM cysteine as a function of adsorption step time. Column: Dionex PCX-500 guard (4 x 50 mm). Eluent: 0.1 M $HClO_4$. Flow Rate: 0.8 mL min^{-1}. Curves: (□) IVD Waveform B, E_{ads} = 1.30 V. (O) PAD waveform, E_{ads} = 0.20 V.

in IVD, the total current resulting from oxidation of all adsorbed CYS is measured. Therefore, it was expected that the benefit from use of a preadsorption step would be most significant for IVD. At present, we cannot explain the observation that the preadsorption step has a large beneficial effect on PAD signals.

Three successive LC-PED peaks are shown in Figure 8 for 1.0 μM CYS obtained using the IVD Waveform A (A & B) and the PAD waveform (C & B) with t_{ads} = 0 ms (A & C) and 1000 ms (B & D). System peaks from elution of the void volumes have been removed. For the IVD waveform, the relative standard deviation (rsd) for three injections was 1.3% for t_{ads} = 0 s (A) and 0.8% for t_{ads} = 1000 ms (B). For the PAD waveform, the rsd was 3.1% for t_{ads} = 0 (C) and 1.4% for t_{ads} = 1000 ms (D). Hence, it is apparent that despite the narrow peaks (*ca.* 9 s FWHM), reproducibility is still acceptable for IVD in spite of the decreased sampling frequency associated with use of the long adsorption time (B). It is also apparent from Figure 8 that the S/N is significantly better for the IVD waveform in comparison to the PAD waveform.

Application of LC-IVD for Mixtures of Organosulfur Compounds. To demonstrate the capabilities of LC-IVD using Waveform B (Table I), a mixture of seven biologically important organosulfur compounds was separated on the PCX-500 analytical column (4 x 250 mm). Represented in the mixture are four thiols: cysteine (CYS), reduced glutathione (GSH), acetylcysteine (ACYS) and homocysteine (HCYS); one sulfide: methionine (MET); and two disulfides: oxidized glutathione (GSSG) and

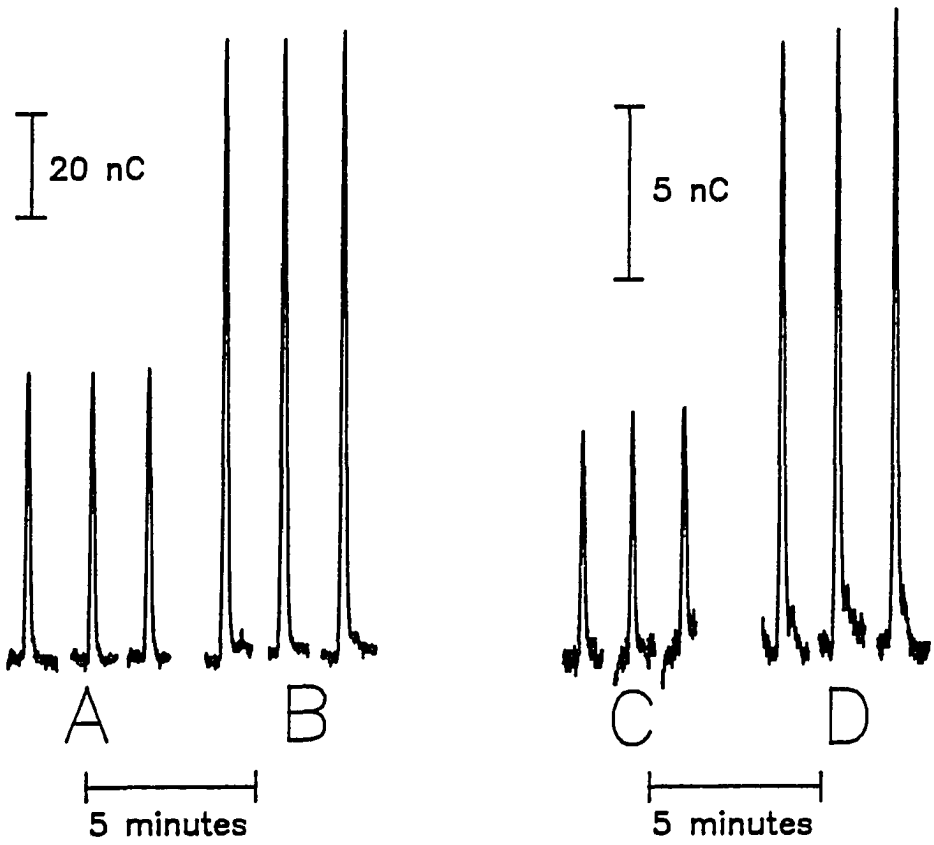

Figure 8. LC-PED response for 1.0 μM cysteine. Column: Dionex PCX-500 guard. Eluent: 0.1 M $HClO_4$. Flow rate: 0.8 mL min^{-1}. Curves: (A) IVD Waveform B with t_{ads} = 0 ms, (B) IVD Waveform B with t_{ads} = 1000 ms, (C) PAD waveform, t_{ads} = 0 ms, (D) PAD waveform, t_{ads} = 1000 ms.

cystine (CYS_2). All concentrations were 10.0 μM except for CYS which was 5.0 μM. Results in Figure 9A correspond to IVD Wave B without a preadsorption step (t_{ads} = 0 ms) and results in Figure 9B correspond to addition of a preadsorption at E_{ads} = 0.30 V (t_{ads} = 1000 ms). A significant increase in response is observed for each compound as a result of the preadsorption step in the IVD waveform. Furthermore, no system peak for O_2 is observed in these data.

It is very significant that both thiols and disulfides are detected by IVD with comparable sensitivity. Other detection procedures described for these compounds in LC require multiple derivatization steps [18] or derivatization at an amine [19], which results in loss of selectivity. Hence, LC-IVD makes possible the study of the biologically important thiol-disulfide couple with relatively little sample preparation. In also is significant that organic sulfides are detected by IVD.

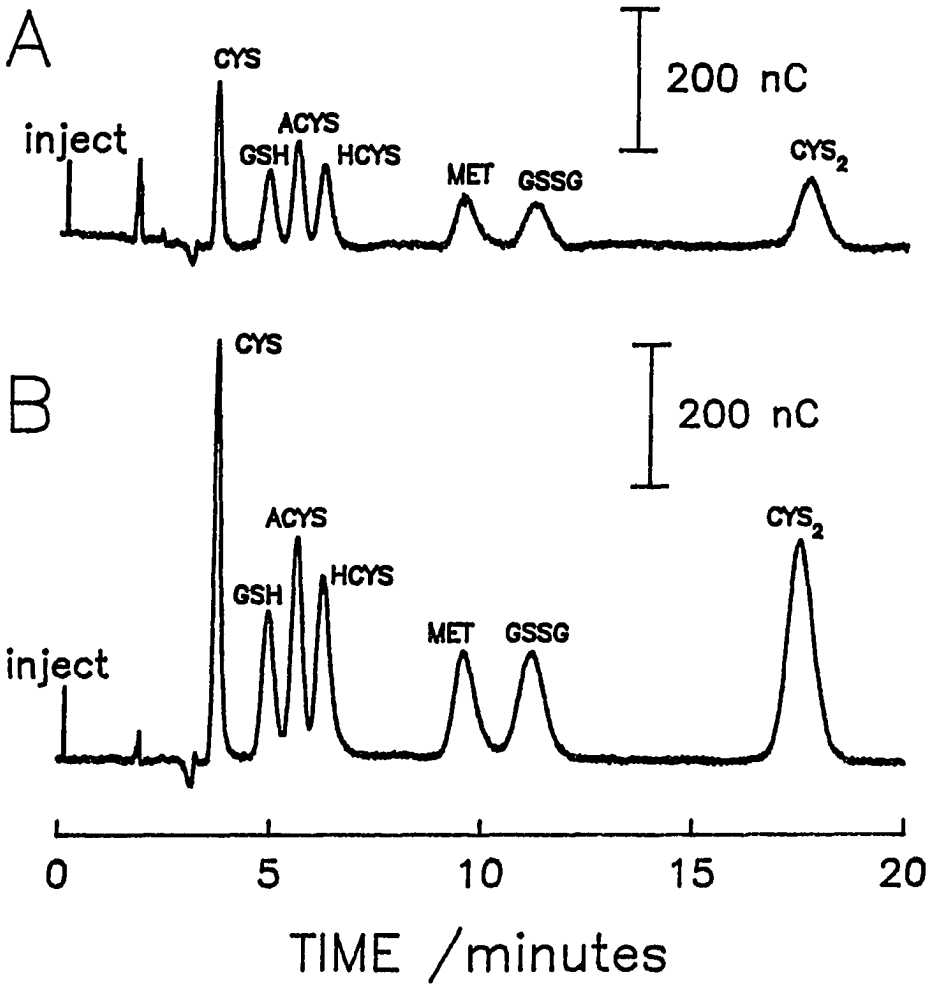

Figure 9. LC separation of biologically important organic sulfur compounds with detection by IVD Waveform B. Column: Dionex PCX-500 analytical. Eluent: 0.10 M $HClO_4$/0.18 $NaClO_4$ with 5% acetonitrile. Flow rate: 1.2 mL min^{-1}. Sample composition: 5.0 μM cysteine (CYS) and 10 μM each reduced glutathione (GSH), acetylcysteine (ACYS), homocysteine (HCYS), methionine (MET), oxidized glutathione (GSSG), and cystine (CYS_2) in H_2O. Curves: IVD Waveform B with (A) no adsorption step and (B) with adsorption step, E_{ads} = 0.30 V, t_{ads} = 1000 ms, prior to detection scan.

CONCLUSIONS

Based on the results shown here, we recommend IVD over PAD in applications at Au electrodes in acidic media for detection of organosulfur compounds following their separation by LC. Advantages of IVD include higher sensitivity, lower noise with a corresponding decrease in detection limit by ca. 4X, and the ability to virtually eliminate the system peak for dissolved O_2. Also improvement is the more rapid equilibration of baseline signal following electrode polishing and decreased response to changes in the mobile phase including additions of organic modifiers and small changes in pH [11,12].

It is significant also that addition of a preadsorption step can improve signal response by a factor of two to three for both IVD and PAD waveforms. Although an adsorption step can be used to increase signal for these PED waveforms, we caution users of this technique that waveforms requiring a long execution time, i.e., low frequency, can result in poor peak definition for very narrow LC peaks.

ACKNOWLEDGEMENTS

This research was supported by grants CHE-8914700 and CHE-9215963 from the U.S. National Science Foundation.

REFERENCES

1 D.C. Johnson and W.R. LaCourse, *Anal. Chem.*, 62 (1990) 589A.

2 D.C. Johnson and W.R. LaCourse, *Electroanal.*, 4 (1992) 367.

3 D.C. Johnson, D.A. Dobberpuhl, R.A. Roberts and P.J. Vandeberg, *J. Chromatogr.*, 640 (1993) 79.

4 T.Z. Polta and D.C. Johnson, *J. Electroanal. Chem.*, 209 (1986) 159.

5 M.V. Thomas and P.E. Sturrock, *J. Chromatogr.*, 357 (1986) 318.

6 A. Ngoviwatchai and D.C. Johnson, *Anal. Chim. Acta*, 215 (1988) 1.

7 D.R. Doerge and A.B.K. Yee, *J. Chromatogr.*, 586 (1991) 158.

8 P.J. Vandeberg, J.L. Kawagoe and D.C. Johnson, *Anal. Chim. Acta*, 260 (1992) 1.

9 P.J. Vandeberg and D.C. Johnson, *Anal. Chem.*, 65 (1993) 2713-2718.

10 D.G. Williams and D.C. Johnson, *Anal Chem.*, 64 (1992) 1785.

11 G.G. Neuburger and D.C. Johnson, *Anal. Chem.*, 60 (1988) 2288.

12 L.E. Welch, W.R. LaCourse, D.A. Mead, Jr., and D.C. Johnson, *Anal. Chem.*, 61 (1989) 555.

13 H. Angerstein-Kozlowska, B.E. Conway, A. Hamelin and L.Stoicoviciu, *Electrochim. Acta*, 31 (1986) 1051.

14 Fawcett et al., *J. Electroanal. Chem.*, in review. (I'll hunt for more information.)

15 W.R. LaCourse and D.C. Johnson, *Anal. Chem.*, 65 (1993) 50.

16 W. Fiddler and R.C. Doerr, *Current Separations.*, 6 (1985) 50.

17 Roy Rocklin, Dionex Corp., Sunnyvale, CA; Personal communication: 1992.

18 T. Toyo'Oka, S. Uchiyama, Y. Saito and K. Imai, *Anal. Chim. Acta*, 205 (1988) 29.

19 D.J. Reed, J.R. Babson, P.W. Beatty, A.E. Brodie, W.W. Ellis and D.W. Potter, *Anal. Biochem.*, 106 (1980) 55.

GENERAL CONCLUSIONS

Sulfur compounds, which adsorb very strongly to the Au surface and may decompose, provide a great challenge for the application of PED. Adequate oxidative cleaning and cathodic regeneration steps must be used to maintain reproducible electrode response. The surface oxide formation, which is necessary for the oxidation of sulfur compounds, causes a large background signal. This background may be eliminated by application of an integrated voltammetric detection waveform, which measures current over both the formation and the reduction of the surface-oxide, resulting in the subtraction of that surface oxide. The IVD waveform makes PED more applicable for use with gradients where changes in pH or organic modifier may affect the surface oxide formation.

The strong adsorption characteristics of organic sulfur compounds at Au may be taken advantage to enhance detection. A low pH can be used for the detection of organic sulfur compounds to eliminate the interference of compounds which are electroactive at high pH, including carbohydrates and amines. In addition, Acetonitrile, which adsorbs to the electrode surface, may be used to block the signal from compounds which adsorb less strongly, yet acetonitrile has little effect on the detection of sulfur species.

In addition to investigations into the electrochemistry and detection process, many applications of PED detection of organic sulfur compounds were presented. The separation and detection of biologically important compounds was demonstrated.

LITERATURE CITED

1. Vetter, R.D.; Matrai, P.A.; Javor, B.; O'Brien, J. in *Biogenic Sulfur in the Environment*, Saltzman, E.S. and Cooper, W.J. Ed.; American Chemical Society, Washington, D.C., 1989; pp 243-269.

2. U.S. Deprtment of Health and Human Services, *Fourth Annual Report on Carcinogens,* GPO, Washington, DC, 1987, p. 208.

3. Bernstein, P.; Hull, M.N., *J. Electroanal. Chem.*, **1970**, *28*, A1-A5.

4. Meister, A. in *Glutathione: Chemical, Biochemical, and Medical Aspects, Part A*, Dolphin, D.; Poulson, R.; Avramovic, O. Ed.; Wiley: New York, 1989, 1-38.

5. Meister, A.; Griffith; O.W. *Cancer Treat. Rep.*,**1979**, *63*, 1115-1121.

6. Chasseaud, L.F. in *Glutathione Conjugation: Mechanisms and Biological Significance*, Sies, H.; Ketterer, B. Ed.; Academic Press: London, 1988; pp. 391-413.

7. Huber, R.E.; Edwards, L.A. in *Glutathione: Chemical, Biochemical, and Medical Aspects, Part A*, Dolphin, D.; Poulson, R.; Avramovic, O. Ed.; Wiley: New York, 1989, 50-51

8. Hogendoorn, E.A.; van Zoonen, P.; Brinkman, U.A.; *Cromatographia*, **1991**, *31*, 285-292.

9. Wauters, D.; De Mol J.; De Temmerman, L. *J. Chromatogr.*, **1990**, *516*, 375-382.

10. Stryer, L. *Biochemistry* 3rd. ed.; Freeman, W.H.: New York, 1988; chapt. 3.

11. Reed, D.J.; Babson, J.R.; Beatty, P.W.; Brodie, A.E.; Ellis, W.W.; Potter, D.W. *Anal. Biochem.* **1980**, *106*, 55-62.

12. Henderson, P.T.; van Doorn, R., Leijdekkers, C.M.; Bos, R.P. *IARC Sci. Publ.*, **1984**, *59*, 173-187.

13. Bossle, P.C.; Martin, J.J.; Sarver, E.W.; Sommer, H.Z. *J. Chromatgr.* **1984**, *283*, 412-416.

14. Fahey, R.C.; Newton, G.L.; Doran, R.; Kosower, E.M. *Anal. Biochem.*, **1980**, *107*, 1-10.

15. Fahey, R.C.; Newton, G.L.; Doran, R.; Kosower, E.M. *Anal. Biochem.*, **1981**, *111*, 357-365.

16. Toyo'oka, T.; Imai, K. *J. Chromatgr.*, **1983**, *282*, 495-500.

17. Toyo'oka, T.; Uchiyama, S.; Saito, Y.; Imai, K. *Anal. Chim. Acta*, **1988**, *205*, 29-41.

18. Ling, B.L.; Baeyens, W.R.G.; Marysael, H.; Imai, K. *Anal. Chim. Acta*, **1989**, *227*, 203-209.

19. Jones, D.P.; Coates, R.J.; Flagg, E.W.; Eley, J.W.; Block, G.; Greenberg, R.S.; Gunter, E.W.; Jackson, B. *Nutr. and Canc.*, **1992**, *17*, 57-75.

20. Allison, L.A.; Shoup, R.E. *Anal. Chem.*, **1983**, *55*, 8-12.

21. Werkhoven-Goewie, C.E.; Niessen, W.M.A.; Brinkman, W.A.Th.; Frei, R.W. *J. Chromatogr.*, **1981**, *203*, 165-172.

22. Hanekamp, H.B.; Bos, P.; Frei, R.W. *J. Chromatogr.*, **1979**, *186*, 489-496.

23. Lawrence, J.F.; Iverson, F.; Hanekamp, H.B.; Bos, P.; Frei, R.W. *J. Chromatogr.*, **1981**, *212*, 245-250.

24. Uddin, Z.; Markuszewski, R.; Johnson, D.C. *Anal. Chim. Acta*, **1987**, *200*, 115-129.

25. Rabenstein, D.L.; Saetre, R. *Anal. Chem.* **1977**, *49*, 1036-1039.

26. Saetre, R.; Rabenstein, D.L. *Anal. Chem.* **1978**, *50*, 276-280.

27. Bergstrom, R.F.; Kay, D.R.; Wagner, J.G. *J. Chromatogr.* **1981**, *222*, 445-452.

28. Krause, R.T.; Wang, Y. *J. Liq. Chrom.* **1988**, *11*, 349-362.

29. Krause, R.T. *J. Liq. Chrom.* **1989**, *12*, 1635-1644.

30. Krause, R.T. *J. Assoc. Off. Anal. Chem.* **1989**, *72*, 975-979.

31. Doerge, D.R.; Yee, A.B.K. *J. Chromatogr.* **1991**, *586*, 158-160.

32. Prince, J.L. *J. Agric. Food Chem.* **1985**, *33*, 93-94.

33. Iriyama, K.; Yoshiura, M.; Iwamoto, T. *J. Liq. Chrom.* **1986**, *9*, 2955-2968.

34. Buchberger, W.; Winsauer, K. *Anal. Chim. Acta* **1987**, *196*, 251-254.

35. Dou, L.; Krull, I.S. *Anal. Chem.* **1990**, *62*, 2599-2606.

36. Cox, J.A.; Dabek-Zlotorzynska, E. *J. Chromatogr.* **1991**, *543*, 226-232.

37. Halbert, M.K.; Baldwin, R.P. *Anal. Chem.* **1985**, *57*, 591-595.

38. Wring, S.A.; Hart, J.P.; Birch, B.J. *Talanta* **1991**, *38*, 1257-1260.

39. Adams, R.N. *Electrochemsitry at Solid Electrodes*, Marcel Dekker, New York, 1969, chap. 10.

40. Parker, V.D. in Baizer, M.M. Ed. *Organic Electrochemistry*, Marcel Dekker, New York, 1973, chap. XVI.

41. Wroblowa, H.; Green, M. *Electrochim. Acta,* **1963**, *8*, 679-692.

42. Andreev, V.N.; Kazarinov, V.E. *Elektrochimiya* **1974**, *10*, 1736-1739.

43. Holze, R.; Schomaker, S. *Electrochim. Acta*, **1990**, *35*, 613-620.

44. Chambers, J.Q.; Moses, P.R.; Shelton, R.N.; Coffen, D.L. *J. Electroanal. Chem.* **1972**, *38*, 245-249.

45. Bucur, R.V.; Marginean, P. *Electrochim. Acta* **1984**, *29*, 1297-1303.

46. Iwamoto, M.; Osteryoung, R.A. *J. Electroanal. Chem.* **1984**, *169,* 181-194.

47. Davis, D.G.; Bianco, E. *J. Electroanal. Chem.* **1966**, *12*, 254-260.

48. Pradac, J.; Koryta, J. *J. Electroanal. Chem.* **1968**, *17*, 167-175.

49. Koryta, J.; Pradac, J. *J. Electroanal. Chem.* **1968**, *17*, 177-183.

50. Koryta, J.; Pradac, J. *J. Electroanal. Chem.* **1968**, *17*, 185-189.

51. Ossendorfova, N.; Pradac, J.; Koryta, J. *J. Electroanal. Chem.* **1970**, *28*, 311-316.

52. Reynaud, J.A.; Malfoy, B.; Canesson, P. *J. Electroanal. Chem.* **1980**, *114*, 195-211.

53. Fawcett, W.R.; Fedurco, M.; Kovacova, Z.; Borkowska, Z. *J. Electroanal. Chem.* submitted.

54. Burke, L.D.; Cunnane, V.J. *J. Electroanal. Chem.* **1986**, *210*, 69-77.

55. Burke, L.D.; O'Leary, W.A. *J. Appl. Electrochem.*, **1989**, *19*, 758-767.

56. Vitt, J.E.; Larew, L.A.; Johnson, D.C. *Electroanal.* **1990**, *2*, 21-30.

57. Roberts, R.A.; Johnson, D.C. *Electroanl.* **1992**, *4*, 741-749.

58. Johnson, D.C.; LaCourse, W.R. *Anal. Chem.* **1990**, *62*, 589A-579A.

59. Johnson, D.C.; LaCourse, W.R. *Electroanal.* **1992**, *4*, 367-380.

60. Johnson, D.C.; Dobberpuhl, D.A.; Roberts, R.A.; Vandeberg, P.J. *J. Chromatogr.* **1993**, *640*, 79-96.

61. Polta, T.Z.; Johnson, D.C. *J.Electroanal. Chem.* **1986**, *209*, 159-169.

62. Polta, T.Z.; Johnson, D.C.; Luecke, G.R. *J. Electroanal. Chem.* **1986**, *209*, 171-181.

63. Polta, T.Z. Ph.D. Dissertation, Iowa State University, Ames, IA, 1986.

64. Thomas, M.B.; Sturrock, P.E. *J. Chromatogr.* **1986**, *357*, 318-324.

65. Ngoviwatchai, A.; Johnson, D.C. *Anal. Chim. Acta* **1988**, *215*, 1-12.

66. Neuburger, G.G.; Johnson, D.C. *Anal. Chem.* **1988**, *60*, 2288-2293.

67. Welch, L.E.; LaCourse, W.R.; Mead, D.A.; Johnson, D.C. *Anal. Chem.* **1989**, *61*, 555-559.

ACKNOWLEDGEMENTS

First and foremost I would like to thank Dr. Johnson for his skillful guidance during my graduate studies. He is the right mix of scientist, mentor, boss, friend, administrator and coworker to be among the best graduate advisors.

I would like to thank the members of the Johnson group, particurly several who led the way ahead of me. I am thankful Therese Polta and Glen Neuburger for their initial work with PED that I was able to build upon. I would like to thank Joe Vitt for his valuable assistance during the first year of my graduate studies. To Rich Roberts and Dave Dobberpuhl I am grateful for their valuable every-day assistance and discussion. They have been like brothers to me the past two years and have made work much more enjoyable.

I would especially like to thank Karin, who has become very special to me and has given me added incentive to complete my PhD in a timely fashion.

Finally I would like to acknowledge my parents, Mary and Vernon and all thirteen of my brothers and sisters: Dan, Tim, Gerard, Jan, Diane, David, Tom, Joe, Bob, Pat, Greg, Pam and Ed. I was really quite fortunate to grow up a set of loving parents and 13 older brothers and sisters who provided me with a rich intellectual atmosphere and continued support in my quest for an education. I only regret the passing of my father who would have been proud to see me receive my PhD.